

**Targeting the Final Step of Blood  
Coagulation:  
Structure-Activity-Relationship Studies  
on the Factor XIIIa Inhibitor Tridegin**

---

D I S S E R T A T I O N

zur Erlangung des Doktorgrades (Dr. rer. nat.)  
der  
Mathematisch-Naturwissenschaftlichen Fakultät  
der  
Rheinischen Friedrich-Wilhelms-Universität Bonn

vorgelegt von  
**Miriam Böhm**  
aus  
Erlabrunn

Bonn, Januar 2015



Angefertigt mit Genehmigung der Mathematisch-Naturwissenschaftlichen Fakultät der  
Rheinischen Friedrich-Wilhelms-Universität Bonn

1. Gutachter: Prof. Dr. Diana Imhof
  2. Gutachter: Prof. Dr. Michael Gütschow
- Tag der Promotion: 02.06.2015  
Erscheinungsjahr: 2015



*Für Robert*



## Abstract

The prophylaxis and therapy of thrombotic diseases is one of the major columns supporting our continuously increasing life expectancy and health. The transglutaminase factor XIIIa (FXIIIa), which is part of the blood coagulation cascade, therefore is an interesting target for antithrombotic and thrombolytic treatment with enzyme inhibitors. Additionally, powerful and specific FXIIIa inhibitors are valuable research tools to elucidate the multiple functions of FXIIIa in more detail. An example for such a powerful inhibitor of FXIIIa can be found in nature: Tridegin, a 66mer peptide was first isolated from the salivary gland of the giant amazon leech *Haementeria ghilianii* in 1997 and is still one of the most potent and specific FXIIIa inhibitors described. The aim of this thesis is to gain access to the peptide by different preparation methods and to characterize in detail the inhibitory mechanism and structure of this interesting peptide. In the course of this research tridegin was synthesized by solid-phase peptide synthesis followed by oxidative self folding to form disulfide bonds. Additionally, recombinant expression of the peptide in *Escherichia coli* was performed. Functional analysis by enzyme activity and binding assays revealed that the major inhibitory action is localized in the C-terminal part of the peptide, whereas the N-terminal part contributes to binding affinity. The disulfide connectivity of both the synthetic and the recombinant peptide variant was elucidated by mass spectrometric analysis and showed that three different disulfide-linked isomers were formed. Subsequently, molecular modeling of all three isomers was performed and the models were docked to the FXIII-A° structure. In general, this work greatly increases the understanding of the natural FXIIIa inhibitor tridegin, which provides the scientific community with a valuable research tool and a potential lead structure for the development of new FXIIIa inhibitors.





## Zusammenfassung

Die Prophylaxe und Therapie thrombotischer Erkrankungen ist eine der wichtigsten Säulen, die unsere stetig steigende Lebenserwartung und Gesundheit trägt. Die Transglutaminase Faktor XIIIa (FXIIIa), die Teil der Blutgerinnungskaskade ist, ist daher ein interessantes Target für antithrombotische und thrombolytische Behandlungen mit Enzyminhibitoren. Zudem sind starke und spezifische FXIIIa-Inhibitoren wertvolle Werkzeuge zur detaillierten Erforschung der verschiedenen Funktionen von FXIIIa. Ein Beispiel für einen solchen wirkungsvollen Inhibitor für FXIIIa kann man in der Natur finden: Tridegin, ein 66mer Peptid, wurde 1997 aus der Speicheldrüse des Amazonas-Riesenblutegels *Haementeria ghilianii* isoliert und ist noch immer einer der potentesten spezifischen bekannten FXIIIa Inhibitoren. Das Ziel dieser Arbeit ist es, Zugang zu Tridegin durch verschiedene Herstellungsverfahren zu erhalten und den inhibitorischen Mechanismus und die Struktur dieses interessanten Peptids im Detail zu charakterisieren. Im Verlauf dieser Untersuchungen wurde Tridegin durch Festphasenpeptidsynthese und anschließende oxidative Selbstfaltung zur Ausbildung der Disulfidbrücken hergestellt. Die rekombinante Expression des Peptids in *Escherichia coli* war ebenfalls erfolgreich. Funktionelle Analysen mittels Enzym-Aktivitäts-Untersuchungen und Bindungsstudien zeigten, dass die hauptsächliche inhibitorische Aktivität im C-terminalen Teil des Peptids lokalisiert ist, wohingegen der N-terminale Teil zur Bindungsaffinität des Inhibitors beiträgt. Die Disulfidverbrückung sowohl der synthetischen als auch der rekombinanten Peptidvariante wurde mit Hilfe von Massenspektrometrie aufgeklärt und es wurde gezeigt, dass drei verschiedene disulfidverbrückte Isomere gebildet wurden. Anschließend wurde eine computergestützte Modellierung aller drei Isomere sowie ein Docking der Modelle an FXIII-A° durchgeführt. Insgesamt erhöht diese Arbeit das Verständnis des natürlichen FXIIIa-Inhibitors Tridegin, welcher der wissenschaftlichen Gemeinschaft ein wertvolles Forschungswerkzeug und eine potentielle Leitstruktur für die Entwicklung weiterer FXIIIa-Inhibitoren zur Verfügung stellt.



# Contents

<b>1</b>	<b>Introduction</b>	<b>1</b>
<b>2</b>	<b>Theoretical Background</b>	<b>3</b>
2.1	Transglutaminases . . . . .	3
2.2	Coagulation Factor XIIIa . . . . .	5
2.2.1	Localization and activation of FXIII . . . . .	5
2.2.2	Structure of FXIII-A . . . . .	7
2.2.3	Substrate specificity of FXIIIa . . . . .	9
2.2.4	Involvement in haemostasis and fibrinolysis . . . . .	11
2.2.5	Other physiological functions . . . . .	13
2.3	Pathophysiology of Factor XIIIa . . . . .	15
2.3.1	Factor XIII deficiency . . . . .	15
2.3.2	Involvement of FXIII in thrombotic diseases . . . . .	16
2.3.3	FXIIIa and cancer . . . . .	17
2.4	Inhibition of FXIIIa . . . . .	18
2.5	Tridegin . . . . .	21
2.5.1	Sequence and homology . . . . .	21
2.5.2	Potency . . . . .	23
2.5.3	Mutational studies . . . . .	24
2.6	Structural Classification of Disulfide Bonds . . . . .	25
<b>3</b>	<b>Aims of this work</b>	<b>27</b>
<b>4</b>	<b>Materials and Methods</b>	<b>29</b>
4.1	Chemicals and Buffers . . . . .	29
4.2	Peptide Synthesis and Purification . . . . .	32
4.2.1	Solid-phase peptide synthesis . . . . .	32
4.2.2	Peptide oxidation . . . . .	34
4.2.3	Peptide purification and analysis by HPLC . . . . .	34
4.3	Chemical Characterization of Peptides . . . . .	35
4.3.1	Mass spectrometry . . . . .	35

4.3.2	Amino acid analysis . . . . .	35
4.3.3	SDS-PAGE . . . . .	38
4.3.4	Ellman's assay . . . . .	38
4.4	Recombinant Expression of Tridegin . . . . .	38
4.4.1	Cloning strategy . . . . .	38
4.4.2	Growth, harvesting and purification . . . . .	40
4.5	Functional Assays . . . . .	41
4.5.1	Chromogenic enzyme activity assay . . . . .	41
4.5.2	Fluorogenic enzyme activity assay . . . . .	41
4.5.3	Microscale thermophoresis experiments . . . . .	41
4.6	Structure Elucidation . . . . .	42
4.6.1	Enzymatic digests and MS analysis . . . . .	42
4.6.2	Molecular modeling . . . . .	42
<b>5</b>	<b>Results and Discussion</b>	<b>43</b>
5.1	Design of Peptides . . . . .	43
5.1.1	Potency of inhibitors from different preparations . . . . .	43
5.1.2	Influence of the N-terminal part on inhibitor function . . . . .	44
5.1.3	Potency and substrate behavior of C-terminal peptides . . . . .	45
5.1.4	Binding affinity of tridegin analogues to FXIII . . . . .	46
5.2	Preparation of Tridegin and Derivatives . . . . .	47
5.2.1	Synthesis . . . . .	47
5.2.2	Recombinant expression of tridegin . . . . .	49
5.3	Functional Characterization . . . . .	51
5.3.1	Substrate behavior of C-terminal peptides . . . . .	51
5.3.2	Evaluation of N-terminally truncated peptides . . . . .	52
5.3.3	Inhibitory potency of different tridegin variants . . . . .	53
5.3.4	Assessment of a fluorogenic FXIIIa assay . . . . .	55
5.3.5	Inhibition type and stoichiometry of the tridegin-FXIIIa-interaction . . . . .	57
5.3.6	Binding studies . . . . .	59
5.4	Structural Analysis . . . . .	60
5.4.1	Crystallization and co-crystallization experiments . . . . .	61
5.4.2	Elucidation of disulfide connectivity . . . . .	63
5.4.3	Side-product formation during oxidation of disulfide-linked tridegin analogues . . . . .	68
5.4.4	Disulfide connectivity of recombinant tridegin . . . . .	69

5.5	Molecular Modeling of Tridegin . . . . .	71
5.5.1	Comparison with other peptides and proteins . . . . .	73
5.6	Structure-Activity-Relationship . . . . .	73
5.6.1	General relationships of the tridegin-FXIIIa-interaction . . . . .	73
5.6.2	Docking of tridegin to FXIII-A° . . . . .	74
<b>6</b>	<b>Conclusion</b>	<b>79</b>
	<b>Abbreviations</b>	<b>83</b>
	<b>List of Figures</b>	<b>85</b>
	<b>List of Tables</b>	<b>87</b>
	<b>Bibliography</b>	<b>89</b>



# 1 Introduction

The connection between leeches and medicine has been established so long ago, that it is hard to tell, when these animals were first applied in therapy. This is stressed by the fact, that “leech” is derived from the Anglo-Saxon word “laece”, which meant physician.<sup>1</sup> Even today, leech therapy continues to play a role, for example, when blood flow needs to be re-established in reattached limbs.<sup>2</sup> When it comes to the molecular mechanisms of leech therapy, the probably most important parts of the leech are the peptides and proteins secreted into the leech saliva, with which the leech numbs the pain of the bitten animal and prevents blood coagulation to occur. The most prominent representative of leech-derived anticoagulants, a peptide named hirudin after the scientific name for the medicinal leech, *Hirudo medicinalis*, was already discovered in the beginning of the 20th century.<sup>3</sup> Since then, hirudin has been investigated in great detail and is now applied in clinical practice as a thrombin inhibitor.<sup>4</sup>

A wide variety of similar substances have been identified to date, some of which are fully characterized, and some of which still need further investigation.<sup>5</sup> One example of the latter group is tridegin, a potent inhibitor of the blood coagulation factor XIIIa. Since its first isolation from the salivary gland of the giant amazon leech *Haementeria ghilianii* in 1997, little has been published concerning structure or inhibitory mechanism of tridegin. Therefore, this thesis is dedicated to intense studies of tridegin with focus on structural analysis of the inhibitor, its interaction with factor XIIIa and the relationship between the structural and functional details.

Tridegin as a well characterized inhibitor might serve as a research tool, a drug or a lead structure for development of new anticoagulants. And the leeches could prove again that they can live up to their name.





## 2 Theoretical Background

### 2.1 Transglutaminases

Transglutaminases (Tgases, EC 2.3.2.13) in general are enzymes that catalyze the formation of  $\epsilon$ -( $\gamma$ -glutamyl)lysine isopeptide bonds between an acyl donor and an acyl acceptor substrate. The reaction proceeds via a covalent enzyme-substrate complex between the active center cysteine side chain and the acyl donor substrate (Figure 2.1).<sup>6,7</sup> While transglutaminases show a high and isoenzyme-dependent substrate specificity for the acyl donor (usually a glutamine residue in a peptide or protein chain), specificity for the acyl acceptor is relatively low.<sup>6</sup> Besides lysine side chains in peptides or proteins, small amines or even water are accepted. Therefore, the enzyme-substrate complex can be resolved by the formation of an isopeptide bond, but also by incorporation of a low molecular weight amine or by hydrolysis (thereby turning the glutamine residue into glutamate). If the incorporated small amine has

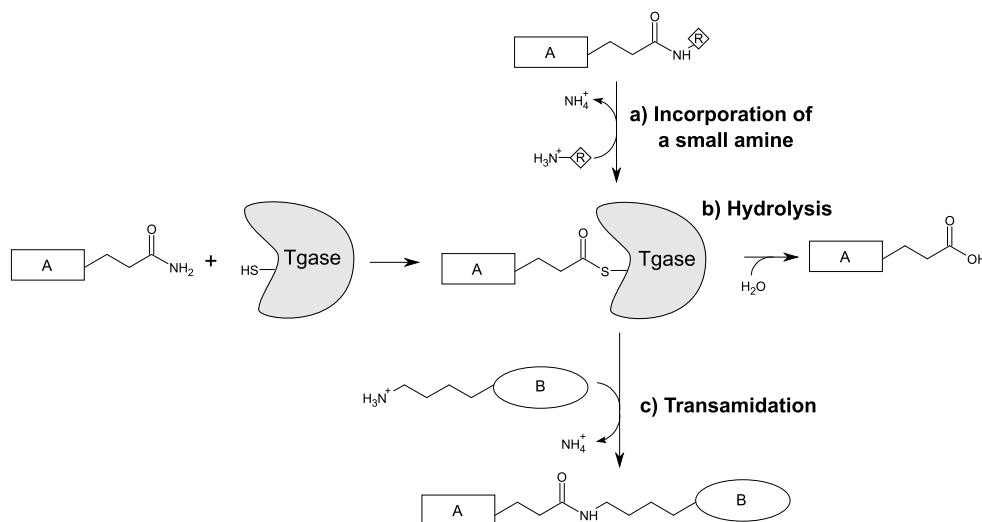


**Figure 2.1:** Overview over the reactions catalyzed by transglutaminases: After formation of the covalent intermediate between the acyl donor and the active site cysteine, three different reactions can follow: a) the incorporation of a small amine, b) hydrolysis of activated thioester, turning the amide substrate into a carboxylic acid or c) transamidation resulting in the formation of an isopeptide bond. Modified from Griffin *et al.*<sup>6</sup>

**Table 2.1:** Human transglutaminases.

Name	Synonym	Preferred substrates	Physiological functions
Tgase 1	Keratinocyte Tgase	Q-x-K/R-φ-x-x-x-W-P <sup>9</sup>	Assembly of the cornified envelope
Tgase 2	Tissue Tgase	Q-x-P-φ <sup>10</sup>	various
Tgase 3	Epidermal Tgase	Y/F/W-Q-S/T-R/K-φ <sup>11</sup>	Assembly of the cornified envelope
Tgase 4	Prostate Tgase	–	Mediator of cell-matrix-adhesion
Tgase 6	Neuronal Tgase	Q-x-x-φ <sup>12</sup>	neuronal differentiation/apoptosis
Factor XIIIa	Fibrin stabilizing factor	Q-x-x-φ-x-W-P <sup>10</sup>	Blood coagulation, wound healing

a second amino group, such as spermidine or spermine, the resulting product can serve as an acyl acceptor in the next reaction (secondary cross-link, Figure 2.1).<sup>6</sup>

There are eight different transglutaminases found in the human genome, which show strong sequence similarity and belong to the superfamily of papain-like cysteine proteases.<sup>6</sup> All members of this family share a common catalytic triad in the active site, consisting of cysteine, histidine and aspartate or asparagine. However, only six of these transglutaminases have been described at protein level so far (Table 2.1). Additionally, “erythrocyte-bound 4.2” has been identified as a homologue, but due to a mutation of the active site cysteine it is no longer enzymatically active and serves structural purposes.<sup>6</sup> All transglutaminases require Ca<sup>2+</sup> for their crosslinking function. Additionally, Tgases 2 and 3 can be negatively regulated by the binding of either GTP or GDP, which is not the case for factor XIIIa or Tgase 1. However, Tgases 1 and 3 as well as Factor XIIIa can be activated by proteolytic cleavage, which, in turn, is not described for Tgase 2.<sup>8</sup>

Of the six transglutaminases in humans, transglutaminase 2 (or tissue transglutaminase) is probably the best characterized. It is ubiquitously expressed and localized both intra- and extracellularly.<sup>13</sup> Besides its transglutaminase activity, it has been shown to act as a GTPase, protein disulfide isomerase and kinase. Tgase 2 plays a role in cell death and differentiation, matrix stabilization, adhesion and migration.<sup>6,13</sup> It is also involved in a number of pathogenic processes, such as celiac disease and cystic fibrosis.<sup>14,15</sup>

Transglutaminase 1 is expressed predominantly in keratinocytes, where it is anchored to the keratinocyte plasma membrane via palmitoylation and myristoylation. It helps in the assembly of the cornified envelope, consisting of heavily cross-linked proteins in the cornified layer of the skin.<sup>16,17</sup> Low levels of Tgase 1 have been shown to be associated with Lamellar ichthyosis, a rare epidermal disorder that results in extensive scaling of the skin.<sup>18</sup> Mice deficient in Tgase 1 show a phenotype similar to the disease and die shortly after birth due to an impaired barrier function of the skin.<sup>19</sup>

Transglutaminase 3 is expressed in the squamous epithelium and is also involved in

cornification.<sup>16,17</sup> Tgase 3 has been described as an auto-antigen, which might be involved in the pathophysiology of dermatitis herpetiformis.<sup>16</sup>

Relatively little is known about transglutaminase 4, which is uniquely expressed in the prostate gland.<sup>20</sup> Recently, Tgase 4 has been shown to increase the aggressiveness of prostate cancer cells by mediating cell-matrix-adhesion.<sup>21</sup>

Transglutaminase 6 is predominantly expressed in the central nervous system. Its expression pattern during embryogenesis suggests a role in neuronal differentiation and/or programmed cell death.<sup>22</sup>

The biochemistry and physiological role of factor XIIIa will be described in detail in the following sections.

## 2.2 Coagulation Factor XIIIa

Factor XIIIa (FXIIIa) was first described in a short article by Laki and Lóránd in 1948 as a thermolabile component of the blood serum that, in presence of calcium ions, renders a blood clot insoluble in highly concentrated urea solutions.<sup>23</sup> Therefore, FXIIIa is also called Laki-Lorand-Factor or fibrin-stabilizing factor. Later, in 1964, it was shown that this fibrin-stabilizing factor was present as a precursor (FXIII) in plasma, and that it needs to be activated by thrombin.<sup>24</sup> Knowledge on FXIII and FXIIIa has increased significantly since then. As more different forms and activation states of FXIII were found, Muszbek *et al.* suggested a nomenclature, which will be used throughout this document.<sup>25</sup>

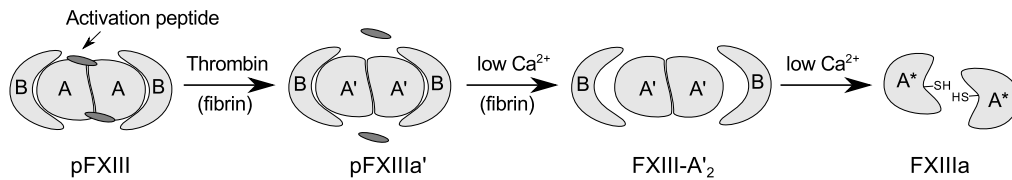
### 2.2.1 Localization and activation of FXIII

FXIII is present in the plasma as an A<sub>2</sub>B<sub>2</sub>-heterotetramer. The two A subunits (FXIII-A) harbor the enzymatic activity, while the B-subunits (FXIII-B) have an inhibitory and carrier function.<sup>26</sup> This tetrameric form is referred to as plasmatic FXIII (pFXIII). Additionally, FXIII can be found in the cytoplasm of different cell types, mainly in platelets and monocytes/macrophages. In this case, it is present as an A<sub>2</sub>-dimer.<sup>27</sup>

The pFXIII (A<sub>2</sub>B<sub>2</sub>) circulates in the blood in an average concentration of 21.0 µg/ml.<sup>28</sup> There is a 50 % excess of the B-subunit over the A-subunit, however, only about 1 % of the A-subunit are present in free form. A recent re-evaluation of the binding constant between the two types of FXIII subunits revealed a K<sub>d</sub> value in the range of 10<sup>-10</sup> M, which is in good agreement with the measured proportions of the free subunits in plasma.<sup>29</sup> The A-subunit is synthesized primarily in bone marrow, whereas the B-subunit originates from liver cells.<sup>29</sup> From patients deficient in FXIII-B, it is known that the B-subunits protects the catalytic A-subunit from clearance (see also section 2.3.1). Therefore, a high proportion of complexed

**Activation of plasma FXIII**

A) proteolytic activation



B) non-proteolytic activation

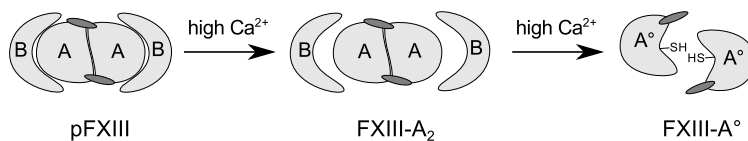


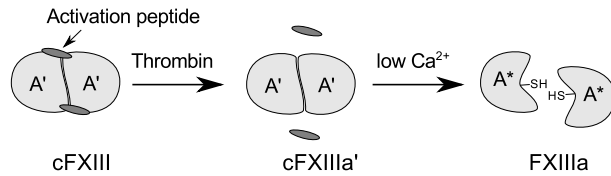
**Figure 2.2:** Different ways of activation for plasma FXIII. Proteolytic activation is probably the physiological way of pFXIII activation (A), while activation with calcium ions alone requires unphysiologically high calcium concentrations (B). Abbreviations as suggested by Muszbek *et al.* are given below. Modified from Muszbek *et al.*<sup>25</sup>

FXIII-A is crucial to maintain FXIII plasma levels. However, the B-subunit also inhibits the activation of pFXIII, so that a multi-step activation process is necessary for the formation of the active enzyme (Figure 2.2). The proposed physiological activation process in plasma involves the concerted action of both thrombin and calcium ions. First, thrombin cleaves the activation peptide of FXIII-A (37 amino acids from the N-terminus), then the binding of calcium ions induces dissociation of the B-subunits and a conformational change in the A-subunit that uncovers the active center.<sup>24,30</sup> The cleavage of the activation peptide is enhanced in the presence of fibrinogen or non-cross-linked fibrin<sup>31</sup> and also the dissociation of the B-subunit is greatly facilitated in the presence of fibrin.<sup>30</sup> Additionally, pFXIII can also be activated by non-physiological high  $\text{Ca}^{2+}$  concentrations (>30 mM). In this case,  $\text{Ca}^{2+}$  ions alone are able to induce dissociation of the B-subunits and a subsequent conformational change in the A-subunits, thereby activating the enzyme (denoted FXIII-A°).<sup>30,32</sup> Whether this mechanism plays any role in the *in vivo* activation of pFXIII remains questionable.

In contrast, intracellular FXIII (cFXIII) behaves differently. While cFXIII is identical to the A-subunit of pFXIII, it is not accompanied by B-subunits and activated more readily by  $\text{Ca}^{2+}$ -ions alone (Figure 2.3). This activation occurs already at concentrations of 2 mM  $\text{Ca}^{2+}$ , albeit very slowly.<sup>33</sup> For maintenance of activity, 2 mM  $\text{Ca}^{2+}$  were required, at lower concentrations the enzyme was shown to deactivate again. Both the  $\text{Ca}^{2+}$ -dependent activation as well as the deactivation are reversible. Still, these calcium concentrations are much higher than the

**Activation of cellular FXIII**

A) proteolytic activation



B) non-proteolytic activation

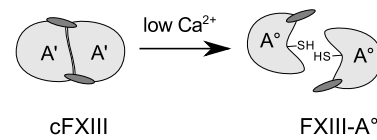


**Figure 2.3:** Cellular FXIII is not bound to B-subunits, therefore activation occurs more readily in presence of calcium ions (A). Proteolytic activation by thrombin or, supposedly, other proteases is nevertheless possible (B). Modified from Muszbek *et al.*<sup>25</sup>

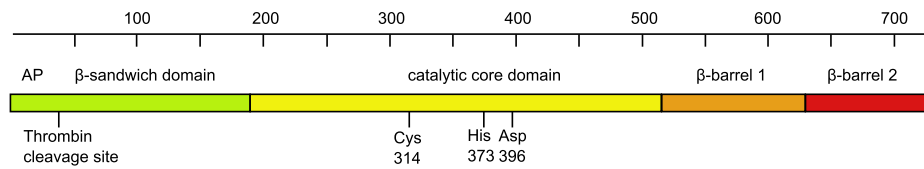
$10^{-4}$  mM of calcium usually found in resting cells.<sup>33</sup> It is suggested that  $\text{Ca}^{2+}$ -ion influx after stimulation of cells could activate cFXIII *in vivo*.<sup>34</sup> Additionally, cFXIII can also be activated by proteolytic cleavage. Activation by thrombin proceeds similar as described for pFXIII, omitting the B-subunit dissociation. In platelets, activation of cFXIII by the cysteine protease calpain has been described.<sup>35</sup> However, in activated platelets no proteolytic truncation has been observed, leaving  $\text{Ca}^{2+}$ -activation as the more likely pathway *in vivo*.<sup>36</sup>

**2.2.2 Structure of FXIII-A**

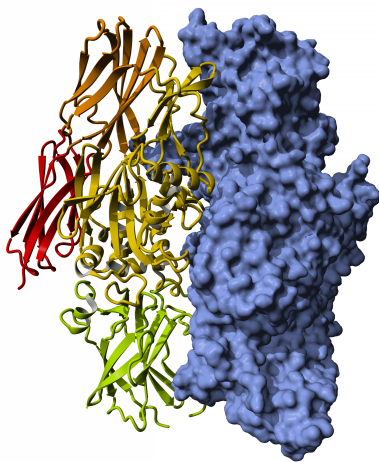
The crystal structure of cFXIII has been first described by Yee *et al.* in 1994.<sup>37</sup> Since then, it has been crystallized several times.<sup>38–40</sup> As crystallization of the activated FXIIIa was not successful in the following years, other approaches were used to gain understanding of the conformational changes that accompany activation of the enzyme. The crystal structure of the homologous Tgase 2<sup>41</sup> was used as a scaffold for homology modeling of FXIIIa.<sup>42</sup> Also, hydrogen-deuterium-exchange has been used to study the conformational dynamics of FXIIIa.<sup>43,44</sup> Finally, in 2013 a probably active conformation ( $\text{Ca}^{2+}$ -activated FXIII-A°) was crystallized with the help of the covalent inhibitor ZED1301.<sup>45</sup> A crystal structure of the B-subunit, the pFXIII ( $\text{A}_2\text{B}_2$ -tetramer) or the proteolytically activated FXIIIa is still not available.

In general, the FXIII-A structure consists of four major domains. The activation peptide (37 N-terminal amino acids) is followed by a  $\beta$ -sandwich domain (38–184), the catalytic core domain, which is also the largest domain (185–515) and two  $\beta$ -barrel domains ( $\beta$ -barrel 1: 516–628 and  $\beta$ -barrel 2: 629–731). This overall structure is conserved in Tgase 2 and Tgase 3 as well.<sup>41,46</sup> The catalytic triad of FXIIIa is formed by Cys314, His373 and Asp396 (Figure 2.4). In the inactive state up to one calcium binding site is populated and the catalytic site is blocked by the  $\beta$ -barrel 1 domain. The side chain hydroxy group of Tyr560 forms a hydrogen bond with the sulfur of the active site cysteine.<sup>37</sup> Upon activation

A



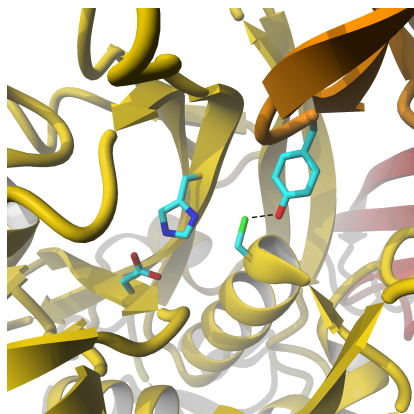
B



C



D



E

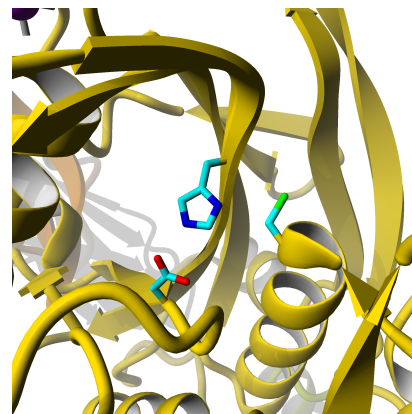


**Figure 2.4:** A) Overall domain structure of FXIII-A B) Structure of the inactive FXIII-A<sub>2</sub>. One monomer is shown in blue, the other monomer is colored according to domain structure.<sup>40</sup> C) Structure of FXIII-A<sup>o</sup>. The irreversible inhibitor ZED1301 is shown in blue, Ca<sup>2+</sup>-ions in violet.<sup>45</sup> D) and E) show enlarged views of the active site in FXIII-A and FXIII-A<sup>o</sup>, respectively. AP: activation peptide.

to FXIII-A<sup>o</sup> by calcium binding, two additional calcium binding sites are populated and the two  $\beta$ -barrel domains move aside to allow access to the active center. The coordination of the two additional calcium ions is suggested to be the driving force for this rearrangement.<sup>45</sup> During this process, a channel for the lysine substrate is opened and an additional catalytic diad is formed by His342 and Glu401, which is supposed to facilitate the nucleophilic attack of the lysine substrate.

In contrast, only little is known about the structure of the B-subunit and the A<sub>2</sub>B<sub>2</sub>-tetramer. The FXIII-B sequence shows a highly repetitive structure containing 10 sushi domains and is similar to fibronectin.<sup>47</sup> Electron microscopy and gradient sedimentation experiments suggest that the B subunit has an asymmetric, elongated shape.<sup>48</sup> The tetramer, in contrast, has a more compact structure, suggesting that the B-subunit is in some way wrapped around the A-subunit.<sup>48</sup> Further investigations showed, that free, recombinant FXIII-B can form homodimers, a function that could be attributed to the ninth sushi domain by comparison with truncated variants. However, the formation of tetrameric complexes with FXIII-A was dependent on the presence of the first (N-terminal) sushi domain, which is therefore thought to be responsible for the binding to FXIII-A. The formation of the A<sub>2</sub>B<sub>2</sub>-tetramer was independent on the ability of the truncated variants to form dimers.<sup>47</sup>

### 2.2.3 Substrate specificity of FXIIIa

Transglutaminases in general show a relatively high substrate specificity for the glutamine containing substrate, whereas specificity for the lysine containing substrate is rather low, so that not only peptides containing lysine residues are accepted, but also small primary amines like glycine ethyl ester.<sup>49</sup> Despite the specificity of FXIIIa for certain glutamine substrates, it proved difficult to derive a universal consensus sequence. Sugimura *et al.* determined a consensus sequence by applying a phage-display library approach. They came up with a preference for substrates containing a Qxx $\phi$ xWP motif ( $\phi$  is any hydrophobic amino acid).<sup>10</sup> The development of an inhibitor based on this consensus sequence validates this approach.<sup>45</sup> Therefore it is even more surprising, that most of the natural substrates of FXIIIa do not share this common sequence (Table 2.2).<sup>50</sup> This indicates that the overall structure of the substrate might also play an important role.

A recent study using a proteomics approach identified 147 substrates of FXIIIa in blood, and 48 proteins that were actually incorporated in the plasma clot. Again, a consensus sequence could not be derived from the data, apart from the complete absence of proline in the first position C-terminal of the glutamine residue. However, they found an over-representation of reactive glutamine residues in loop regions after categorizing their hits according to secondary structure.<sup>51</sup> A list of selected FXIIIa substrates is given in Table 2.2. Further FXIIIa substrates can be found in the transdab database.<sup>52</sup>

**Table 2.2:** Selected glutamine containing substrates of FXIIIa. Updated from Böhm, 2010.<sup>53</sup>

Sequence			Origin	Ref.
<b>Natural substrates</b>				
...WNSGSSGTGSTGN	Q <sup>328</sup>	NPGSPRPGSTGTW...	Fibrinogen $\alpha$ -chain	54
...HWTSESSUSGSTG	Q <sup>366</sup>	WHSESGSFRPDSP...	Fibrinogen $\alpha$ -chain	54
...IIPFNRLTIGEGQ	Q <sup>398</sup>	HHLGGAQAGDV-OH	Fibrinogen $\gamma$ -chain	54
H-EA	Q <sup>3</sup>	QIVQPQSPLTVSQ...	Fibronectin	54
...SKIRKPKMCPQLQ	Q <sup>670</sup>	YEMHGPEGLRVGF...	$\alpha_2$ -Macroglobulin	54
H-N	Q <sup>2</sup>	EQVSPLTLLKLG...	$\alpha_2$ -Antiplasmin	55
H-FQSG	Q <sup>5</sup>	VLAALPRTSRQVQ...	TAFI <sup>a</sup>	56
...NQIKAYISMHSYS	Q <sup>292</sup>	HIVFPYSYTRSKS...	TAFI	56
...MTPENFTSCGFMQ	Q <sup>83</sup>	IQKGSYPDAILQA...	plasminogen activator inhibitor 2 <sup>b</sup>	57
...TSDLQAQSKGNPE	Q <sup>93</sup>	TPVLPEEEAPAPE...	Vitronectin	54
...TVMFPPQSVLSLS	Q <sup>167</sup>	SKVLPVPEKAVPY...	$\beta$ -Casein	54
...QERCVDGCSCPEG	Q <sup>313</sup>	LLDEGLCVESTEC...	von Willebrand factor	58
...PVIPANMDKKYRS	Q <sup>378</sup>	HLDNFSNQIGKHY...	coagulation factor V	51,59
<b>Putative natural substrates<sup>c</sup></b>				
...DKLGEVNTYAGDL	Q <sup>77</sup>	KKLVPFATELHER...	Apolipoprotein A-IV	51
...GTAFVIFGIQDGE	Q <sup>280</sup>	RISLPESLKRIPI...	Complement C3	51
...EEVDQVTLYSYKV	Q <sup>78</sup>	STITSRMATTMIQ...	ITI <sup>d</sup> heavy chain H2	51
...SVVHLGVPLSVGV	Q <sup>42</sup>	LQDVPRGQVVKGS...	Complement C4-B	51
...PVVAEFYGSKEDP	Q <sup>111</sup>	TFYYAVAVVKKDS...	Serotransferrin	51
...NGDRIDSLENDR	Q <sup>168</sup>	QTHMLDVMQDHFS...	Clusterin	51
...WLLVAVGSACRFL	Q <sup>64</sup>	EQGHRAEATTLHV...	Complement C8 $\gamma$ -chain	51
<b>Artificial substrates</b>				
H-LGPG	Q <sup>5</sup>	SKVIG-OH	K9-peptide (Berichrom <sup>®</sup> -substrate)	60
H-N	Q <sup>2</sup>	EQVSPLTLLKLG-OH	derived from $\alpha_2$ -Antiplasmin	60
H-N	Q <sup>2</sup>	EQVSPLTLLK-OH	derived from $\alpha_2$ -Antiplasmin	55
H-D	Q <sup>2</sup>	MMLPWPAVKL-OH	Screening	10
H-W	Q <sup>2</sup>	HKIDLRYNGA-OH	Screening	10
H-S	Q <sup>2</sup>	HPLPWVLMML-OH	Screening	10
H-SVLSLS	Q <sup>7</sup>	SKVLPVPE-NH <sub>2</sub>	derived from $\beta$ -Casein	61

<sup>a</sup>Thrombin-activatable fibrinolysis inhibitor. Q2 is also a substrate glutamine. <sup>b</sup>Q82 and Q86 are also substrate glutamines.

<sup>c</sup>Frequently, more than one reactive glutamine residue was found. In this case, only the most N-terminal representative is chosen here. <sup>d</sup>Inter-alpha-trypsin inhibitor.



### 2.2.4 Involvement in haemostasis and fibrinolysis

The most important biological function of FXIIIa is its involvement in blood coagulation. It differs from most of the other coagulation enzymes in that it is not a serine protease, but a transglutaminase. In the final stages of blood coagulation, thrombin cleaves fibrinogen to form fibrin and also activates FXIII. The fibrin monomers assemble to a non-covalent fibrin clot, which is then covalently cross-linked by FXIIIa. This is also the reaction that was originally observed by Laki *et al.* when they discovered FXIIIa.<sup>23</sup> The covalent crosslinking of fibrin makes the clot insoluble even at high concentrations of urea, while non-cross-linked fibrin clots dissolve readily under these conditions. Later, measurements of the viscoelastic properties of cross-linked and non-cross-linked clots showed a remarkable increase in clot stiffness after FXIIIa treatment.<sup>62,63</sup> This is attributed to the crosslinking of  $\alpha$ - and  $\gamma$ -fibrin chains. The fastest reaction is  $\gamma$ -chain dimerization by the reciprocal cross-linking between Lys406 on one chain, and Gln398 or Gln399 on another chain. This is then followed by the slower  $\alpha$ -chain cross-linking, in which multiple lysine and glutamine residues are involved and which results in high molecular weight polymers. It is suggested that the second, slower reaction, has more influence on clot stiffness.<sup>27</sup>

The action of FXIIIa on fibrin also renders a clot more resistant to fibrinolysis by plasmin. Initially it was thought that this also results from fibrin cross-linking. However, it was shown by Fraser *et al.* that the resistance of the clot to fibrinolysis is almost solely influenced by  $\alpha_2$ -antiplasmin ( $\alpha_2$ -AP), which is covalently attached to the fibrin chains by FXIIIa.<sup>64</sup>  $\alpha_2$ -AP is a natural inhibitor of the fibrinolytic protease plasmin. It is secreted by the liver as Met1- $\alpha_2$ -AP, which is a mediocre substrate for FXIIIa, but antiplasmin cleaving enzyme (APCE), a protease present in the blood, partially converts Met1- $\alpha_2$ -AP to Asn1- $\alpha_2$ -AP by removing 12 N-terminal amino acids. Asn1- $\alpha_2$ -AP is an excellent substrate of FXIIIa and is rapidly incorporated into the clot.<sup>36</sup> The importance of this physiological process is underlined by the fact that  $\alpha_2$ -AP-deficiency leads to severe bleeding tendency very similar to FXIII-deficiency (see section 2.3.1).<sup>65</sup>

Another component of the fibrinolytic system that is cross-linked to fibrin by FXIIIa is plasminogen activator inhibitor 2 (PAI-2).<sup>57</sup> This protein is usually found in monocytes, but can also be secreted and is detectable in plasma during pregnancy.<sup>66,67</sup> It is an inhibitor of urokinase (also called urokinase-type plasminogen activator or u-PA). PAI-2 prevents urokinase from converting plasminogen to plasmin, and therefore has an antifibrinolytic function.<sup>67</sup>

Thrombin-activatable fibrinolysis inhibitor (TAFI) is a more recently described inhibitor of fibrinolysis, which is also incorporated in the clot by FXIIIa.<sup>56</sup> It is activated by thrombin, most efficiently in the presence of thrombomodulin, resulting in activated TAFI (TAFIa). It

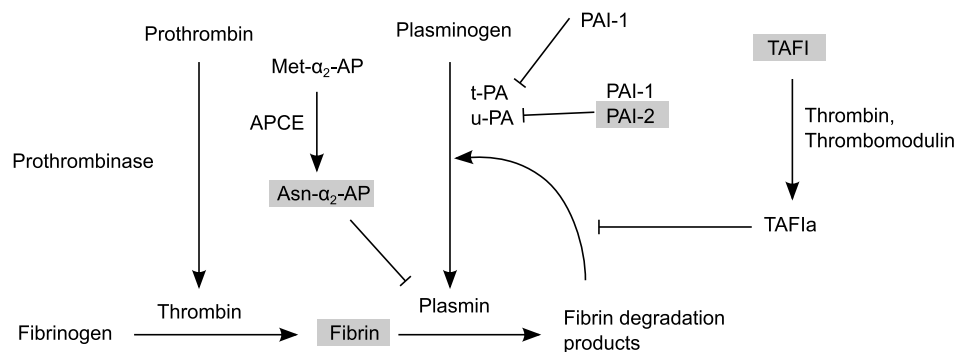


**Figure 2.5:** Overview of fibrinolytic and anti-fibrinolytic processes. Substrates of FXIIIa are marked in gray.

then acts by inhibiting a positive feedback mechanism in the activation of plasmin: Plasmin cleaves fibrin after selected lysine and arginine residues. These free C-terminal lysine residues enhance the formation of plasmin from plasminogen, thereby increasing fibrinolysis.<sup>36,68</sup> TAFIa eliminates these C-terminal lysine and arginine residues from the partially degraded fibrin and reduces this positive feedback mechanism. The covalent cross-linking of TAFI and fibrin is suggested to facilitate the activation of TAFI and protect it from degradation.<sup>56</sup>

The interaction of FXIIIa with platelets and the involvement of the intracellular cFXIII of platelets in the coagulation process seems to be more complex. Although cFXIII is present in platelets in huge amounts reaching about 3 % of total cell protein,<sup>69</sup> the influence of cFXIII from platelets on the crosslinking of the clot is negligible and cFXIII is not released during platelet activation.<sup>36,70</sup> The presence of platelets themselves, however – independently on whether or not they contain cFXIII – did accelerate the fibrin cross-linking reaction of pFXIIIa, indicating that platelets provide a catalytic surface by a yet unknown mechanism.<sup>36</sup> The role of cFXIII inside platelets has also been investigated in more detail. There are contradictory findings on whether or not cFXIII is involved in clot retraction, i.e. a platelet mediated shrinking of the clot that pulls the edges of the lesion closer together.<sup>36,71,72</sup> Studies on the localization of cFXIII inside the platelets showed a diffuse, cytoplasmatic distribution of cFXIII in resting platelets, but upon activation of the platelets by either thrombin or Ca<sup>2+</sup>-influx, cFXIII rapidly relocates to the periphery. As this is a region of major cytoskeletal reorganization in activated platelets, and as FXIIIa has been shown to associate with cytoskeletal proteins, an involvement of FXIIIa in cytoskeletal stabilization was suggested.<sup>73</sup>

The whole process of fibrinolysis is summarized in Figure 2.5. With these findings in mind, it is evident that FXIIIa is a key player in the regulation of fibrinolysis and clot stability and has an overall anti-fibrinolytic effect. However, recently other physiological roles for FXIII have been suggested, and will be reviewed in the following section.

### 2.2.5 Other physiological functions

Multiple physiological functions for FXIIIa have been suggested apart from the involvement in blood coagulation. This includes a participation in wound healing, angiogenesis, maintenance of pregnancy, inflammation, immune response, cardiac protection and bone metabolism, which have recently been reviewed.<sup>36,50,74</sup> Figure 2.6 gives an overview on this topic.

**Wound healing and angiogenesis** An important additional function of FXIIIa is its influence on wound healing processes. An impaired wound healing has been documented both in FXIII-A deficient humans and mice.<sup>75,76</sup> When the closure of cutaneous wounds was studied in FXIII-A deficient mice, they showed poor epidermal regeneration, formation of abnormal scar tissue and necrosis. Only 73 % of total wound closure was reached after 11 days, a time span sufficient for wound closure in control animals. The substitution of FXIII in the deficient mice, in contrast, resulted in nearly normal wound healing.<sup>76</sup> This suggests that pFXIII is sufficient to restore the normal phenotype, despite the cFXIII deficiency of the mice, which was not affected by FXIII substitution.<sup>76</sup> The molecular mechanism is not fully understood yet. The most important physiological processes involved in wound healing are fibrin gel formation, invasion of macrophages, migration and proliferation of fibroblasts, production of extracellular matrix and angiogenesis.<sup>36</sup> FXIIIa seems to be involved in several steps of this process. It was shown that FXIIIa (but not inactivated FXIIIa) significantly enhances proliferation and migration of monocytes and fibroblasts and also reduces apoptosis in these cell types.<sup>77</sup> Additionally, FXIIIa is known to cross-link certain matrix proteins, for example fibronectin, which is covalently cross-linked by FXIIIa and is also attached to fibrin-clots, thereby enhancing fibroblast migration into the clot.<sup>36,50</sup> Finally, FXIIIa is also pro-angiogenic, a property not uncommon among coagulation enzymes that is also the case for thrombin, factor VII and tissue factor.<sup>78</sup> Dardik *et al.* showed that FXIIIa had a positive influence on migration and proliferation of endothelial cells and inhibited apoptosis. Additionally, FXIIIa treatment lowered the expression of thrombospondin 1, a well-characterized anti-angiogenic factor, in these cells. Again, these effects were not seen with inactivated FXIIIa.<sup>79</sup> The effect of FXIIIa on angiogenesis *in vivo* was also evaluated. In a murine neonatal cardiac allograft model, a dose dependent increase in blood vessels was found when injected with FXIIIa.<sup>80</sup> This angiogenic function of FXIIIa is assumed to play an important role in wound healing.

**Maintenance of pregnancy** Besides bleeding, premature abortion is a common symptom in FXIII deficient women. Of 124 reported cases of pregnancies in FXIII deficient patients without prophylactic therapy, 91 % resulted in miscarriages. When pFXIII is substituted,

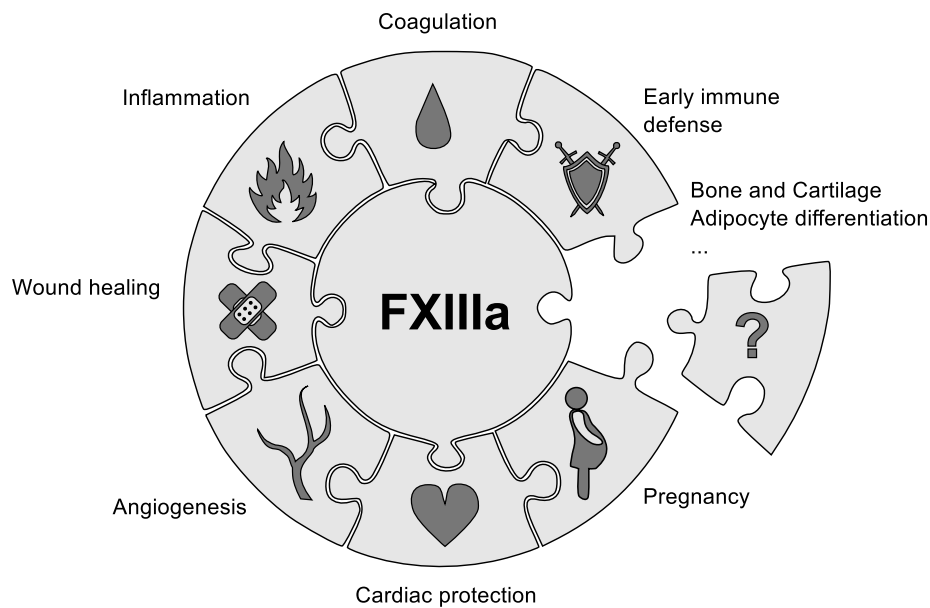


**Figure 2.6:** Physiological functions of FXIIIa.

pregnancy is largely normal in these patients.<sup>81</sup> An interesting finding is the proliferation of cFXIII containing cells in the placenta in the first trimester of pregnancy.<sup>82</sup> However, the fact that pFXIII substitution is sufficient to maintain pregnancies leads to the conclusion, that pFXIII is of primary importance.<sup>36</sup> It has been shown in case of a deficient patient that the absence of FXIIIa impaired the formation of the cytotrophoblastic shell, a layer that connects the fetal and maternal parts of the placenta. It is thought that FXIIIa serves an important function in the cross-linking of extracellular matrix proteins in this region thereby stabilizing the placenta.<sup>83</sup>

**Inflammation and immune response** The connections between FXIII and infection control have been reviewed recently.<sup>84</sup> Entrapment of bacteria in blood or similar body fluids is an evolutionary old mechanism of immune systems, which is still a primary line of defense in animals like the horseshoe crab, whose hemolymph reacts with coagulation after contact with bacterial endotoxins.<sup>84</sup> This mechanism is still conserved in humans, as shown by the activation of the blood coagulation upon contact with bacteria. Moreover, FXIII may also be activated in this process and has been shown to efficiently cross-link bacteria into the forming clot, thereby immobilizing them. This entrapment can also be seen *in vivo*, a mechanism that was shown to be impaired in FXIII deficient mice where bacteria were distributed more widely in the early stages of infection compared to normal mice.<sup>85</sup>

Besides this very ancestral line of immune defense, there is also a cross talk between FXIIIa, the complement system and immune cells.<sup>34,74</sup> An example for this is mannan-binding lectin-

associated serine protease-1 (MASP1), a component of the complement system, that has a similar substrate specificity as thrombin. It was shown to activate FXIII, but more slowly than thrombin.<sup>86</sup> This could be one of the mechanisms also involved in the cross-linking of bacteria and fibrin clots. Interestingly, a study on potential substrates of FXIIIa identified a number of other complement proteins as FXIIIa substrates.<sup>51</sup>

An example for the connection between FXIIIa and immune cells is the already mentioned pro-proliferative effect of FXIIIa on monocytes.<sup>77</sup>

**Cardiac protection** In 2006, Nahrendorf *et al.* discovered a novel functional impairment in FXIII deficient mice. They could show that both homozygous and heterozygous FXIII deficient mice died due to a cardiac rupture a few days after an experimental myocardial infarct was introduced. They could also demonstrate that FXIII was present within the healing infarct in wild-type mice.<sup>87</sup> This finding was strengthened by a study on the life span of FXIII deficient mice, which revealed that especially male mice tended to die of heart bleeding.<sup>88</sup> Also, a similar human case has been reported, which underlines the possible clinical relevance of this topic.<sup>89</sup>

**Various** Additionally, other potential physiological functions of FXIII have been described. Among these are an involvement in bone and cartilage development. FXIII has been found in hypertrophic, i.e. terminally differentiated, chondrocytes.<sup>90</sup> Furthermore, it has been shown to participate in the differentiation of these chondrocytes and an involvement in osteoarthritis is discussed.<sup>91</sup> FXIII also came up in a genome wide association study on genes correlated with obesity<sup>92</sup> and most recently, FXIII was shown to be a negative regulator of adipogenesis.<sup>93</sup>

## 2.3 Pathophysiology of Factor XIIIa

Despite the ongoing, thorough investigations of the physiological functions of FXIIIa, its pathophysiology is only partly understood. While the deficiency in FXIII is well studied, the implications of FXIII levels on other diseases are still a matter of debate.

### 2.3.1 Factor XIII deficiency

Factor XIII deficiency is a rare bleeding disorder caused by low levels of (functional) FXIII in the plasma. Clinical symptoms include frequent bleeding events, for example subcutaneous hematomas, intramuscular and joint hemorrhage, and intracranial hemorrhage.<sup>75</sup> The latter is also the most frequent cause of fatality and disability in FXIII deficient patients.<sup>75,94</sup>

Rebleeding of wounds is a common symptom as well. However, due to the multiple functions of factor XIII in man, bleeding is not the only symptom of a FXIII deficiency. Most notably, deficient patients suffer from impaired wound healing and scar formation. In women, FXIII deficiency leads to recurrent pregnancy losses (see also section 2.2.5).<sup>81</sup>

Factor XIII deficiency can be inherited (congenital) or acquired. Congenital FXIII deficiency is a very rare, autosomal recessive disease with a prevalence of 1 in 2 or 3 million people.<sup>75,95</sup> It can present as either FXIII-A or FXIII-B deficiency, depending on whether the A- or the B-subunit is affected. FXIII-A deficiency can be further classified into type I or type II. Type I deficiency is a quantitative defect. The plasma level of FXIII-A is low or not detectable, usually caused by a mutation in the *F13A*-gene which leads to a misfolded or truncated protein. More than 100 mutations have been reported so far.<sup>96</sup> On the other hand, FXIII-A type II deficiencies are caused by a dysfunctional FXIII-A-subunit. Up to now, there is only one such example, where an amino acid exchange at the thrombin cleavage site renders the protein resistant to thrombin cleavage and thereby prevents activation of FXIII.<sup>75</sup> A nonfunctional FXIII-B subunit on the other hand results in increased clearance of FXIII-A from the plasma, thereby also lowering the plasma levels of FXIII. However, the phenotype is somewhat milder compared to FXIII-A deficiencies, which is probably due to small amounts of FXIII-A (about 10 % of the normal value) still present in the plasma.<sup>75</sup>

Acquired FXIII deficiency may have a variety of causes. As known for other coagulation factors as well, a high consumption of these enzymes for example during major surgery or inflammatory bowel disease, can lead to a significant decrease in plasma levels.<sup>75</sup> On the other hand, autoantibodies against FXIII (in most cases the A-subunit, rarely the B-subunit<sup>96</sup>) have been reported, which can inhibit FXIIIa, prevent the activation of FXIII or the binding of FXIII to fibrinogen.<sup>97</sup> Most commonly these autoantibodies are found in patients suffering from autoimmune diseases such as systemic lupus erythematosus.<sup>98</sup> Treatment is more difficult in these cases, as substitution of FXIII is often not successful. Therefore, treatment is usually focused on suppressing the immune response and/or treating the underlying autoimmune condition.<sup>75</sup>

### 2.3.2 Involvement of FXIII in thrombotic diseases

Since FXIII plays an important role in coagulation and haemostasis, it seems stringent to look for an involvement of the enzyme in thrombotic diseases (Figure 2.7). However, there is relatively few evidence that elevated levels of FXIII could influence this type of disease.<sup>99</sup> For example, two studies on deep vein thrombosis (DVT) and venous thromboembolism (VTE) did not find a link between FXIII levels and risk of DVT.<sup>100,101</sup> However, it was shown that FXIII is significantly decreased in patients with pulmonary embolism, and the decrease

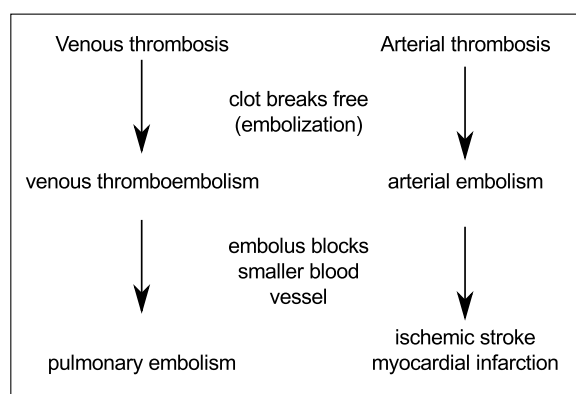


**Figure 2.7:** Overview over different complications arising from venous and arterial thrombus formation. In case a thrombus forms in veins, embolization (i.e. breaking free of the thrombus) can lead to obstruction of smaller blood vessels in the lung, causing life threatening pulmonary embolism. Thrombi formed in the arteria may also embolize and can for example block capillaries in the brain or heart muscle, also causing potentially fatal obstruction of these.

was correlated with the pulmonary occlusion rate. This indicates a consumption of FXIII in the course of the disease and therefore direct contribution of FXIII to the clot formation.<sup>102</sup> On the other hand, high FXIII levels have been linked to an increased risk for myocardial infarction. This correlation is gender specific and applies only to women.<sup>103</sup>

A lot of attention has been given to the influence of a common polymorphism of FXIIIa (Val34Leu) on pathological conditions. The frequency of this allele is about 25 % in Caucasians, but significantly lower in Africans or Asians.<sup>104</sup> The Val34Leu substitution is close to the thrombin cleavage site in FXIII and has indeed been shown to enhance the activation rate by thrombin and affect the cross-linked fibrin structure.<sup>105</sup> Studies demonstrated that the risk of DVT is slightly decreased in both homozygous and heterozygous carriers of the Val34Leu polymorphism.<sup>100</sup> However, there seems to be no influence of this polymorphism on ischemic stroke, as a recent meta-analysis suggests.<sup>106</sup>

A more indirect influence of FXIII on atherosclerotic diseases has been investigated by AbdAlla *et al.* The group could demonstrate that angiotensin 1 receptors (AT<sub>1</sub> receptors) in monocytes can be cross-linked by cFXIII in the presence of calcium ions and angiotensin II. This leads to dimerization of the AT<sub>1</sub> receptors which renders them hyperresponsive. Interestingly, an increased level of these AT<sub>1</sub> receptor dimers was found in patients that already showed hypertension.<sup>107</sup> Therefore it is suggested that activation of intracellular FXIII may be a risk factor for the development of atherosclerosis.<sup>107</sup>

### 2.3.3 FXIIIa and cancer

There is some evidence that FXIIIa is associated with oncogenesis. For example, FXIII-A has been shown to be present in acute promyelocytic leukemia cells.<sup>108</sup> Activity of FXIIIa in plasma was elevated in patients with non-small cell lung carcinoma.<sup>109</sup> A more detailed analysis on the function of FXIII in tumor metastasis revealed, that the absence of FXIII impairs the formation of metastases by hematogenous tumor cells. FXIII is suggested to

enhance the survival of micrometastases by providing a cross-linked fibrin rich matrix that prevents natural killer cells from entering the metastatic site and eliminating the tumor.<sup>110</sup> A similar effect was described for brain tumors, where fibrin deposition and the presence of FXIII were described.<sup>111</sup> The whole picture of FXIII influence on tumors is not yet understood, but will probably be addressed in more detail in the future.

### 2.4 Inhibition of FXIIIa

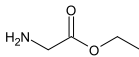
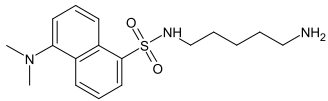
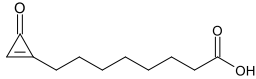
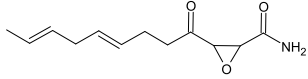
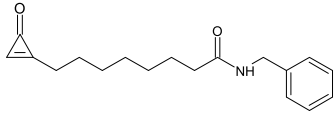
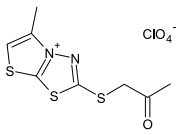
The aforementioned association of FXIIIa with pathological conditions makes it an interesting target for inhibitor design. The earliest “inhibitors” described for fibrin cross-linking were in fact small, primary amines that were incorporated into fibrin clots and thereby prevented fibrin cross-linking.<sup>49</sup>

In the 1980's, Merck Sharp & Dohme developed imidazolium and thiadiazolium derived transglutaminase inhibitors.<sup>112,113</sup> Additionally, some naturally occurring FXIIIa inhibitors have been identified, among them the antibiotic cerulenin<sup>114</sup> as well as alutacenoic acids<sup>115</sup> and derivatives<sup>116</sup> and the peptide inhibitor tridegin (see section 2.5). Some experiments have already shown the potential benefit of FXIIIa inhibitors. One of them was conducted by Shebuski *et al.* in 1990 and showed an enhanced t-PA induced thrombolysis in a canine model, when a FXIIIa inhibitor (L722151, see Table 2.3) was applied prior to thrombus formation.<sup>117</sup> Another study nine years later showed a similar result on a pulmonary embolism model in ferrets.<sup>118</sup> The group administered an inhibitory antibody against FXIIIa and could demonstrate that not only thrombus lysis after t-PA administration was increased after FXIIIa inhibition, but also the endogenous thrombolysis without addition of t-PA.<sup>118</sup> Matlung *et al.*, in contrast, could demonstrate that the inhibition of transglutaminase activity (by L682777) did not influence the early stage development of atherosclerotic lesions in a mouse model.<sup>119</sup>

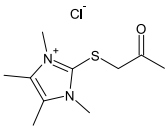
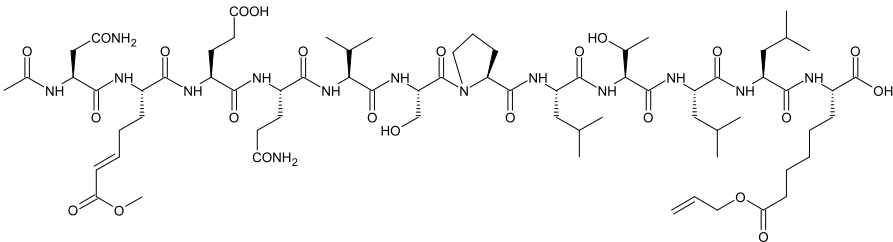
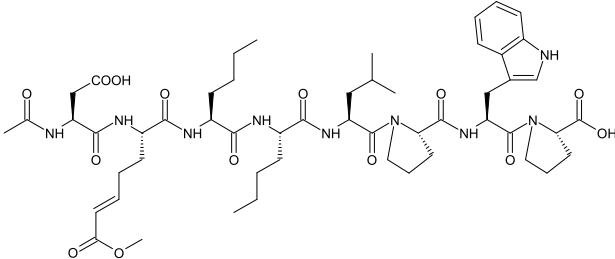
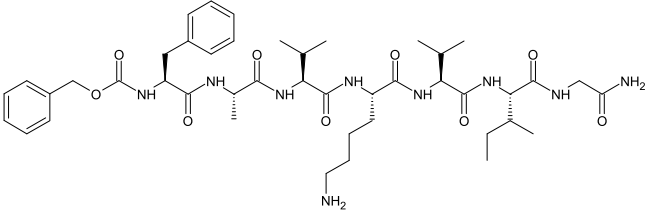
While these inhibitors gave valuable insights in *in vivo* experiments, they suffer from two shortcomings: First, most of the small molecule inhibitors did not discriminate well between the tissue transglutaminase Tgase2 and FXIIIa. Second, they showed only a short plasma half life of 5-10 min.<sup>117</sup> Therefore, in the last years inhibitor design concentrated on peptide-derived inhibitors. One of them, ZED1301, has been successfully applied for co-crystallization with active FXIII.<sup>45</sup> Because of this, specific FXIIIa inhibitors are both, valuable tools for the investigation of FXIIIa *in vitro* and *in vivo* and potential drug candidates.



**Table 2.3:** FXIIIa inhibitors. Potency is given as IC<sub>50</sub> and/or k<sub>2nd</sub> (apparent second-order rate constant), depending on what information was available.

Inhibitor	Potency	Specificity
<b>Chemical agents</b>		
EDTA (depletion of Ca <sup>2+</sup> -ions) <sup>120</sup>	–	unspecific
iodoacetamide (alkylation of active site cysteine) <sup>121</sup>	–	unspecific
<b>Competitive substrates</b>		
 glycine ethyl ester <sup>49</sup>	–	does not discriminate between FXIIIa and Tgase2
 dansylcadaverine <sup>49</sup>	–	does not discriminate between FXIIIa and Tgase2
<b>Small molecule inhibitors</b>		
 alutacenoic acid B <sup>115</sup>	IC <sub>50</sub> =0.61 μM	does not inhibit papain, calpain or cathepsin, inhibits Tgase2 with 20fold higher IC <sub>50</sub>
 Cerulenin <sup>114</sup>	IC <sub>50</sub> <6.2 μM <sup>122</sup>	has also antibiotic activity
 alutacenoic acid derivative <sup>116</sup>	IC <sub>50</sub> =0.026 μM	unknown
 L722151 <sup>112,113</sup>	IC <sub>50</sub> <0.5 μM <sup>122</sup> k <sub>2nd</sub> =23000 M <sup>-1</sup> s <sup>-1</sup>	no effect on thrombin, plasmin, papain, <sup>112</sup> but does inhibit Tgase2 <sup>123</sup>

**Table 2.3:** FXIIIa inhibitors (*continued*). MAP: Michael acceptor pharmacophore, CMK:Chloro methyl ketone.

Inhibitor	Potency	Specificity
 L682777 <sup>113,124</sup>	$IC_{50} < 0.08 \mu M$ <sup>124</sup> $k_{2nd} = 63000 M^{-1} s^{-1}$	no inhibition of papain or calpain, but apparent second-order rate constants are in the same range for FXIIIa and Tgase2 <sup>113</sup>
<b>Peptide derived inhibitors</b>		
 ZED1251 <sup>125</sup> (Ac-Asn-MAP-Glu-Gln-Val-Ser-Pro-Leu-Thr-Leu-Leu-Lys(alloc)-OH)	$k_{2nd} = 5500 M^{-1} s^{-1}$	unknown
 ZED1301 <sup>45</sup> (Ac-Asp-MAP-Nle-Nle-Leu-Pro-Trp-Pro-OH)	$IC_{50} \approx 100 nM$ <sup>126</sup> $k_{2nd} = 4600 M^{-1} s^{-1}$ <sup>127</sup>	$IC_{50}$ for Tgase2 about 3000 nM, i.e. 30-fold lower inhibition. <sup>126</sup>
 Cbz-Phe-Glu(CMK)-Val-Lys-Val-Ile-Gly-NH <sub>2</sub> <sup>128</sup>	$k_{2nd} = 681 M^{-1} s^{-1}$	unknown

## 2.5 Tridegin

The natural FXIIIa inhibitor tridegin was first described in 1997 by Finney *et al.*<sup>129</sup> It was shown that the salivary gland extract of the giant amazon leech *Haementeria ghilianii* could inhibit FXIIIa and subsequently a peptide of approx. 7.3 kDa was isolated. With the help of an ammonia-release assay, the group determined an IC<sub>50</sub> value of about 10 nM and was furthermore able to derive the 66 amino acid peptide sequence by Edman sequencing, with few ambiguities. These include the insufficient separation of (carbamidomethylated) cysteine from glutamate and three positions that could not be determined at all and are suggested to be post-translationally modified (Figure 2.8A). While the group could directly show that tridegin inhibited the fibrin cross-linking, an effect of tridegin on other components of the coagulation cascade (thrombin, factor Xa) or cysteine proteases (bromelain, papain, cathepsin C) was not detectable. However, tridegin did inhibit Tgase 2, albeit with an IC<sub>50</sub> value of about 23-fold the value which was found for FXIIIa. Tridegin is therefore a highly specific and highly active FXIIIa inhibitor. It is also the first and up to now only natural peptidic FXIIIa inhibitor described.<sup>129</sup>

### 2.5.1 Sequence and homology

Between 2000 and 2002 two patent applications on tridegin were filed<sup>130,131</sup> and one more containing the tridegin sequence as an example for glucose dehydrogenase fusion proteins.<sup>132</sup> Two of these patents describe the recombinant expression of tridegin and contain a full tridegin sequence (no ambiguities) with two additional amino acids (N-terminal methionine and C-terminal glutamate).<sup>131,132</sup> However, no details are given on how this sequence was derived.

A first clear homologue of tridegin was found by an expressed sequence tag (EST) sequencing approach of the salivary complexes of *Haementeria depressa*.<sup>133</sup> An alignment of this sequence with the originally published peptide sequence performed by T. Kühl resulted in almost the same sequence as published in the patents (see Figure 2.8).<sup>134</sup> The *H. depressa* gene product of the homologous sequence has not been isolated. Salivary gland extracts from the *H. depressa* leech, however, show a significant inhibition of FXIIIa. This is also true for the related species *Haementeria officinalis*, suggesting that compounds similar to tridegin can be found in various species of the *Haementeria* genus.<sup>130</sup> Since there is not much sequence information on leeches available, clear homologues in more distantly related species have not been found. Some homology can be assumed to sequence stretches from the leech *Helobdella robusta* (of which the whole genome has been sequenced) and the well-characterized thrombin inhibitor hirudin from the medicinal leech *Hirudo medicinalis*. The latter is especially similar to tridegin concerning the spacing of cysteine residues and



therefore might show structural homology to tridegin (see Figure 2.8). However, the overall identity (19.7%) and similarity (23.7%) are relatively low, therefore it cannot be said whether the sequences are truly homologous (“twilight zone”<sup>135</sup>). Alignment with two other leech-derived peptides, ornatin from *Placobdella ornata* and decorsin from *Macrobodella decora* yields similar results. Therefore, using structural information from hirudin, ornatin or decorsin to derive the tridegin structure (i.e the three dimensional fold or the disulfide bond network) is not a reliable way and other means of structure determination need to be used (see also section 5.5.1).

### 2.5.2 Potency

The activity of FXIIIa and thereby also the potency of FXIIIa inhibitors is conveniently measured *in vitro* by different assays. The earliest assays available were an amine-incorporation assay<sup>137</sup> as well as different ammonia-release assays.<sup>138,139</sup> Later on, the isopeptidase activity of FXIIIa was exploited to measure activity by the use of fluorogenic or chromogenic assays. In this case, release of a chromophore, fluorophore or quencher coupled to the glutamine residue of a FXIIIa substrate is monitored.<sup>128,140,141</sup>

The potency determined for native (i. e. leech isolated) tridegin determined by Finney *et al.* with an ammonia-release assay was given as an IC<sub>50</sub> value of approx. 9.2 nM.<sup>129</sup> They also noted that this IC<sub>50</sub> value varied with the concentration of FXIIIa in the assay and suggested a 1:1 stoichiometry of tridegin and FXIIIa.<sup>129</sup>

Since then, several other preparations of tridegin have been analyzed, but none of them from the original organism. Early investigations on tridegin produced recombinantly in *E. coli* showed IC<sub>50</sub> values of 2-4 μM,<sup>131</sup> optimization of the expression procedure (most notably periplasmic instead of cytoplasmic expression) resulted in an IC<sub>50</sub> of 20-40 nM.<sup>142</sup> Analysis of the same substance with an isopeptidase assay<sup>141</sup> resulted in IC<sub>50</sub> values of 92-200 nM.<sup>134,143</sup> Tridegin synthesized by solid-phase peptide synthesis and subsequent oxidation yielded an IC<sub>50</sub> of 300-600 nM.<sup>53,134,143</sup>

The exact reason for these deviations is not clear. They may partly be due to different preparation strategies, resulting in different post-translational modifications (in case of the native tridegin) or different disulfide bonds. Furthermore, the assay conditions may play a role as well as the method of concentration determination (Bradford assay vs. amino acid analysis). It is of interest that the values published for the leech-extracted tridegin have never been reached with any preparation since then, but without access to the native material, it is impossible to determine whether structural or methodological reasons apply.

### 2.5.3 Mutational studies

In one of the patents, Giersiefen *et al.* started to investigate which part of the tridegin sequence was most important for inhibitor function. Therefore, they split the sequence into 25 overlapping 20mer peptides and assayed the inhibitor potency of these relative to full-length tridegin (Figure 2.9A). The experiment revealed that the main inhibitory activity resides in the C-terminal part of the peptide.<sup>131</sup> They then concentrated on the most potent 20mer found and sequentially exchanged every amino acid to alanine (alanine scanning, Figure 2.9B) which resulted in a number of candidate amino acids with major influence on the inhibitor function.

Based on this data, R. Coch continued with the synthesis of longer variants containing an I50A mutation. Both a full-length variant and a C-terminal 30mer with the mutation

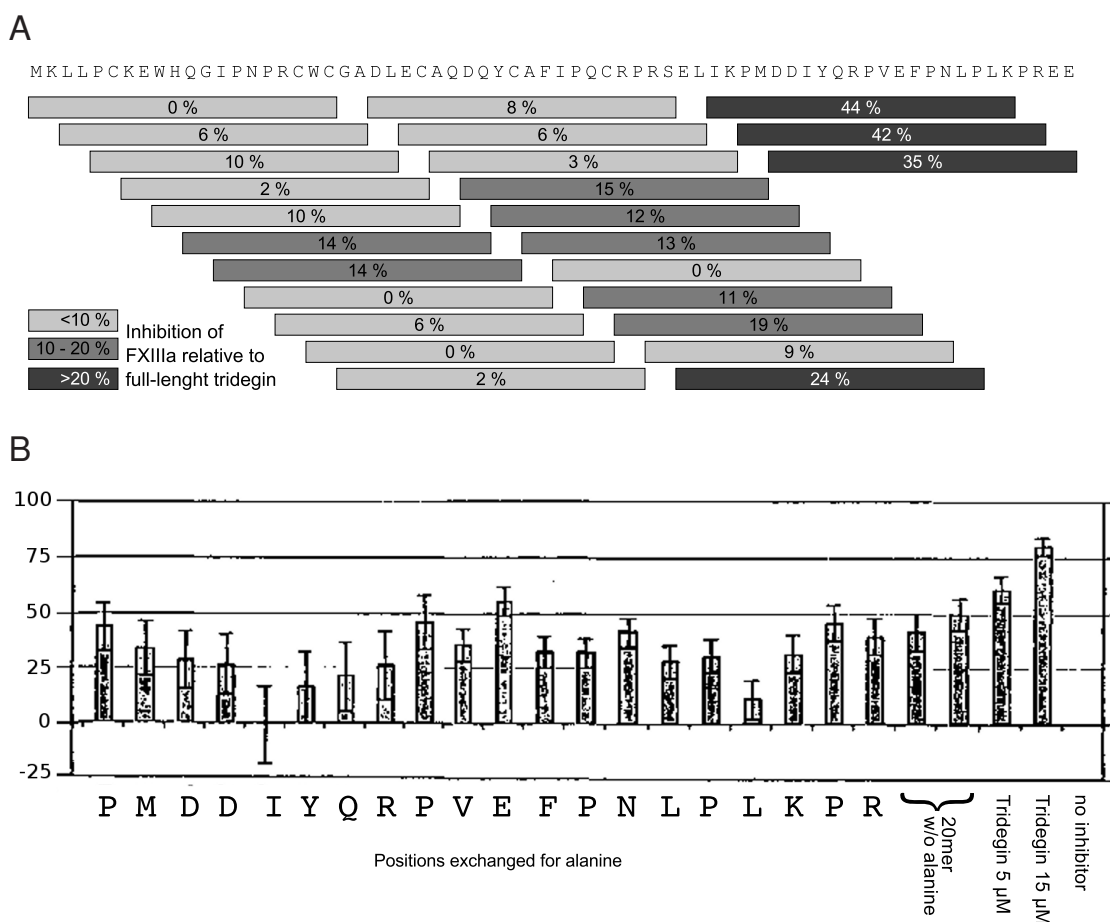


**Figure 2.9:** Early truncation and mutation studies on tridegin by Giersiefen *et al.*<sup>131</sup> A) A series of 20mer peptides from tridegin localizes the major inhibitory function in the C-terminal part of tridegin. B) Alanine scanning in the most potent 20mer pinpoints influential positions. Concentration of peptides  $\approx 7.3 \mu\text{M}$ . Modified from Giersiefen *et al.*<sup>53,131</sup>

**Table 2.4:** Effect of mutations in the sequence of tridegin or a truncated analogue on inhibitor potency<sup>53,143</sup>

Peptide	No. of amino acids	Mutation	IC <sub>50</sub> [ $\mu$ M]
Tridegin	66	none	0.48
Tridegin	66	I50A	1.12
C <sup>37</sup> -E <sup>66</sup>	30	none	1.71
C <sup>37</sup> -E <sup>66</sup>	30	I50A	13.8
C <sup>37</sup> -E <sup>66</sup>	30	I50A, L62A	68.0

showed strongly decreased inhibitor potency, confirming the importance of the I50 position for inhibitor function.<sup>143</sup> A later analysis of a 30mer with an additional L62A mutation, a position also suggested to be important by Giersiefen *et al.*, confirmed the expected decrease in potency (Table 2.4).<sup>53</sup>

## 2.6 Structural Classification of Disulfide Bonds

Disulfide bonds, i.e. the oxidative covalent linkage between two cysteine sulfur atoms, are a major structural feature in proteins and peptides. About 40% of all mammalian proteins contain disulfide bonds, the vast majority of these proteins are localized extracellularly.<sup>144,145</sup> Mostly, these disulfide bonds serve structural purposes, as they protect the protein structure in the (sometimes harsh) extracellular environment. However, in some cases these disulfides are catalytically active, as for example in thiol-disulfide oxidoreductases. More recently it has become evident that also allosteric influences of disulfide formation or reduction on protein function plays a regulatory role.<sup>145,146</sup>

A classification of the three dimensional conformation of disulfide bonds on the basis of their bond angles has first been introduced by Richardson in 1981<sup>147</sup> and has since been refined.<sup>145</sup> A basic classification can be done on the orientation of the  $\chi_2$ ,  $\chi_3$  and  $\chi_2'$  bond angles (Figure 2.10). The disulfide bonds are characterized as being either right- or left-handed depending on whether  $\chi_3$  is positive or negative, respectively. Furthermore, if  $\chi_2$ ,  $\chi_3$  and  $\chi_2'$  all have the same orientation (either positive or negative) the disulfide bond is referred to as a “spiral”, while “hook” refers to a bond where only one of the angles  $\chi_2$  and  $\chi_2'$  share the same orientation with the  $\chi_3$  angle. Finally, a disulfide bond where both  $\chi_2$  and  $\chi_2'$  have the opposite orientation compared to  $\chi_3$  are referred to as “staples”.<sup>145,147</sup> These are then abbreviated as either right hand (RH) or left hand (LH) spirals, hooks or staples. For example a right hand spiral is denoted RHSpiral. With this classification, six different disulfide bonds are possible (the disulfides are treated as symmetrical, i.e. there is only one

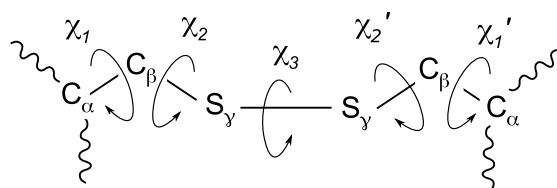


**Figure 2.10:** There are five  $\chi$ -angles of the disulfide bond. When only the orientation of these angles is taken into account (i.e. – or +) and the disulfide bond is treated as symmetrical, 20 different conformations arise. Modified from Schmidt *et al.*<sup>145</sup>

RHHook, independent on which of the two  $\chi_2$  angles is positive).

For a more detailed classification, the orientation of  $\chi_1$  and  $\chi_1'$  angles was added. In this case, a plus or minus sign indicates whether both angles are positive or negative, respectively. A  $-/+$  oder  $+/-$  indicate that  $\chi_1$  and  $\chi_1'$  have different orientations. Thus,  $-RHStaple$  would indicate a minus right handed staple, i.e. the angles for  $\chi_1$ ,  $\chi_2$ ,  $\chi_3$ ,  $\chi_2'$  and  $\chi_1'$  are  $-$ ,  $-$ ,  $+$ ,  $-$  and  $-$ . Note that there is only one possibility to form a  $+/-RHStaple$ , but there are both  $+/-RHHook$  and  $-/+RHHook$  possible. According to this, there are 20 disulfide bond configurations possible, all of which have been shown to exist in proteins.<sup>145</sup> However, not all showed the same prevalence. The  $-LHSpiral$  is the most prevalent in disulfide containing X-ray structures (24.7 %) and also has the lowest dihedral strain energy. It is therefore assumed to be the primary structural disulfide.<sup>145</sup> In contrast,  $+RHHook$ ,  $+RHStaple$  and  $+LHStaple$  showed a prevalence of  $<1\%$  in the same dataset. The conformation of disulfide bonds is also closely linked to function: while almost all catalytic disulfides are  $+/-RHHooks$ , most allosteric disulfides are  $-RHStaples$ .<sup>145</sup> When comparing the results from X-ray structures with NMR structures of the same protein, it became obvious that these are not tightly fixed conformations. Different NMR structures often showed different conformations. However, in most cases, the conformation found in X-ray structures could also be confirmed in one of the NMR structures.<sup>148</sup>

In general, although there is a lot of information available on the conformation of the peptide backbone, disulfide conformation is still not very well characterized. This is a problem especially for multiply bridged, disulfide-rich peptides, because in these the contribution of the disulfide bonds to the overall structure is extraordinarily large.



### 3 Aims of this work

This work aims at a comprehensive understanding of the natural FXIIIa inhibitor tridegin and its interaction with FXIIIa on a molecular level. Both structural and functional aspects of the enzyme-inhibitor interaction should be investigated in detail, to deepen our understanding of the biochemistry of FXIIIa and to provide the scientific community with a well characterized tool for studying the multiple functions of FXIIIa *in vitro* and *in vivo*.

To achieve this, the functional characterizations should be performed. The sequence stretch of tridegin that probably interacts with FXIIIa has been localized in the C-terminal region of the peptide.<sup>131,134</sup> However, it is known that the presence of the N-terminal part enhances inhibitor potency, but it remains unclear by what mechanism. This should be investigated in a first step. Therefore, a series of peptides lacking different parts of the N-terminal region should be synthesized and their inhibitory potency should be compared to the full length inhibitor. The N-terminal part of tridegin also harbors six cysteine residues which are, to current knowledge, fully oxidized to form three disulfide bonds. Both their function and the pattern by which they are connected are not known. Therefore, tridegin analogues lacking the disulfide bonds or the cysteine residues will be analyzed in more detail. All enzyme activity assays are to be performed in cooperation with Prof. Dr. Torsten Steinmetzer (University of Marburg).

For structural analysis, different approaches should be tested. Crystallization experiments, which have unfortunately not been successful with pure synthetic tridegin in the past, should be continued in presence of FXIII in cooperation with Dr. Manuel Than (FLI Jena). Furthermore, the disulfide connectivity of tridegin should be investigated in parallel, to learn about the number and type of disulfide-connected isomers present in the differentially produced substances. To help this aim, a smaller peptide with all cysteine residues will be synthesized and its disulfide pattern after oxidation will be evaluated. The method of choice for this task should be a detailed MS and MS/MS analysis of the peptides. From the results, a computational model of tridegin will be generated in cooperation with Dr. Arijit Biswas (University Hospital Bonn).

### *3 Aims of this work*

---

Once both functional and structural information have been gathered, these should be combined and evaluated to derive structure-activity-relationships. Based on the structural information derived from tridegin and the recently published structure of FXIIIa,<sup>149</sup> computer models of the tridegin-FXIIIa-interaction will be generated. The results are then to be compared with the experimental data.

## 4 Materials and Methods

### 4.1 Chemicals and Buffers

**Table 4.1:** Chemicals and reagents

Chemical	Supplier
<b>Solvents</b>	
Acetic acid	Roth
Acetonitrile (HPLC grade)	VWR
n-Butanol	Roth
Dichlormethane (DCM, HPLC grade)	VWR
Dimethylformamide (DMF, technical grade)	VWR
Dimethylformamide (DMF, analytical grade)	VWR
Ethyl acetate	Roth
Isopropanol (HPLC grade)	VWR
Methanol (HPLC grade)	Fisher Scientific
Phenol	FLUKA Chemika
Pyridine	Riedel-de Haën
Water (HPLC grade)	VWR
<b>Reagents for peptide synthesis</b>	
Carboxyfluorescein (5-FAM)	Novabiochem
<i>N,N</i> -Diisopropylethylamine (DIEA)	ACROS
Ethandithiole	FLUKA Chemika
<i>O</i> -benzotriazol- <i>N,N,N',N'</i> -tetramethyl-uronium-hexafluorophosphate (HBTU)	Iris Biotech GmbH
<i>N</i> -methyl-morpholine (NMM)	Aldrich
Piperidine	Sigma-Aldrich
Benzotriazol-1-yl-oxytripyrrolidinophosphonium hexafluorophosphate (PyBOP)	Novabiochem

**Table 4.1:** Chemicals and reagents (*continued*)

Chemical	Supplier
Thioanisole	FLUKA Chemika
Trifluoroacetic acid (TFA, synthesis grade)	Merck
<b>Amino acid derivatives and resins</b>	
Fmoc-Ala-OH, Fmoc-Arg(Pbf)-OH, Fmoc-Arg(Pbf)-OH, Fmoc-Asn(Trt)-OH, Fmoc-Asp(OtBu)-OH, Fmoc-Cys(Trt)-OH, Fmoc-Gln(Trt)-OH, Fmoc-Glu(OtBu)-OH, Fmoc-Gly-OH, Fmoc-His(Trt)-OH, Fmoc-Ile-OH, Fmoc-Leu-OH, Fmoc-Lys(Boc)-OH, Fmoc-Met-OH, Fmoc-Orn(Boc)-OH, Fmoc-Phe-OH, Fmoc-Pro-OH, Fmoc-Ser(tBu)-OH, Fmoc-Thr(tBu)-OH, Fmoc-Trp(Boc)-OH, Fmoc-Tyr(tBu)-OH, Fmoc-Val-OH	ORPEGEN Pharma
Fmoc rink amide AmphiSphere 40 RAM PS PEG2000, 0.28 mmol/g	Varian
TentaGel amide resin, 0.24 mmol/g	Intavis
<b>Buffer components</b>	
Ammonium sulfate ((NH <sub>4</sub> ) <sub>2</sub> SO <sub>4</sub> )	Grüssing
Calcium chloride (CaCl <sub>2</sub> )	Fluka
Dithiothreitol (DTT)	Applichem
Ethylenediaminetetraacetic acid (EDTA)	Roth
Glutathione, reduced (GSH)	Sigma-Aldrich
Glutathione, oxidized (GSSG)	Merck
Glycine	Merck
Hydrochloric acid (HCl)	Merck
Magnesium sulfate (MgSO <sub>4</sub> )	Merck
Potassium dihydrogen phosphate (KH <sub>2</sub> PO <sub>4</sub> )	Merck
Sodium chloride (NaCl)	Roth
Sodium dihydrogen phosphate (NaH <sub>2</sub> PO <sub>4</sub> )	Merck
Sodium dodecyl sulfate (SDS)	Applichem
Sodium hydrogen phosphate (Na <sub>2</sub> HPO <sub>4</sub> )	Fluka
Tricin	Applichem
Tris(hydroxymethyl)aminomethane (Tris)	Roth

**Table 4.1:** Chemicals and reagents (*continued*)

Chemical	Supplier
<b>Electrophoresis reagents</b>	
Acrylamide, Bisacrylamide	Applichem
Agarose (SeaKem™ LE)	Lonza
Ammonium persulfate (APS)	Applichem
Bromophenol blue	Fluka
Coomassie brilliant blue G-250	Applichem
GelRed	Biotium
Glutaraldehyde 25 % in water	Merck
Glycerol (water free, 99 %)	Grüssing GmbH
β-Mercaptoethanol	Applichem
Page ruler unstained, Low Range Protein Ladder	Thermo Scientific
Tetramethylethanediamine (TEMED)	VWR
<b>Amino acid analysis</b>	
Ready to use buffers A–F	ONKEN
Ready to use Reagent R	ONKEN
Sample dilution buffer (PVP)	ONKEN
<b>Proteins</b>	
Faktor XIII-A, Faktor XIII-B, FXIIIa (recombinantly produced in insect cells)	Zedira
Fibrogammin®	CSL Behring
<b>Cloning, nucleic acids and nucleic acid analysis</b>	
BioMix Red PCR master mix	Bioline
BL21 (DE3) Singles™ competent cells	Novagen
Clonables™ ligation/transformation kit	Novagen
pEN08H (Trid.)	Entelechon
pET22b(+) vector	Novagen
T7 Promoter primer	Novagen
T7 Terminator primer	Novagen
ZR plasmid Miniprep™ Classic	Zymo Research
<b>Miscellaneous</b>	
Ammonia, 25 % in water	Fluka

**Table 4.1:** Chemicals and reagents (*continued*)

Chemical	Supplier
Ampicilline	Applichem
Iodoacetamide (IAA)	Applichem
LB medium (Lennox)	Applichem
Ninhydrin	Chemapol
$\alpha$ -Cyano-4-hydroxycinnamic acid	Sigma Aldrich
Peptide Calibration Standard	Bruker
Phosphoric acid (H <sub>3</sub> PO <sub>4</sub> )	Merck
Potassium iodide	Fluka
Protein Calibration Standard I	Bruker
o-Tolidine	Serva

**Table 4.2:** Composition of buffers and media

Buffer	Composition
SDS-PAGE cathode buffer	0.1 M tricine, 0.1 M Tris, 0.1 % SDS
SDS-PAGE running buffer	236 mM glycine, 25 mM Tris, 0.1 % SDS
SDS-PAGE sample buffer (2 $\times$ )	150 mM Tris-HCl (pH 6.8), 1.2 % (w/v) SDS, 30 % glycerol, 15 % (v/v) $\beta$ -mercaptoethanol, 36 $\mu$ g/ml bromophenol blue
M9 medium	33 mM Na <sub>2</sub> HPO <sub>4</sub> , 22 mM KH <sub>2</sub> PO <sub>4</sub> , 8.55 mM NaCl, 18.7 mM NH <sub>4</sub> Cl, 2 mM MgSO <sub>4</sub> , 0.1 mM CaCl <sub>2</sub> , 0.4 % glycerol and 100 $\mu$ g/ml ampicillin
Coomassie staining solution <sup>150</sup>	0.1 % Coomassie brilliant blue G-250, 10 % ammonium sulfate, 10 % phosphoric acid, 20 % methanol

## 4.2 Peptide Synthesis and Purification

### 4.2.1 Solid-phase peptide synthesis

Solid-phase peptide synthesis (SPPS) was mainly performed at an automatic peptide synthesizer (Economy Peptide Synthesizer EPS 221, ABIMED) using an Fmoc protecting group approach. All peptides were synthesized as C-terminal amides using an Fmoc rink amide AmphiSphere resin. The peptide synthesizer was programmed to perform the following protocol (all amounts given for 100 mg resin):

1. Preparation of the resin

- 1× rinsing with DMF I (2500 µl)
- 1× rinsing with DCM (1400 µl)
- 1× rinsing with DMF I (1400 µl)
- 1× flushing with air (300 µl)
- 1× rinsing with DMF I (2500 µl)

2. Cleavage of the Fmoc protecting group

- 2× Fmoc-cleavage with 20 % piperidine in DMF (1000 µl) – 6 min
- 1× rinsing with DMF I (4000 µl)
- 1× rinsing with DMF I (1400 µl)
- 1× flushing with air (300 µl)
- 2× rinsing with DMF I (2000 µl)

3. Coupling

- mixing of reagents in separate vial: 450 µl HBTU, 125 µl NMM/DMF (1:1), 10 µl DMF II und 420 µl Fmoc-amino-acid in DMF
- 1× coupling – ca. 13 min
- mixing of reagents as above
- 1× coupling – ca. 13 min
- 1× rinsing with DMF I (3000 µl)
- 2× rinsing with DMF I (1400 µl)
- 2× rinsing with DMF I (2000 µl)

4. Final Fmoc-cleavage and rinsing of resin

- 2× Fmoc cleavage with 20 % piperidine in DMF (1000 µl) – 20 min
- 1× rinsing with DMF I (4000 µl)
- 1× rinsing with DMF I (1400 µl)
- 1× flushing with air (300 µl)
- 2× rinsing with DMF I (2000 µl)
- 4× rinsing with DCM (1400 µl)
- 2× flushing with air (4500 µl)

In cases where carboxyfluorescein coupling was required, this was done by manually after automated synthesis of the unlabeled precursor. The resin was incubated with 2 eq. 5-FAM, 4 eq. PyBOP and 4 eq. DIEA for 1 h. After washing with DMF, the coupling was repeated for maximum yield.

Cleavage of peptides from the resin was performed as follows: Per 100 mg resin, 1 ml of TFA (95 % in water) and 150  $\mu$ l “reagent K” (0.75 g phenol, 0.25 ml ethanedithiol, 0.5 ml thioanisole) were added. The mixture was then incubated on the shaker for 3 h, then filtered and precipitated in cold ether. Peptide pellets were washed three times with ether and then redissolved in a suitable solvent.

#### 4.2.2 Peptide oxidation

For the formation of disulfide bonds, the purified linear peptides were subjected to oxidative folding in buffer. The reaction mixture contained the peptide at a concentration of 0.01 mM, 1 mM oxidized glutathione and 2 mM reduced glutathione in 40 % isopropanol and 60 % buffer (0.1 M Tris-HCl, 1 mM EDTA, pH 8.7). All solvents were degassed for 15 min in an ultrasonic bath and the reaction mixture was repeatedly evacuated and flushed with argon after addition of every component. Finally, oxidative folding was performed under argon atmosphere at 4 °C for 24 h.

#### 4.2.3 Peptide purification and analysis by HPLC

Peptides were purified by high performance liquid chromatography (HPLC). Semi-preparative HPLC was performed on a LC 8A-system (SHIMADZU) equipped with an Eurospher 100 column (KNAUER, C18 reversed phase, 250 $\times$ 32 mm, 5  $\mu$ m particle size, 100 Å pore size) for amounts between 20 and 100 mg and a Vydac 218TP1022 column (C18 reversed phase, 250 $\times$ 22 mm, 10  $\mu$ m particle size, 300 Å pore size) for amounts below 20 mg. For analytical HPLC an LC 10AT-system (SHIMADZU) with a Vydac 218TP54 column (C18 reversed phase, 250 $\times$ 4.6 mm, 5  $\mu$ m particle size, 300 Å pore size) was used. All separations were done by gradient elution and UV absorption was monitored at 220 nm. For details on gradients and

**Table 4.3:** HPLC methods applied for semi-preparative and analytical separations.

Method	Flow rate	Gradient (eluent B)	Eluent A	Eluent B
<b>semi-preparative HPLC</b>				
method A	10 ml/min	10%–60% in 120 min	0.1 % TFA in water	0.1 % TFA in 90 % acetonitrile/water
method B	10 ml/min	15%–65% in 120 min		
method C	10 ml/min	20%–70% in 120 min		
<b>analytical HPLC</b>				
method D	1 ml/min	0%–60% in 60 min	0.1 % TFA in water	0.1 % TFA in acetonitrile
method E	1 ml/min	20%–60% in 40 min		



eluent, please refer to table 4.3. Peptides (see section 5.1) were purified by the following methods: **P4**, **P7** and **P18** with method A, **P2**, **P15** and **P5** with method B, **P1**, **P15** with method C. **P3** was purified on analytical scale with method E. Peptide **P6** was purified using method C before and method A after oxidation.

### 4.3 Chemical Characterization of Peptides

Peptides were analyzed for purity by analytical HPLC, TLC and/or SDS-PAGE. Analytical data is listed in table 4.4

#### 4.3.1 Mass spectrometry

Mass spectrometry was performed at either a MALDI-TOF-device (Bruker Daltonics Autoflex II) or at an LC-ESI-device (Bruker Daltonics MircoTOF-Q) coupled to a Dionex UltiMate 3000 LC system.

For MALDI measurements, the dissolved samples were mixed with an equal volume of matrix solution (7 mg/ml solution of  $\alpha$ -cyano-4-hydroxycinnamic acid in 50% acetonitrile/water with 0.1% TFA). Mixing was done either directly on the target plate or separately in advance. A total of 2  $\mu$ l was spotted on the target plate and left to dry. The instrument was calibrated prior to each series of measurements with Peptide Calibration Standard (Bruker) for smaller (400-4000 Da) or Proteins Calibration Standard I for larger (up to 30 000 Da) samples.

For ESI-measurements the samples were either directly injected into the source or pre-separated by the coupled LC device on a Macherey Nagel NUCLEOSHELL column (C18 reversed phase, 100 $\times$ 2 mm, 2.7  $\mu$ M particle size, 90 Å pore size). In this case, a solvent system of water with 0.1% acetic acid (eluent A) and acetonitrile with 0.1% acetic acid (eluent B) was used. The separation was done using a gradient of 0% eluent B to 60% eluent B in 12 min.

#### 4.3.2 Amino acid analysis

Amino acid analysis was performed to determine peptide concentration in solutions and peptide content in lyophilized powders. Peptide samples were freeze dried, dissolved in 6 N HCl and subsequently incubated at 110 °C for 24 hours to achieve total hydrolysis. The samples were afterwards dried by vacuum centrifugation at 60 °C and redissolved in an acidic sample buffer (PVP, as purchased from Orpegen). Amino acid analysis was then performed in an amino acid analyzer (LC 3000, EPPENDORF-BIOTRONIK). For concentration determination an external standard containing 200 nM of all detectable amino acids was used.

**Table 4.4:** Chemical characterization of synthesized peptides. For HPLC methods please refer to table 4.3.  $t_R$ : retention time,  $R_f$ : retardation factor TLC. PAGE gives the apparent molecular weight in SDS-PAGE. If higher charged states than  $[M+H]^+$  were detected in MS,  $[M+H]^+$  was calculated from these.

Peptide	Sequence number	Length (aa)	$t_R$ method E [min]	$R_{f,1}^a$	$R_{f,2}^a$	PAGE [kDa]	mass (calc.) [Da]	mass ( $[M+H]^+$ ) [Da]
<b>Tridegin (full length)</b>								
Tridegin linear	P1	66	22.4	0.56 system 1	0.49 system 3	7.1	7782.1 <sup>b</sup>	7783.4 <sup>b</sup>
Tridegin oxidized	P2	66	20.4	0.50 system 1	0.47 system 3	8.0	7777.0 <sup>b</sup>	7778.7 <sup>b</sup>
Tridegin dimer	P3	2×66	20.1	n.d.	n.d.	8.1 16.1 <sup>c</sup>	15554.0 <sup>b</sup>	15553.5 <sup>b</sup>
Tridegin recombinant	P4	66	21.3	n.d.	n.d.	8.4	7776.0 <sup>b</sup>	7777.1 <sup>b</sup>
Tridegin all-C-to-S	P5	66	18.9	0.01 system 1	0.05 system 2	7.4	7685.8 <sup>b</sup>	7688.3 <sup>b</sup>
<b>Shorter derivatives</b>								
K <sup>01</sup> -C <sup>37</sup> (N-terminal seg.)	P6	37	20.0	n.d.	n.d.	5.5	4255.9	4256.9
R <sup>38</sup> -E <sup>66</sup> (C-terminal seg.)	P7	29	13.7	0.01 system 1	0.09 system 2	5.1	3531.9	3532.9
A <sup>32</sup> -E <sup>66</sup>	P8	35	17.3	0.07 system 1	0.47 system 2	n.d.	4191.2 <sup>b</sup>	4192.0 <sup>b</sup>
D <sup>22</sup> -E <sup>66</sup>	P9	45	19.0	0.36 system 1	0.26 system 2	n.d.	5363.2 <sup>b</sup>	5363.4 <sup>b</sup>
C <sup>17</sup> -E <sup>66</sup>	P10	50	20.9	0.36 system 1	0.55 system 2	n.d.	5883.8 <sup>b</sup>	5884.8 <sup>b</sup>

<sup>a</sup> TLC systems: system 1: n-butanol/acetic acid/water 48:18:24, system 2: pyridine/ethyl acetate/acetic acid/water 5:5:1:3, system 3: t-butanol/ethyl acetate/acetic acid/water 1:1:1:1

<sup>b</sup> average mass

<sup>c</sup> under non-reducing conditions

n.d.: not determined .

**Table 4.4:** Chemical characterization of synthesized peptides. (*continued*)

Peptide	Sequence number	Length (aa)	t <sub>R</sub> method E [min]	R <sub>f,1</sub> <sup>a</sup>	R <sub>f,2</sub> <sup>a</sup>	PAGE [kDa]	mass (calc.) [Da]	mass ([M+H] <sup>+</sup> ) [Da]
I <sup>12</sup> -E <sup>66</sup>	P11	55	21.2	0.32 system 1	0.24 system 2	n.d.	6461.5 <sup>b</sup>	6462.6 <sup>b</sup>
E <sup>07</sup> -E <sup>66</sup>	P12	60	21.1	0.32 system 1	0.18 system 2	n.d.	7099.2 <sup>b</sup>	7099.9 <sup>b</sup>
L <sup>43</sup> -L <sup>60</sup>	P13	18	16.6	0.36 system 1	0.45 system 2	n.d.	2186.1	2191.6
L <sup>43</sup> -L <sup>60</sup> , Q52E	P14	18	17.2	0.29 system 1	0.39 system 2	n.d.	2187.1	2188.0
<b>Flourescence labeled peptides</b>								
cf-Tridegin linear	P15	66	21.3	0.50 system 1	n.d.	7.1	8140.5 <sup>b</sup>	8142.7 <sup>b</sup>
cf-Tridegin oxidized	P16	66	20.8	0.50 system 1	n.d.	7.1	8146.5 <sup>b</sup>	8149.7 <sup>b</sup>
cf-N-terminal segment	P17	37	23.0	0.54 system 1	0.62 system 2	n.d.	4617.0 <sup>b</sup>	4618.1 <sup>b</sup>
cf-C-terminal segment	P18	29	17.3	0.53 system 1	0.53 system 2	n.d.	3890.2	3892.0

<sup>a</sup> TLC systems: system 1: n-butanol/acetic acid/water 48:18:24, system 2: pyridine/ethyl acetate/acetic acid/water 5:5:1:3, system 3: t-butanol/ethyl acetate/acetic acid/water 1:1:1:1

<sup>b</sup> average mass

n.d.: not determined.

### 4.3.3 SDS-PAGE

For analysis of peptides by polyacrylamide gel electrophoresis (PAGE), resolving gels with 18 % acrylamide/bisacrylamide and 5 % crosslinking were prepared in 0.75 M Tris-HCl pH 8.4, 0.1 % SDS, 0.1 % APS, 0.05 % TEMED. Stacking gels contained 3 % acrylamide/bisacrylamide with 3.3 % crosslinking and were prepared in 0.75 M Tris-HCl pH 8.4, 0.1 % SDS, 0.1 % APS, 0.1 % TEMED. Peptide solutions were mixed with an equal volume of SDS-PAGE sample buffer and applied to the gel. The gel was allowed to run at a voltage of 45 V for 1 h and at a voltage of 100 V for another 2-3h. The gels were fixed in 5 % glutaraldehyde for 30 min, washed 3×5 min in water and prepared for staining in 45 % methanol, 10 % acetic acid at 60 °C for 30 min. Then staining was done with colloidal Coomassie staining solution overnight. Apparent molecular weights were determined with GelAnalyzer 2010a.

### 4.3.4 Ellman's assay

Ellman's assay was used to determine the concentration of free thiol groups in peptide solutions. Ellman's reagent (5,5'-dithiobis-(2-nitrobenzoic acid), DTNB) was prepared at a concentration of 1.76 mg/ml in 0.2 M sodium phosphate buffer pH 8. In a microtiter plate, 150 µl of sample or standard solution were mixed with 100 µl of Ellman's reagent. After 10 min, absorption at 410 nm was measured. For calculation of free thiol groups in solution, a standard curve was prepared using a cysteine solution at concentrations between 3 and 167 µM. The standard curve was linear in this range with  $R^2 > 0.999$ .

## 4.4 Recombinant Expression of Tridegin

### 4.4.1 Cloning strategy

The recombinant expression of tridegin in *Escherichia coli* was performed according to Arkona et al.<sup>151</sup> As there was no access to the original DNA from *Haementeria ghilianii*, a synthetic cDNA sequence was used. The cDNA, optimized for expression in *E. coli*, was purchased from Entelechon (Regensburg, Germany). This sequence already contained the MscI and BamHI restriction sites necessary for cloning into the pET22b(+) vector and was provided in a pEN08H vector (see figure 4.1A). This vector was amplified in *E. coli* NovaBlue (Novagen) cells. After purification of the vector with ZR Plasmid Miniprep Classic, the synthetic fragment was excised, purified by agarose gel electrophoresis on a 1 % agarose gel and ligated into pET22b(+) with Clonables™ ligation/transformation kit (Merck Millipore). The synthetic DNA fragment was designed in a way that ligation could be done in frame with the pelB-leader sequence present in pET22b(+) ( see figure 4.1B). The success of the ligation was confirmed

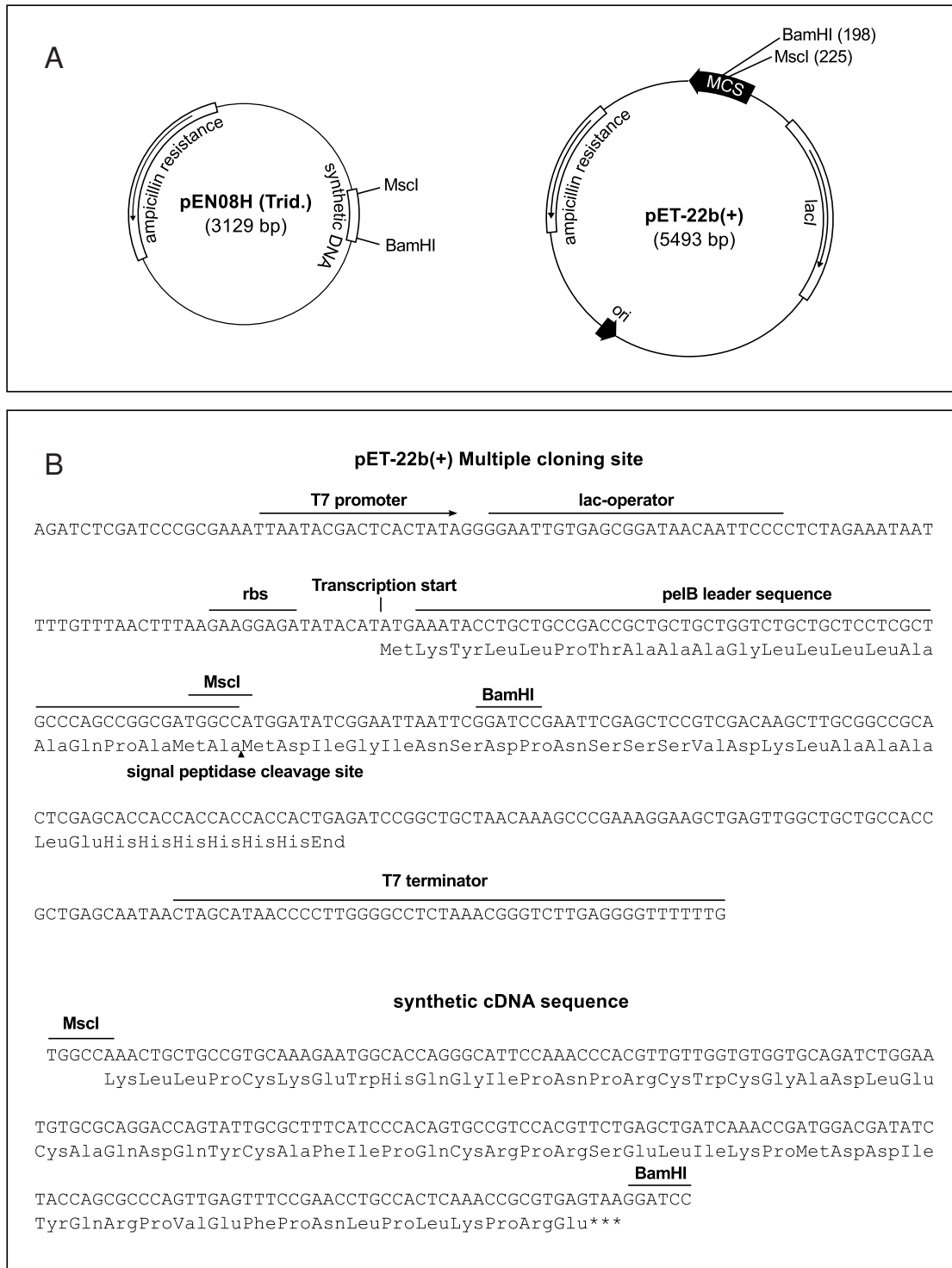


**Figure 4.1:** Cloning strategy for recombinant tridegin. A: schematic depiction of the vectors. B: Sequences of the multiple cloning site of the empty vector as well as the sequence of the synthetic cDNA. Restriction sites are indicated in both sequences.

by polymerase chain reaction (PCR), using T7 promoter and T7 terminator primers. The PCR program was as follows:

1. Initialization – 95 °C, 4 min
2. Denaturation – 95 °C, 1 min
3. Annealing – 50 °C, 1 min
4. Elongation – 72 °C, 3 min
5. Final elongation – 72 °C, 10 min
6. Hold – 4 °C

Steps 2 to 4 were repeated for 30 cycles. The reaction was performed in BioMix Red master mix and the reaction products were analyzed on a 1 % agarose gel containing GelRed for visualization. The correct sequence of the ligation site was verified by DNA sequencing (using T7 promoter primer, by GATC biotech). The sequence allows expression of a tridegin variant carrying the N-terminal pelB-leader sequence for periplasmic localization. The vector was again amplified in NovaBlue cells, purified and then transformed into competent BL21 (DE3) cells for expression.

#### 4.4.2 Growth, harvesting and purification

The bacterial starter cultures were grown over night in LB medium and then M9 medium was inoculated with the starter culture. The bacteria were allowed to grow at 37 °C until an optical density of 0.4 at 600 nm was reached. Then the culture was induced by addition of 1 mM IPTG and allowed to grow at 24 °C over night. The cells were then harvested by centrifugation. For analysis of protein in the medium fraction, 1 ml of medium was mixed with 5 ml of cold (-80 °C) acetone for precipitation of protein. After centrifugation, the pellet was redissolved in SDS-PAGE sample buffer.

Preparation of the periplasmic fraction from the cell pellet was done by a protocol adapted from the PeriPreps periplasting kit (Biozym Scientific, Germany). Per 1 g of wet cell pellet 4 ml of periplasting buffer (200 mM Tris-HCl, pH 7.5, 20 % sucrose, 1 mM EDTA and 30 U/ $\mu$ l lysozyme) were added. The suspension was incubated at room temperature for 5 min, then 6 ml of cold (4 °C) water was added to induce an osmotic shock. After 10 min on ice the mixture was centrifuged and the supernatant containing the periplasmic fraction was isolated.

All fractions were analyzed for tridegin by SDS-PAGE. As most of the peptide was found in the medium fraction, this fraction was used for purification. The medium was freeze dried and subsequently redissolved in 1/30 of the original volume in water. Insoluble particles and substances were removed by centrifugation and the clear solution was purified by HPLC method A (see table 4.3). Purity was confirmed by SDS-PAGE and analytical HPLC.

## 4.5 Functional Assays

### 4.5.1 Chromogenic enzyme activity assay

The chromogenic enzyme activity assay was performed essentially as described.<sup>141,151</sup> An aliquot of 100  $\mu$ l Fibrogammin® (6.25 U in total) was diluted with 500  $\mu$ l Tris-HCl-buffer pH 7.5 (50 mM), then 360  $\mu$ l 0.9 % (w/v) NaCl solution and 10  $\mu$ l 1 M CaCl<sub>2</sub> solution were added. Activation was started by addition of 1.42 U thrombin. After 20 min at 37 °C the reaction was stopped by the addition of 10  $\mu$ l of a 1 mg/ml hirudin solution, thereby inhibiting further thrombin activity. Measurements were performed on microtiter plates in a Labsystems iEMS Reader MF spectrophotometer. Each measurement contained 50  $\mu$ l of the enzyme solution, 50  $\mu$ l of inhibitor solution, 100  $\mu$ l Tris-HCl buffer pH 7.5 and 50  $\mu$ l of a 400  $\mu$ M substrate solution. The substrate used was H-Tyr-Glu(pNA)-Val-Lys-Val-Ile-Gly-NH<sub>2</sub>.<sup>141</sup> Absorption was measured at 405 nm for up to 1 h. For evaluation of the data, OriginPro 8 was used.

### 4.5.2 Fluorogenic enzyme activity assay

Activation of FXIII for these measurements was done as above. For measurement of enzyme activity by fluorescence, a novel fluorogenic substrate H-Tyr(3-NO<sub>2</sub>)-Glu(NH-(CH<sub>2</sub>)<sub>4</sub>-NH-Abz)-Val-Lys-Val-Ile-NH<sub>2</sub> · 3 TFA was used based on previous substrates.<sup>128</sup> In contrast to the chromogenic measurements, only 1/5 of the enzyme amount per measurement was required. Otherwise, measurements were performed as above at a substrate concentration of 20  $\mu$ M. For correct evaluation of enzyme kinetic parameters, an inner filter correction was necessary.<sup>152</sup> For this purpose, the reference fluorophor 2-Abz-NH-(CH<sub>2</sub>)<sub>4</sub>-NH<sub>2</sub> · 2 TFA was used to establish a calibration curve for the fluorescence signal at different concentrations (0.05  $\mu$ M to 20  $\mu$ M). Then, inner filter correction was performed by measuring the fluorescence of the substrate at different concentrations (1  $\mu$ M to 20  $\mu$ M) in presence and absence of the reference fluorophor. From this, a correction factor was calculated for each substrate concentration as described.<sup>128</sup> Synthesis of the substrate and fluorophor as well as the inner filter correction were done by T. Steinmetzer and K. Hardes (University of Marburg).

### 4.5.3 Microscale thermophoresis experiments

For binding studies on fluorescence labeled molecules in solution, Microscale thermophoresis (MST) can be used. The method is based on differences in thermophoretic behavior that occur when the size, hydration or charge of a molecule or complex is altered upon binding.<sup>153</sup> For these studies, carboxyfluorescein-labeled inhibitor derivatives were synthesized and incubated with varying concentrations of FXIIIa, FXIII-A and FXIII-B. The measurements were done on a Monolith NT 115 instrument from Nanotemper (Munich, Germany). A

solution of 62.5-250 nM carboxyfluorescein-labeled peptide was prepared in buffer (50 mM Tris- HCl pH 7.5, 0.9 % w/v NaCl), finally 0.1 % Tween-20 was added. A serial dilution of the unlabeled protein was performed in the same buffer (omitting Tween20) and was then mixed with an equal volume of inhibitor solution. After incubation for at least 20 min, the solutions were transferred into a glass capillary and thermophoresis was measured at a IR-laser power of 50 %. The data were evaluated using NT analysis 1.2 and OriginPro 8G.

### 4.6 Structure Elucidation

#### 4.6.1 Enzymatic digests and MS analysis

For structure elucidation, peptides were digested with chymotrypsin. Per 100  $\mu$ g peptide, 20  $\mu$ g chymotrypsin were added from a stock solution of 0.1 mg/ml chymotrypsin in 1 mM HCl. Digests were performed in slightly acidic buffer (50 mM phosphate buffer pH 6.5) to suppress disulfide shuffling. After incubation at 37 °C for 1.5 h reaction was stopped by the addition of an equal volume of 0.1 % TFA. Samples were freeze-dried and either analyzed directly by mass spectrometry or subjected to analytical HPLC separation (Method D). Samples were collected from the analytical HPLC run and freeze-dried again. All samples were analyzed on the MicroTOF Q device (see 4.3.1) before and after reduction with 10 mM DTT in 10 mM phosphate buffer pH 8.5. Both MS and MS/MS experiments (CID) have been performed. Evaluation of the MS and MS/MS data was done with BioTools (Bruker).

#### 4.6.2 Molecular modeling

Molecular modeling and docking was done by A. Biswas (University Hospital Bonn). The models of three different disulfide-linked isomers of tridegin were generated by restraining the  $\gamma$ -S atom of the cysteine residues participating in disulfide bonds at a bond length of 2 Å. The models were afterwards energy minimized and then refined by running a molecular dynamics (MD) simulation for 500 ps (YAMBER force field). Then, the three different structures with the energy minimum in the simulation trajectory were used for a blind docking to FXIII-A° (after removal of ZED1301 from the crystal structure).<sup>149</sup> Blind docking was done on a Z-Dock docking server.<sup>154</sup>



## 5 Results and Discussion

The results of this thesis are a direct continuation of a diploma thesis from 2010.<sup>53</sup> The results presented here have been published in two full articles in 2012<sup>151</sup> and 2014<sup>155</sup> and represent the major contribution to this thesis. Furthermore, part of the work described herein was published in a master thesis<sup>156</sup> recently.

### 5.1 Design of Peptides

Earlier investigations on tridegin already established the synthesis of the compound<sup>134</sup> as well as some functional<sup>53,143</sup> and structural<sup>53</sup> characteristics. These results need to be taken into account to derive compounds that would allow a more detailed exploration of the characteristics of the inhibitor.

#### 5.1.1 Potency of inhibitors from different preparations

The potency of tridegin has been studied previously *in vitro* with the help of a FXIIIa activity assay.<sup>134,143</sup> It was shown that the synthetic, fully oxidized tridegin had an IC<sub>50</sub> value between 0.3 and 0.6 μM, while a recombinant variant was substantially more potent with an IC<sub>50</sub> of approx. 0.1 μM. Different explanations for this discrepancy are possible. First, the oxidation of recombinant tridegin, which was produced in *E.coli*, is assumed to take place in the periplasm of the bacteria, to where it is exported in the expression process.<sup>142</sup> This is an environment significantly different from the oxidation buffer used in the production of synthetic tridegin, especially concerning the presence of oxidoreductases and other enzymes. Therefore, a different disulfide connectivity might result. Second, the recombinant tridegin is reported to be a disulfide-linked dimer, which might also influence potency.

To address the question, how these different potencies (including the high potency of the “native” tridegin described in the literature) arise, different tridegin variants were chosen. First, a linear, synthetic analogue **P1** was prepared, as well as the buffer-oxidized version thereof (**P2**). Moreover, as a side product of this oxidation reaction, a synthetic, dimeric variant **P3** was isolated which would allow a direct comparison of monomeric and dimeric tridegin from the same source. Additionally, the recombinant expression of tridegin **P4** was

necessary to validate the potency obtained with recombinant tridegin earlier. This results in the following sequences:

KLLPCKEWHQ GIPNPRCWCG ADLECAQDQY CAFIPQCRPR SELIKPMDDI YQRPVEFPNL PLKPRE	(P1)
oxidized version of P1	(P2)
oxidized, dimerized version of P1	(P3)
recombinant version of P1	(P4)

### 5.1.2 Influence of the N-terminal part on inhibitor function

In previous investigations it was shown that the N-terminal part (i.e. K1-Q36) did not inhibit FXIIIa at all, while the C-terminal part (C37-E66) retained about 25 % of inhibitor potency.<sup>53,134</sup> While this indicates that the major inhibitor function resides in the C-terminal part of the peptide, the reason for the approx. 4fold increase in potency in the presence of the N-terminal part is still of interest. Also, the question arises how much this is influenced by the oxidation state of the cysteine residues, which are concentrated in the N-terminal region. Therefore, besides the linear peptide P1 and the oxidized tridegin P2, a variant where all cysteine residues are exchanged for serine is needed, because this efficiently eliminates the possibility to form disulfide bonds, which might still be present in P1 due to spontaneous oxidation.

Furthermore, due to experimental reasons, the earlier studies on the isolated N- and C-terminal parts of tridegin split the peptide sequence between Q36 and C37, leaving five cysteine residues in the N-terminal part and one in the C-terminal part.<sup>134</sup> Therefore, proper disulfide formation was not possible in the N-terminal part, which might have influenced the result concerning the inhibitory actions of this part. To correct this, two more peptides with the structurally more reasonable split between C37 and R38 need to be synthesized (P6 and P7). This leaves the following additional sequences necessary to investigate the function of the N-terminal cysteine network:

KLLPSKEWHQ GIPNPRSWG ADLESAQDQY SAFIPQSRPR SELIKPMDDI YQRPVEFPNL PLKPRE	(P5)
KLLPCKEWHQ GIPNPRCWCG ADLECAQDQY CAFIPQC	(P6)
RPRSELIKPM DDIYQRPVEF PNLPLKPRE	(P7)

### 5.1.3 Potency and substrate behavior of C-terminal peptides

The potency of different sequence stretches of tridegin has previously been studied on the basis of a series of peptides derived from a C-terminal 30mer of the inhibitor (C37-E66) by sequentially shortening this peptide by two amino acids (one in the N-terminus and one in the C-terminus) down to an 8mer (D48-V55).<sup>53</sup> The rationale behind this approach was to find a minimal effective sequence around the I50 residue, that was established earlier as an important position (see section 2.5.3).<sup>143</sup> This investigation revealed that inhibitor potency did not vary much when the 30mer was shortened to a 22mer and was only slightly impaired in the 20mer and 18mer. However, further shortening the peptides resulted in significantly decreased potency and both the 10mer and the 8mer showed almost no inhibition of FXIIIa (Figure 5.1).<sup>53</sup>

Another finding came up in the course of the earlier performed investigation: all the N-terminally truncated peptides showed a progress curve in the FXIIIa activity assay that indicated that they were competing substrates rather than true inhibitors, which was not the case for tridegin. From this finding it was concluded that the only glutamine residue present in all peptides (Q52) was responsible for the substrate-like behavior of these peptides in the presence of FXIIIa and that this position might be altered by either deamidation or transamidation which then results in a non-inhibitory compound. To test this hypothesis, the Q52 position was mutated in one of the model peptides to ornithine, glutamate and alanine. All of the mutant peptides showed substantial loss of inhibitor potency, which supported the

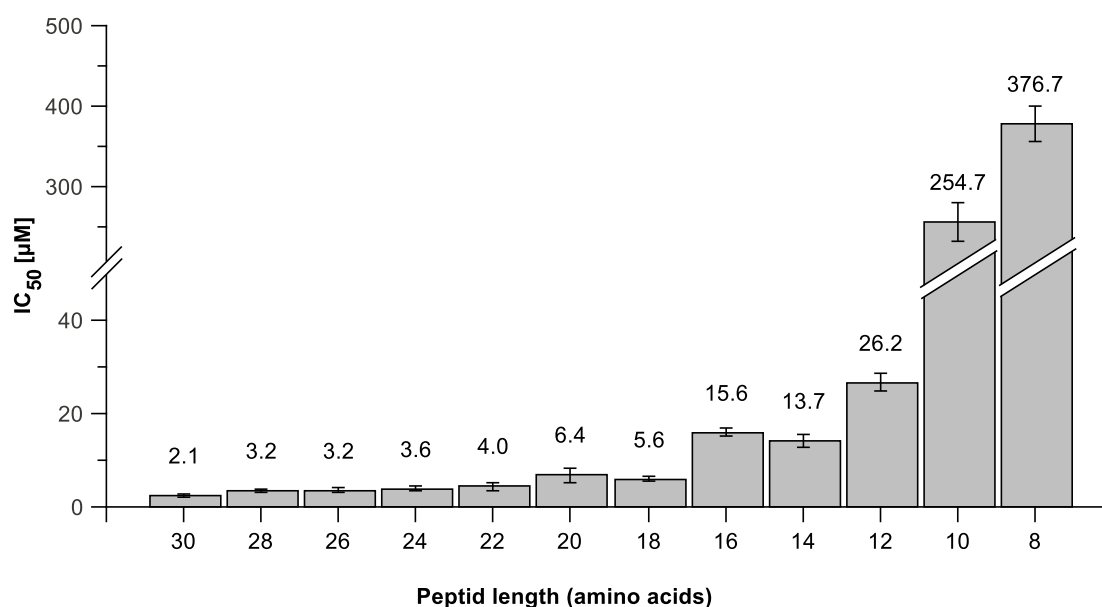


**Figure 5.1:** IC<sub>50</sub> values of peptides from the C-terminal part of tridegin. Modified from Böhm, 2010.<sup>53</sup>

theory.<sup>53</sup>

As a consequence of these findings, the question arises how long or short a sequence stretch from tridegin must be to work as a substrate or a “true” inhibitor. Therefore, longer peptides needed to be synthesized, which contain the full C-terminal region and truncated N-terminally to different extent. The shortest of these peptides is the 35mer **P8** and the longest is the 60mer **P12**. Furthermore, two short peptides of the former series<sup>53</sup> were chosen to investigate the changes that occur in the presence of FXIIIa: the 18mer **P13** and as a comparison the deamidated version **P14**. In summary, the peptides chosen for investigation of the substrate-behavior of the C-terminal tridegin sequence are:

AFIPQCRPRS ELIKPMDDIY QRPVEFPNLP LKPRE	<b>(P8)</b>
DLECAQDQYC AFIPQCRPRS ELIKPMDDIY QRPVEFPNLP LKPRE	<b>(P9)</b>
CWCGADLECA QDQYCAFIPQ CRPRSELIKP MDDIYQRPVE FPNLPLKPRE	<b>(P10)</b>
IPNPRCWCGA DLECAQDQYC AFIPQCRPRS ELIKPMDDIY QRPVEFPNLP LKPRE	<b>(P11)</b>
EWHQGIPNPR CWCGADLECA QDQYCAFIPQ CRPRSELIKP MDDIYQRPVE FPNLPLKPRE	<b>(P12)</b>
LIKPMDDIYQRPVEFPNL	<b>(P13)</b>
LIKPMDDIYERPVEFPNL	<b>(P14)</b>

#### 5.1.4 Binding affinity of tridegin analogues to FXIII

A question that has not been addressed so far is the binding affinity of tridegin or derivatives towards different variants of FXIII. Binding affinity measurements are able to detect interactions between the peptides and FXIII/FXIIIa even in the cases where no enzyme activity can be measured. This allows to answer the question, whether or not tridegin or analogues bind to inactive forms of FXIII, e.g. FXIII-A (non-activated) or FXIII-B. Furthermore, it can be analyzed, whether peptides that do not exert inhibitory action on FXIIIa still bind to the enzyme.

One binding assay capable of addressing these questions is microscale thermophoresis (MST, see section 5.3.6), which requires one binding partner to be fluorescence-labeled. As most of the peptides used here are prepared by solid-phase peptide synthesis, a labeling of the

N-terminus with carboxyfluoresceine can conveniently be performed. Therefore, fluorescence-labeled derivatives of linear and oxidized tridegin (**P1** and **P2**) as well as the isolated N- and C-terminal parts **P6** and **P7** were prepared resulting in the following analogues:

cf-KLLPCKEWHQ GIPNPRCWCG ADLECAQDQY CAFIPQCRPR SELIKPMDDI YQRPVEFPNL PLKPRE	(P15)
oxidized version of <b>P15</b>	(P16)
cf-KLLPCKEWHQ GIPNPRCWCG ADLECAQDQY CAFIPQC	(P17)
cf-RPRSELIKPM DDIYQRPVEF PNLPLKPRE	(P18)

## 5.2 Preparation of Tridegin and Derivatives

Access to native tridegin – which has originally been extracted from the salivary gland of *Haementeria ghilianii* – is very limited. Therefore, other ways of production have been applied. As already described, solid-phase peptide synthesis is a fast and reliable way of producing tridegin.<sup>134</sup> However, there is also the possibility of recombinant production.<sup>131,151</sup> Both ways to gain access to tridegin need to overcome the problem of oxidation, i.e. the formation of three disulfide bonds in the tridegin structure. As the “native” disulfide linkage of tridegin is currently unknown, both procedures were performed in a way that relied on the self-folding capabilities of the peptide.

### 5.2.1 Synthesis

**Synthesis of linear precursors** All of the analyzed peptides, with exclusion of **P4**, were prepared as linear precursors by standard solid-phase peptide synthesis. In case of the carboxyfluoresceine-labeled peptides, after coupling of the last (i.e. most N-terminal) amino acid, carboxyfluoresceine was coupled to the N-terminus. The yields for raw and purified products are given in Table 5.1.

**Peptide oxidation** The oxidation of the linear precursors – when required – was carried out in a glutathione-containing buffer, which is supposed to support folding of the peptide into its energy minimized state and formation of disulfide bonds. However, in all cases when it was applied (**P2**, **P6**, **P16** and **P17**), oxidation was not finished after 24 h. Furthermore, in case of **P6**, oxidation gave rise to multiple HPLC peaks with several of them containing fully oxidized peptide (as determined by iodoacetamide derivatization and subsequent MS analysis). As

**Table 5.1:** Yields of synthesized peptides (per 100 mg resin, loading capacity 0.28 mmol/g)

Peptide	Length (aa)	Yield raw product		Yield purified product	
		[mg]	[%]	[mg]	[%]
<b>P1</b>	66	73.4	33.7	15.2	7.0
<b>P2</b>	66	–	–	2.9	19.3 <sup>1</sup> (1.4 <sup>2</sup> )
<b>P5</b>	66	71.2	33.1	2.7	1.8
<b>P6 (reduced)</b>	37	40.3	33.8	2.4	2.0
<b>P6</b>	37	–	–	0.7	29.2 <sup>1</sup> (0.6 <sup>2</sup> )
<b>P7</b>	29	side product of <b>P18</b>		–	–
<b>P8</b>	35	41.6	35.2	12.4	10.6
<b>P9</b>	45	72.8	48.5	7.4	4.9
<b>P10</b>	50	68.0	41.3	6.4	3.8
<b>P11</b>	55	76.4	42.2	7.0	3.9
<b>P12</b>	60	82.2	41.4	5.9	2.9
<b>P13</b>	18	52.3	99.6	12.5	23.8
<b>P14</b>	18	49.5	94.3	21.8	41.5
<b>P15</b>	66	128.0	56.1	4.7	2.0
<b>P16</b>	66	–	–	0.7	14.9 <sup>1</sup> (0.3) <sup>2</sup>
<b>P17</b>	37	–	–	0.5 <sup>3</sup>	0.4 <sup>3</sup>
<b>P18</b>	29	37.0	33.9	0.9	1.7

<sup>1</sup> oxidation step only. <sup>2</sup> whole synthesis. <sup>3</sup> raw product was oxidized directly

further oxidation even in the presence of oxygen did not change the HPLC profile, it was concluded that the reaction had reached its equilibrium. Therefore, the oxidation product was again purified by HPLC to remove partly oxidized product. Due to the low amount of product after oxidation, yields could not be determined in all cases (table 5.1). Still, sufficient amounts for functional analyses were generated.

**Purification of a synthetic tridegin dimer** The chemical synthesis of the linear tridegin precursor is followed by an oxidation protocol that has already been described in detail.<sup>53,134,143</sup> It was also shown that the synthesized tridegin product after oxidation did not only contain monomeric, oxidized tridegin, but also a reduction labile dimeric form and probably some higher multimers.<sup>134</sup> The formation of these dimers occurs randomly, if oxidation is carried out in a self-folding procedure under oxidative conditions. Preferential formation of monomer is achieved by a high dilution of the peptide during this process (in this case 10  $\mu$ M) thereby kinetically disfavoring multimer formation. However, formation of these side products may still occur.

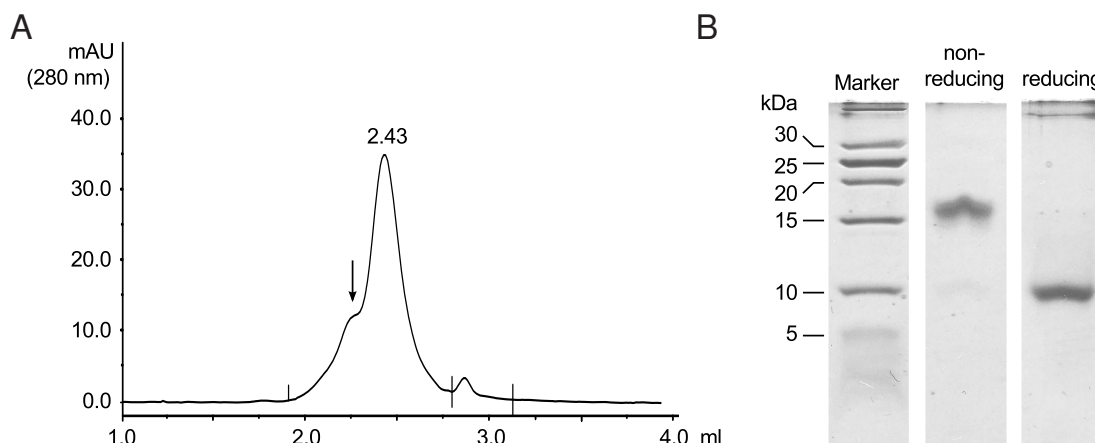


**Figure 5.2:** A) The gel filtration chromatogram shows the presence of dimeric tridegin (indicated by arrow) in the synthetic tridegin preparation. B) SDS-PAGE performed under reducing and non-reducing conditions proves that the isolated dimer is stable under denaturing conditions but labile in the presence of a reducing agent.

It has been suggested by Coch<sup>143</sup> that the dimer might have a higher inhibitory potency compared to the monomer. Therefore it was isolated from the major, monomeric product by gel filtration chromatography (Figure 5.2A). This was done in cooperation with M. Than (FLI Jena), to whom tridegin was provided for crystallization experiments and who kindly returned the dimeric side fractions after purification of the monomer. These fractions were then purified and desalted by HPLC, which resulted in a pure dimeric tridegin (**P3**) preparation. With SDS-PAGE it was shown that the dimer is indeed labile in the presence of a reducing agent ( $\beta$ -mercaptoethanol), but stable in the presence of the denaturing detergent SDS (Figure 5.2B). This indicates that the dimer is covalently cross-linked by disulfide bonds. Mass spectrometry after iodoacetamide treatment confirmed that the dimer is fully oxidized.

### 5.2.2 Recombinant expression of tridegin

The lacking knowledge of the “correct” disulfide connectivity of tridegin made it necessary to explore an alternative way of preparation, i.e. the recombinant expression of the peptide, as well. As an expression host, *E. coli* was selected. The bacterial cytoplasm does not provide a suitable oxidative environment for disulfide formation, therefore a *pelB* leader sequence was added to the N-terminus of the peptide sequence, which translocates the polypeptide chain to the periplasmic space. During this translocation, the leader sequence is removed. In the periplasmic compartment, oxidoreductases are present, which assist in disulfide formation.<sup>157</sup>

Due to the fact that there is no published DNA sequence of tridegin from *H. ghilianii*, an artificial DNA sequence was generated from the known peptide sequence and optimized

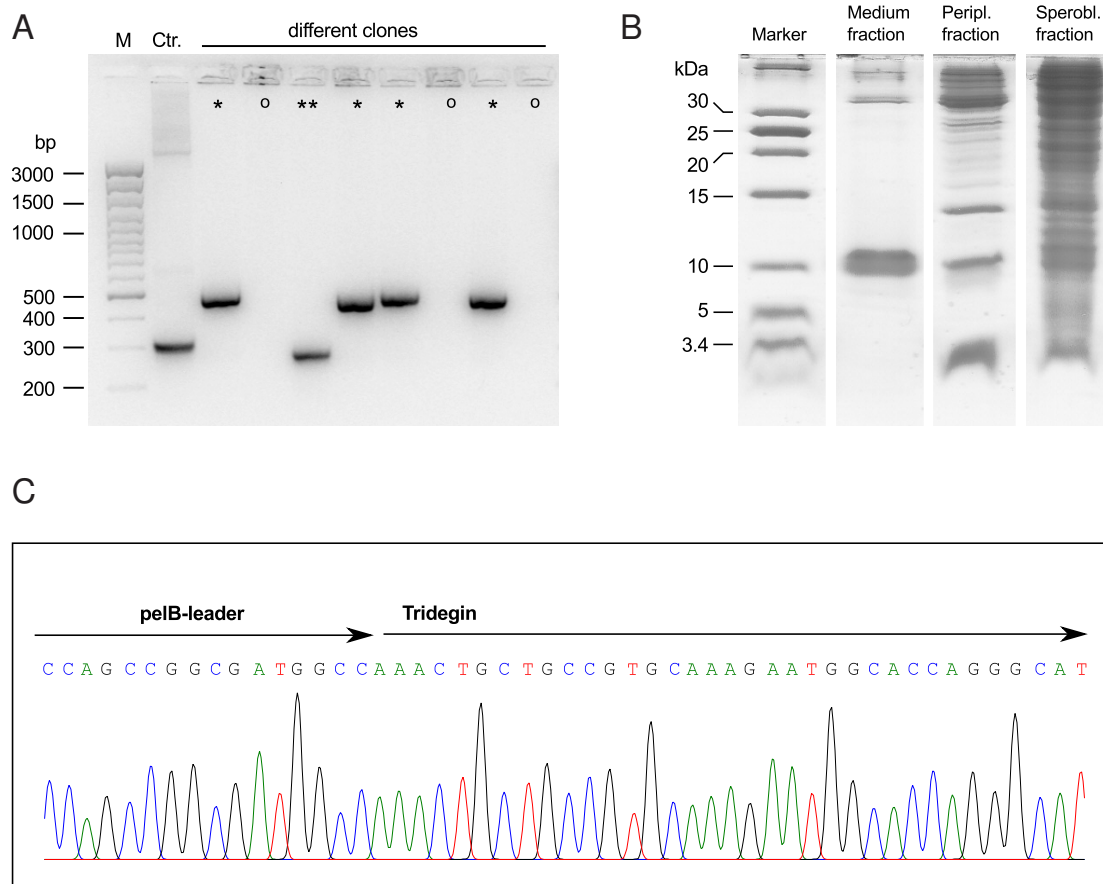


**Figure 5.3:** Recombinant expression of tridegin. A) DNA gel electrophoresis of PCR products. M: Marker, Ctr: empty vector, \* correctly ligated clones, \*\* probable re-ligation of empty vector, ° no detection of vector. B) SDS-PAGE of different fractions after tridegin expression. Tridegin (ca. 10 kDa) can be found primarily in the periplasmic and medium fractions. The prominent band at 14 kDa in the periplasmic and spheroblastic fraction is lysozyme, which was added in the purification procedure. C) DNA sequencing of the expression vector confirmed the correct ligation at the MscI ligation site.

for expression in *E. coli* (Entelechon, Germany) which was then cloned in a suitable expression vector that already contained the periplasma localization sequence (pelB leader, see section 4.4.1 for sequences). Subsequent analysis by PCR was used to identify clones that carried the correctly ligated vector and DNA sequencing revealed that in-frame ligation of the pelB leader and the tridegin sequence was indeed successful (Figure 5.3A and C). After transformation into the expression host, tridegin production was confirmed by SDS-PAGE of the medium and the periplasmic and spheroblastic fractions, showing predominantly monomeric tridegin (Figure 5.3B). The correct processing, i.e. cleavage of the pelB leader sequence upon translocation into the periplasma and the full oxidation of the product were verified by MALDI-MS of the crude extract as well.



Tridegin was expressed without a purification tag to keep the recombinant sequence identical to the synthetic variant (the only difference being the free C-terminus in the recombinant tridegin). However, this made purification more challenging. An experiment to fractionate the periplasmic extract by gel filtration chromatography and subsequent purification by HPLC revealed, that after the gel filtration procedure tridegin was isolated as a dimer. This effect was attributed to the neutral pH used for gel filtration (pH 7.0, 50 mM phosphate buffer, 150 mM NaCl), which might have allowed disulfide shuffling. Since the aim was to extract tridegin in the fold generated in the *E. coli* periplasm, this purification procedure was discarded. Instead, purification was carried out by direct HPLC of the concentrated medium fraction. This resulted in the purification of monomeric recombinant tridegin. With this protocol, approx. 300 µg of pure recombinant tridegin were isolated from 600 ml medium, which corresponds to a yield of 0.5 mg per liter culture. The recombinant peptide was used for further structural and functional investigations.

## 5.3 Functional Characterization

### 5.3.1 Substrate behavior of C-terminal peptides

It has been shown previously that isolated peptides from the C-terminal part of tridegin are substrates for FXIIIa, and that the resulting product no longer shows inhibitory potential.<sup>53</sup> It was then assumed that Gln52 is the residue responsible for this substrate behavior and that it is deamidated by FXIIIa or, in the presence of a small amine such as glycine ethyl ester (H-Gly-OEt), transamidation occurs. However, the experiment proving this was still missing and was therefore performed in the following step in cooperation with T. Steinmetzer (University of Marburg). FXIII from Fibrogammin was activated with thrombin and incubated with a short peptide stretch from the C-terminal part of tridegin (L43-L60, **P13**) in the presence and absence of H-Gly-OEt. The results were compared with a peptide variant, in which Gln52 was substituted by Glu52, i. e. the suspected reaction product (**P14**). Both peptides (**P13** and **P14**, for sequences see section 5.1.3) have been synthesized and characterized in previous works.<sup>53</sup>

The analysis revealed that **P13** is indeed modified by FXIIIa both in the presence and absence of H-Gly-OEt (Figure 5.4). Comparison of the reaction product (in absence of H-Gly-OEt) with **P14** showed similarity in retention time. Mass spectrometric analysis of the reaction products confirmed the hypothesis that **P13** can indeed be coupled to H-Gly-OEt by FXIIIa. Furthermore, analysis of HPLC peak areas after different time points showed that incorporation of H-Gly-OEt occurred much faster than deamidation of the substrate.

Interestingly, incubation of tridegin (**P2**) with FXIIIa did not result in a decreasing inhibitory

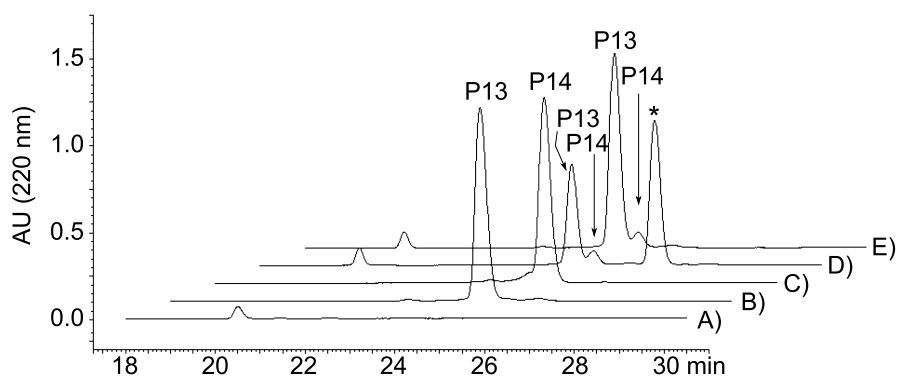


**Figure 5.4:** HPLC of FXIIIa-catalyzed modification of **P13** in the presence and absence of H-Gly-OEt. A) activated fibrogammin, B) pure **P13**, C) pure **P14**, D) incubation of **P13** with FXIIIa for 90 min in the presence and E) in absence of H-Gly-OEt. The asterisk indicates the Glu(Gly-OEt)-containing product.

potency, both in the presence and absence of H-Gly-OEt. Also, no transamidation could be detected. It was concluded that a part of the N-terminal region of tridegin did either prevent or slow down a reaction with FXIIIa or retain the inhibitory function of the de-/transamidated inhibitor. To evaluate this, a series of N-terminally truncated peptides was synthesized, ranging from 35 to 60 amino acids in length (**P8-P12**).

### 5.3.2 Evaluation of N-terminally truncated peptides

The truncated peptides **P8-P12** were synthesized as linear (reduced) peptides, because none of them contained all cysteine residues present in tridegin and therefore oxidative folding would not result in the correct disulfide connectivity. After purification, stock solutions were prepared in water at concentrations between 0.3 and 2.0 mM and the oxidation state of cysteine residues was assessed with Ellman's test. This showed that the peptides were still predominantly in reduced state (77% reduced for **P8**, 90% for **P9**, 97% for **P10**, 100% for **P11** and 95% for **P12**). All peptides were studied with the help of a chromogenic enzyme activity assay.<sup>141</sup> The shape of progression curves was evaluated to determine, whether the substrate-like behavior was similar to that of the shorter C-terminal peptides (see section 2.5). A linear progression curve indicates a constant enzyme activity and stability of the inhibitor, while a progression curve with increasing slope is explained by the turnover of the inhibitor into a species with no or lower inhibitory potency.

Surprisingly, all of the synthesized peptides showed non-linear progression curves (Figure 5.5A). Inhibition of FXIIIa was strongest in the beginning of the measurement and decreased over time. Full enzyme activity was not regained during the course of the measurements, indicating that the reaction product (probably again a deamidated variant of the

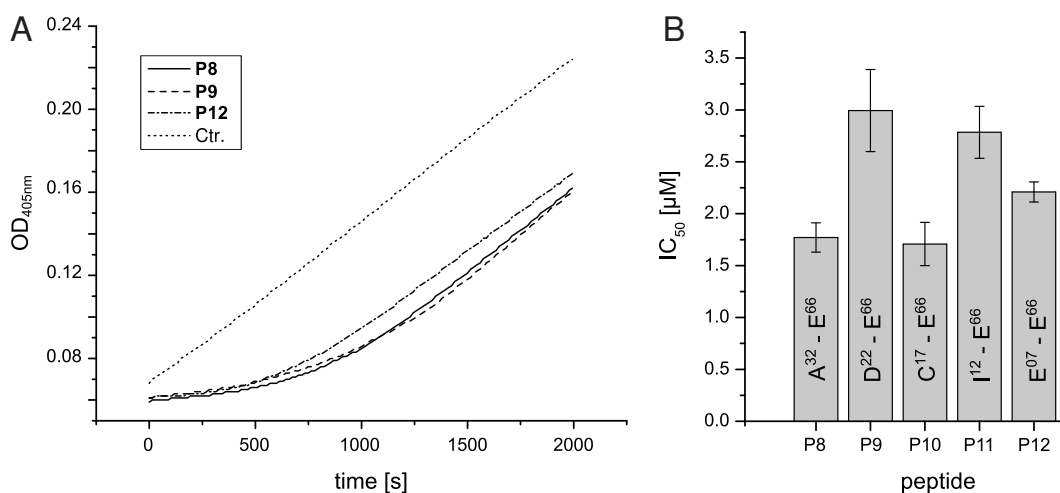


**Figure 5.5:** A) Progress curves showing enzymatic activity in the presence of some of the N-terminally truncated peptides (12.5 µM of **P8** and **P9**, 10 µM of **P12**). Ctr.: control without inhibitor. The curves show strong inhibition (i.e. substrate competition) in the beginning, but inhibition is almost completely lost later on. B) IC<sub>50</sub>-values of the N-terminally truncated peptides (determined from the initial, linear range in the progress curves).

peptides) did still retain a low inhibitory potency. Nevertheless this result was unexpected, as the aim of the experiment had been to find a “threshold” length at which a true inhibitory behavior as seen in full-length tridegin would occur. Therefore the experiment led to the conclusion that either the mentioned “threshold” length was higher than the longest peptide **P12** (60 aa) or that the observed substrate behavior did not depend primarily on peptide length, but on the three dimensional oxidized structure of the N-terminal region in full-length tridegin. Therefore, this question was addressed separately (see section 5.3.3).

Furthermore, IC<sub>50</sub> values were determined for all peptides using the linear range in the progress curves at the beginning of the measurement. The IC<sub>50</sub> values for peptides **P8** to **P12** ranged between 1.7 µM and 3.0 µM without any correlation with peptide length (Figure 5.5B). This was expected, as earlier experiments already showed that an increase in the length of the C-terminal part did not change IC<sub>50</sub> values strongly at a length higher than 24 amino acids. The IC<sub>50</sub> values of peptides **P8** to **P12** can therefore be regarded as similar and deviations can at least partially be attributed to the fact that spontaneous oxidation of the peptide might occur in the assay environment, thereby influencing the inhibitory potency in a yet unknown way.

### 5.3.3 Inhibitory potency of different tridegin variants

For further elucidation of structure-activity-relationships, different tridegin variants were analyzed by an enzyme activity assay. One question that arose from the previous investigations

on tridegin-derived N-terminally truncated peptides was, how the N-terminal part of tridegin functioned in preventing the inhibitor from being “inactivated” by FXIIIa. Therefore it was of interest, whether the mere presence of the full N-terminal sequence was sufficient to stabilize the inhibitor in the presence of FXIIIa, or whether oxidation of the cysteine residues was required. To analyze this, three tridegin variants were compared: full-length oxidized tridegin (**P2**), full-length linear tridegin (**P1**) and a full-length tridegin variant, in which all cysteine residues were exchanged for serine (**P5**) to effectively exclude any possible oxidation. Evaluation of the  $IC_{50}$ -values revealed that **P2** indeed had the highest potency ( $IC_{50}$  ca.  $0.5 \mu\text{M}$ ), while **P1** and **P5** displayed  $IC_{50}$ -values of  $1.5 \mu\text{M}$  and  $2.1 \mu\text{M}$ , respectively. The difference between **P1** and **P5** is probably not significant, especially since a slow or partial oxidation of **P1** under the assay conditions can be expected. This leaves a final 3-4-fold decrease in  $IC_{50}$  that can be attributed to the oxidative folding of the N-terminal part of the peptide. Surprisingly, peptide oxidation or the presence of cysteine residues in general did not influence the inhibitory behavior compared to full-length oxidized tridegin, i.e. no loss of inhibitory action was seen in peptides **P1**, **P2** or **P5**. Therefore it can be concluded that the oxidation of cysteine residues does increase inhibitor potency, but is not required for inhibitor stability in the presence of FXIIIa (Figure 5.6).

Moreover, the influence of the production technique (i.e. recombinant vs. synthetic) and the dimerization on the  $IC_{50}$  values of the inhibitor were analyzed. In contrast to former findings,<sup>151</sup> where recombinant tridegin was most active with an  $IC_{50}$  value of  $40 \text{ nM}$ ,<sup>142</sup> the recombinant tridegin **P4** showed an  $IC_{50}$  of about  $1.2 \mu\text{M}$ , which is twice as high as for **P2**. However, the dimeric tridegin **P3** was significantly more potent than the monomer

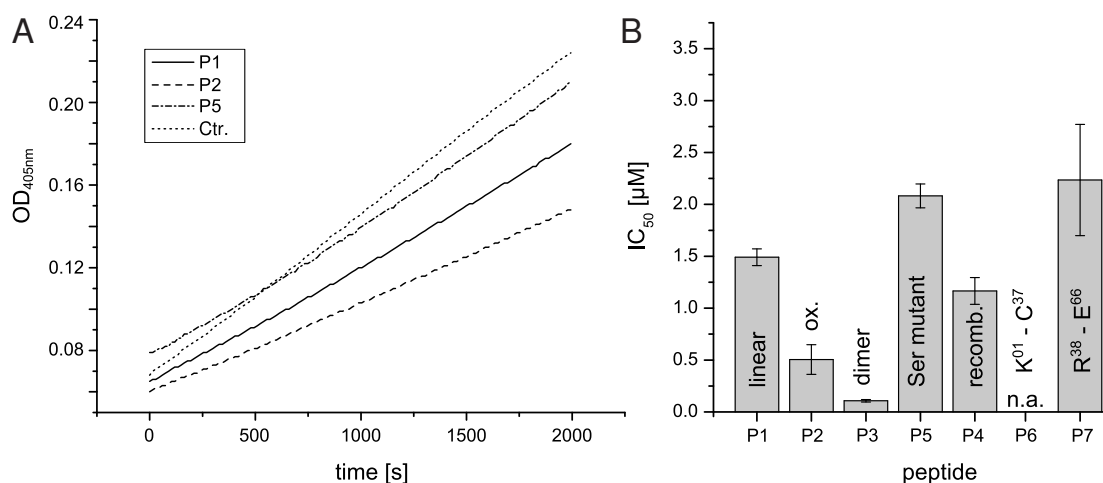


**Figure 5.6:** A) Progress curves showing enzymatic activity in the presence of selected tridegin derivatives. Ctr.: control without inhibitor. The curves are nearly linear. B)  $IC_{50}$ -values of selected peptides in comparison. n.a.: not active.

with an  $IC_{50}$ -value of  $0.11 \mu\text{M}$ . This value is calculated with the correct molecular weight of the dimer, when adjusted to “per monomer”, the  $IC_{50}$  is  $0.22 \mu\text{M}$ , which is still about twice as potent as the synthetic monomer. From these two findings it was concluded that the higher potency that was originally described for the recombinant tridegin can at least partially be attributed to the dimeric form of this earlier preparation.<sup>151</sup> The fact that it is still slightly less potent than the synthetic variant **P2** might be correlated with a different distribution of disulfide-linked isoforms in both preparations, as will be discussed in more detail in section 5.4.4. Why the potency of the dimer is higher than that of the monomer remains unclear. However, these results indicate that the dimer might be the “native” form of tridegin.

In earlier studies it was already suggested that the N-terminal part alone was not capable of inhibiting FXIIIa.<sup>151</sup> However, the variant used in this study was not oxidized since it lacked one cysteine residue (C37), which is why the experiment was repeated with the oxidized, isolated N-terminal part of tridegin (**P6**). It was shown that also the oxidized isolated N-terminal part does not inhibit FXIIIa to a measurable degree ( $IC_{50} > 50 \mu\text{M}$ ). For reasons of comparison, the corresponding C-terminal part of tridegin (**P7**), which was not part of the formerly tested peptide series, was analyzed as well and revealed an  $IC_{50}$ -value of  $2.2 \mu\text{M}$  which is in accordance with what has been found for tridegin-derived peptides of similar length and sequence (see section 2.5).<sup>53</sup>

One further tridegin derivative that was tested was a carboxyfluoresceine-labeled variant of oxidized tridegin (**P16**). This was done in preparation of binding assays, in which **P16** was to be used to assess binding to FXIIIa. The enzyme activity assay was supposed to show, whether the fluorescence label influenced inhibitory action of tridegin. Indeed the  $IC_{50}$ -value of this variant was  $5.2 \mu\text{M}$ , which is about 10-fold worse compared to the unlabeled variant. However, as the inhibitor was still working, this variant was applied for later binding studies, keeping in mind that the detected binding might be weaker than for the unlabeled **P2**.

#### 5.3.4 Assessment of a fluorogenic FXIIIa assay

In addition to the chromogenic enzyme activity assay that was used to determine all  $IC_{50}$ -values, a novel fluorogenic enzyme activity assay was tested. Therefore, a FRET (Förster resonance energy transfer) substrate was applied. It carries the fluorophore 2-aminobenzoic acid (Abz) in the glutamate side chain and the quencher 3-nitrotyrosine directly adjacent to it in the N-terminus of the following sequence: H-Tyr(3- $\text{NO}_2$ )-Glu(NH-( $\text{CH}_2$ )<sub>4</sub>-NH-Abz)-Val-Lys-Val-Ile-NH<sub>2</sub> · 3 TFA.<sup>155</sup> Upon cleavage of the Abz-glutamine-bond by FXIIIa, the fluorophore is released and separated from the quencher, resulting in increasing fluorescence. In comparison to former fluorogenic substrates, this substrate is conveniently synthesized

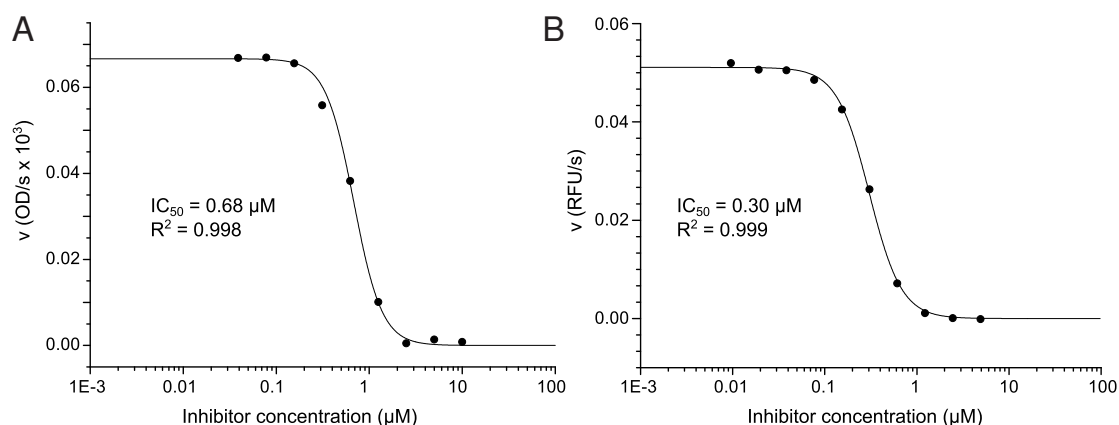


**Figure 5.7:**  $IC_{50}$  determination of tridegin with A) a chromogenic and B) a fluorogenic assay. Curves were fitted with a three parameter logistic model.

and shows a Michaelis constant  $K_m$  of  $2.5 \mu\text{M}$ , which is more than 15-fold lower than the  $K_m$  of the chromogenic substrate ( $44 \mu\text{M}$ ).<sup>141</sup>

Oxidized tridegin **P2** was analyzed with both assays in comparison and  $IC_{50}$ -values were determined as shown in Figure 5.7. The  $IC_{50}$ -value is about 2-fold lower for the fluorogenic ( $0.30 \mu\text{M}$ ) compared to the chromogenic assay ( $0.68 \mu\text{M}$ ). This is in itself not surprising, because the  $IC_{50}$  is, in contrast to  $K_i$ , strongly dependent on assay conditions. However, for the classical inhibition types (competitive, non-competitive and uncompetitive) equations have been derived that allow the calculation of  $K_i$  from  $IC_{50}$ -values using the Michaelis constant  $K_m$  and the substrate concentration  $[S]$ .<sup>158</sup> For competitive inhibition, for example, the relationship is as follows:

$$K_i = \frac{IC_{50}}{\frac{[S]}{K_m} + 1} \quad (5.1)$$

For uncompetitive inhibition, in contrast,  $K_i$  is calculated:

$$K_i = \frac{IC_{50}}{\frac{K_m}{[S]} + 1} \quad (5.2)$$

and for non-competitive inhibition:

$$K_i = IC_{50} \quad (5.3)$$

Application of these equations to calculate  $K_i$  of tridegin from both the chromogenic and the fluorogenic measurements results in the values given in Table 5.2. As can be seen from this table, for none of the classical inhibition types a similar  $K_i$  was found for both assay types, which would be expected if one of these pure inhibition types would apply to the tridegin FXIIIa interaction. This indicated that tridegin might display a mixed inhibition type.

**Table 5.2:** Calculation of  $K_i$  values for tridegin using different assays and inhibition types.

Assay	$[S]$ [ $\mu\text{M}$ ]	$K_m$ [ $\mu\text{M}$ ]	$\text{IC}_{50}$ [ $\mu\text{M}$ ]	$K_i$		
				competitive	uncompetitive	non-competitive
Chromogenic	80	44	0.68	0.24	0.44	0.68
Fluorogenic	20	2.5	0.30	0.03	0.27	0.30

### 5.3.5 Inhibition type and stoichiometry of the tridegin-FXIIIa-interaction

To further investigate the inhibition type, an analysis with different substrate concentrations was carried out with both assays. The aim of this investigation was to generate a Dixon plot that would allow to determine inhibition type and  $K_i$ . Three different substrate concentrations were tested in both assays, which were roughly  $1\times$ ,  $2\times$  and  $5\times K_m$ . The reaction velocity  $v$  was derived from the progress curves and  $1/v$  was plotted over the inhibitor concentration according to Dixon.<sup>159</sup> Unexpectedly, the resulting curves were not linear, but showed a shape similar to an exponential or potential relationship. For the FRET-substrate this is depicted in Figure 5.8A. A possible explanation for this is deviation from the 1:1 stoichiometry between enzyme and inhibitor that is usually assumed in standard inhibitory models. A model for an enzyme capable of binding two molecules of the same inhibitor in a random manner has been suggested by Segel,<sup>160</sup> and recently an example for a similar mechanism has been shown by Kovalevsky *et al.* with small-molecule inhibitors of HIV-protease (Figure 5.8D and E).<sup>161</sup> In this case, a strong cooperativity between the two inhibitor binding sites was assumed. The results reported in the study on HIV protease are similar to the findings for tridegin in that the Dixon plot is non-linear.

To test the hypothesis of an alternate stoichiometry, another graphical representation was used: the re-plotting of the slopes of Lineweaver-Burk-plots. For this, Lineweaver-Burk-plots were generated by plotting the reciprocal velocity ( $1/v$ ) versus the reciprocal substrate concentration ( $1/[S]$ ). The slope of the resulting linear curves is then again plotted versus the corresponding inhibitor concentration. In case of a 1:1 stoichiometry of enzyme and inhibitor, this re-plot is expected to be linear, while for a 1:2 stoichiometry a parabolic shape is expected.<sup>160</sup> Although the data presented is error prone, due to the low number of substrate concentrations tested, the non-linearity of the re-plot is obvious in Figure 5.8B. However, fitting of the data points to functions suggested by Segel or Kovalevsky was not successful, either due to low data quality or a possible deviation from the described models.

To analyze the correct binding stoichiometry, a Hill-plot was generated. In this case, the reaction velocity at a certain inhibitor concentration ( $v_i$ ) and the reaction velocity in absence of the inhibitor  $v_0$  are used to calculate  $\log(v_i/(v_0 - v_i))$  and to plot this value versus the

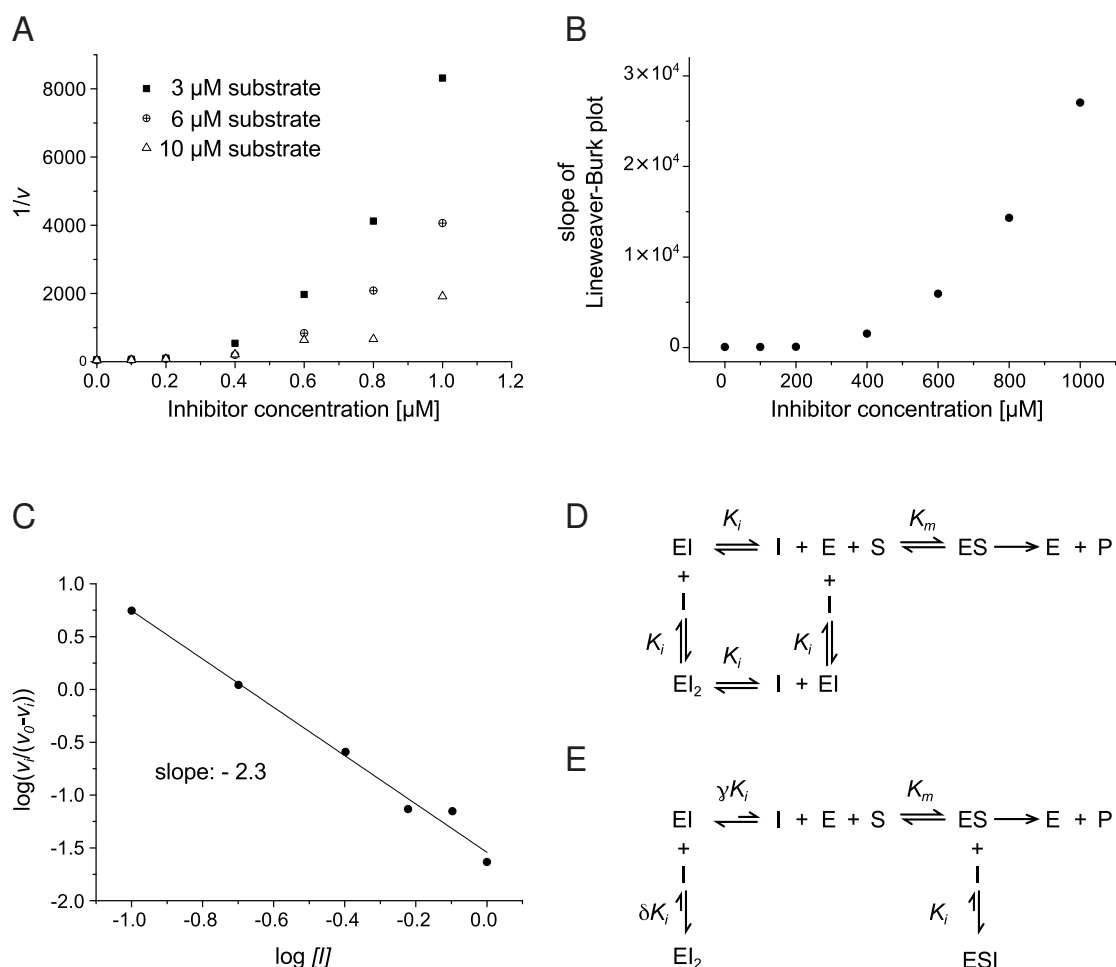


**Figure 5.8:** Analysis of FXIIIa-tridegin stoichiometry. A) Dixon plots are non-linear for all three FRET-substrate concentrations. B) Re-plotting the slope from Lineweaver-Burk plots versus the inhibitor concentration is non-linear as well, suggesting a stoichiometry different from 1:1. C) Determination of the slope in the Hill plot is used to estimate a 1:2.3 stoichiometry. D) Model with random sequence of inhibitor binding proposed by Segel (modified).<sup>160</sup> E) Inhibition model found for Darunavir inhibition of HIV protease by Kovalevsky *et al.* (modified).<sup>161</sup>

logarithm of the inhibitor concentration  $\log[I]$ . From the negative slope of the plot, the stoichiometry can be estimated. In case of oxidized tridegin **P2** a slope of 2.3 was found, which suggests a 1:2 stoichiometry between enzyme and inhibitor (Figure 5.8C).

Re-evaluation of the data for the dimeric tridegin was performed next, to test, whether the dimer **P3** shows a 1:1 stoichiometry, which was, however, not the case. Stoichiometry for the dimer was comparable to the results found for the monomer. Instead, a 1:1 stoichiometry was found for the isolated C-terminal part **P7** (Figure 5.9) as well as for the other short C-terminal derivatives tested previously (data not shown).<sup>53</sup> This indicates that the shorter



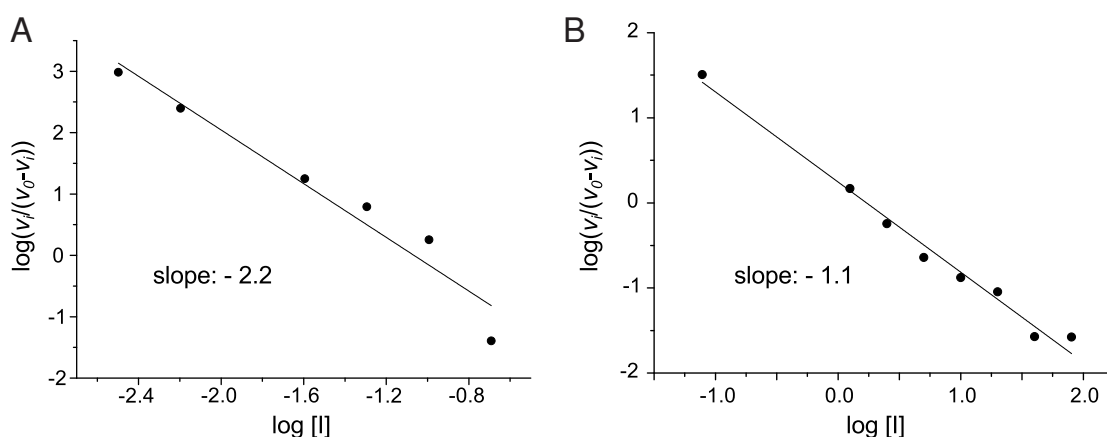


**Figure 5.9:** Hill plots of A) the dimer **P3** and B) the C-terminal peptide **P7**.

derivatives do not only show the discussed substrate behavior, but also bind to FXIIIa in a different way and stoichiometry than the full-length variants.

In conclusion, these analyses revealed that tridegin is not a “simple” competitive inhibitor, as was initially expected. In contrast, the inhibition mechanism seems to be very complex and can, with the data available, not be described with any of the standard models.

### 5.3.6 Binding studies

Binding studies were performed to show the binding affinity of different tridegin-derived peptides to FXIII. In total, four peptides (**P1**, **P2**, **P6** and **P7**) were prepared as N-terminally carboxyfluoresceine-labeled variants (**P15**, **P16**, **P17** and **P18**, respectively). Binding studies were performed by microscale thermophoresis. The labeled peptide was kept at a constant concentration and concentration of the protein was varied. In total three different forms of FXIII were tested: FXIIIa, FXIII-A (inactive) and FXIII-B. While none of the peptides bound to the inactive FXIII-A or the carrier B-subunits FXIII-B, all four showed binding to FXIIIa. For three of the peptides, **P16**, **P17** and **P18**,  $K_d$  values could be estimated from the binding curves (Figure 5.10). For **P16** and **P17**,  $K_d$  values were in the range of <100 nM, while for **P18** a  $K_d$  of  $\approx 800$  nM was found. For **P15**, no  $K_d$  value could be derived, because the binding curve did not reach saturation under given condition. As all these measurements were performed only once, one can not yet rely on the quantitative results, but the question whether binding does occur can be answered in the cases analyzed here.

While binding of oxidized tridegin **P16** to FXIIIa was expected, the strong binding of the non-inhibitory N-terminal part **P17** was surprising. In comparison, the binding affinity of the C-terminal part **P18** to FXIIIa was relatively low. However, this value might not reflect the true binding affinity, since **P18**, like the other C-terminal derivatives, probably is a substrate

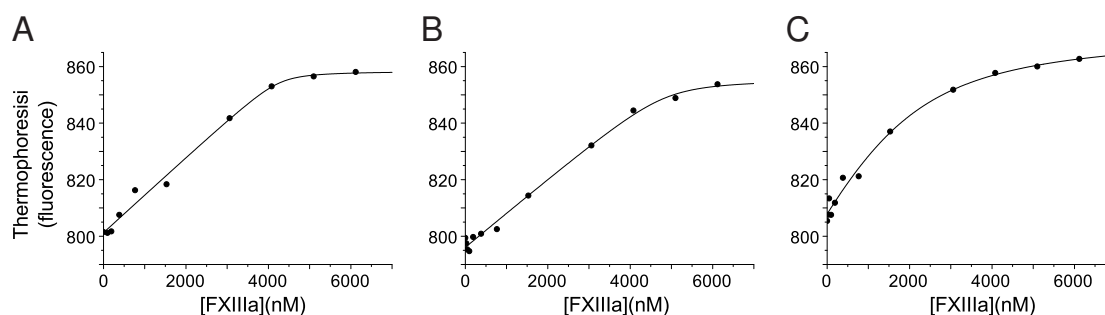


**Figure 5.10:** Binding curves from MST experiments for A) **P16** ( $K_d < 100$  nM), B) **P17** ( $K_d < 100$  nM) and C) **P18** ( $K_d \approx 800$  nM) to FXIIIa.

which is transformed rapidly in the presence of excess FXIIIa. Therefore, this value might represent the binding affinity of the corresponding Glu52 peptide. Future experiments will help to answer this question.

In general, the binding assay suggests a strong contribution of the N-terminal region to binding of tridegin to FXIIIa. However, due to limited availability of substances and equipment, experiments have been done only once and a repetition or confirmation with another binding assay is required to derive final conclusions. Anyway, these findings are highly interesting with respect to the discussion of a mixed binding/inhibition mode.

## 5.4 Structural Analysis

Elucidation of the three dimensional structure of tridegin was of major importance for structure-activity-relationship studies. Experiments with circular dichroism (CD) measurements had already been performed in earlier investigations on the tridegin structure.<sup>53</sup> This estimation of secondary structures in tridegin (Figure 5.11) predicted low percentages of  $\alpha$ -helices and  $\beta$ -sheets and a high amount of  $\beta$ -turns and unordered structures. However, CD is only a very rough method for secondary structure determination, and without detailed knowledge on the disulfide bonding of tridegin, the overall fold of the peptide cannot be determined. Therefore, methods that would give more detailed structural insights were required.

Basically, three different methods for this were considered: 2D nuclear magnetic resonance (NMR) spectroscopy, crystallization with subsequent X-ray structural analysis and elucidation of the disulfide connectivity via mass spectrometry with subsequent molecular modeling. The idea to perform NMR spectroscopy, although successful with other disulfide bridged peptides such as hirudin<sup>165</sup> and conotoxins,<sup>166</sup> was not pursued further due to two reasons: 1) tridegin tends to form aggregates at concentrations higher than 1 mg/ml and 2) the purity of the compound, especially with respect to the disulfide connectivity, was not clear, which

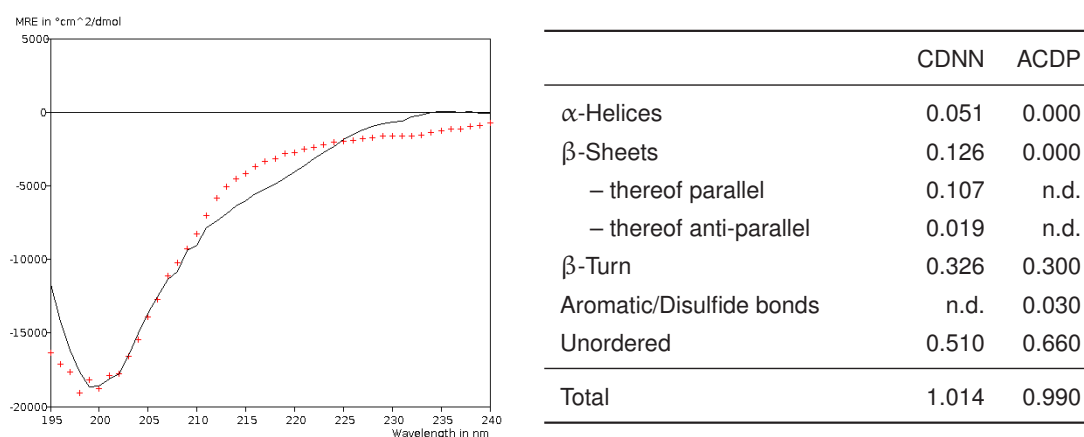


**Figure 5.11:** Left: Measured (black) and fitted (red) CD-spectrum of tridegin. Right: Results of secondary structure prediction based on CD-data. Two software packages were used: CDNN<sup>162</sup> and ACDP.<sup>163,164</sup> Modified from Böhm, 2010<sup>53</sup>

would complicate the already challenging assignment of a 66-mer peptide. Therefore, efforts were concentrated on crystallization experiments and MS analysis including subsequent modeling studies.

#### 5.4.1 Crystallization and co-crystallization experiments

Crystallization experiments were performed by Dr. M. Than (FLI Jena) and coworkers.<sup>155</sup> First, crystallization of pure tridegin was attempted. Synthetic tridegin was purified from the oxidized product and concentrated up to 1 mg/ml. Higher concentrations were not possible due to above mentioned risk of aggregation and precipitation. Approximately 300 crystallization experiments at nanoliter scale were performed and promising conditions were evaluated in subsequent finescreens. However, no peptide crystals were formed. This could be either due to insufficient purity of the peptide (e.g. the presence of different isomers) or a too flexible peptide structure.

In order to stabilize the tridegin structure and thereby help tridegin crystallize, co-crystallization with the target protein was tried. Co-crystallization of tridegin with FXIIIa had already been attempted without success and was therefore not repeated.<sup>167</sup> However, earlier reports from Arkona *et al.* suggested that tridegin also bound to inactive FXIII.<sup>142,151</sup> The binding data discussed in section 5.3.6, which does not support binding of tridegin to FXIII, was not available at the time. As crystallization of FXIII alone occurs readily and has been done several times in the past,<sup>37,40</sup> it was assumed that crystallization of a tridgin-FXIII-complex was feasible. To assess, whether tridegin and FXIII form a stable complex in solution, the molecules were analyzed both separately and in mixture by gel filtration chromatography

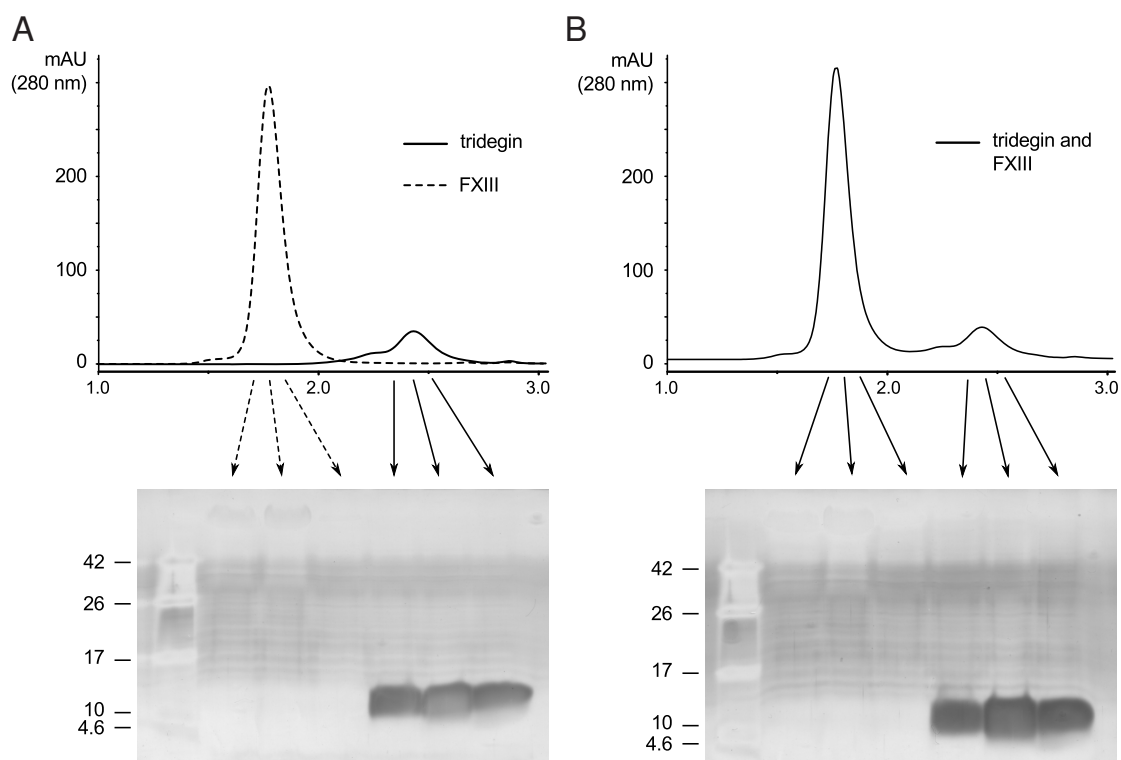


**Figure 5.12:** Gel filtration chromatogram of A) FXIII and tridegin and B) a FXIII/tridegin 1:1 mixture. Fractions were collected and analyzed by SDS-PAGE (silver stain). The higher molecular weight fractions in the mixture B did not contain tridegin, i.e. no stable complex could be isolated.

(Figure 5.12). However, the complex, if formed, was not stable enough to be isolated by this method. Therefore, co-crystallization experiments were performed at varying tridegin:FXIII ratios (between 1.3:1 and 5:1) to facilitate complex formation. Again, several thousand crystallization experiments and subsequent finescreens were performed which resulted in a variety of crystals. Analysis of these crystals revealed, however, only the presence of the already known FXIII structure with no additional electron density, indicating the absence of tridegin. The reason for the absence of co-crystals is suggested to be caused by the low binding affinity of tridegin to FXIII, which has been shown later by a binding affinity assay. Yet also other factors might be critical, such as the presence of different disulfide-linked isomers, which may also explain the contradictory findings on whether or not tridegin binds to FXIII.

### 5.4.2 Elucidation of disulfide connectivity

In parallel to the aforementioned crystallization experiments, elucidation of disulfide connectivity by mass spectrometry was performed. There are different possibilities for disulfide bridge determination via MS or MS/MS including partial reduction and alkylation,<sup>168</sup> enzymatic digest and subsequent MS(/MS) analysis<sup>169</sup> as well as direct MS<sup>n</sup> fragmentation.<sup>170</sup> For elucidation of the disulfide connectivity in tridegin, an enzymatic digest protocol was chosen.<sup>169</sup> Analysis of possible cleavage sites in the tridegin sequence revealed that chymotrypsin was the most suitable enzyme for this purpose. Chymotrypsin cleaves C-terminal of aromatic residues (tryptophane, phenylalanine and tyrosine) as well as methionine and leucine. This means that in between two cysteine residues of the tridegin sequence there is at least one possible cleavage site (Figure 5.13). The enzymatic digest protocol was then optimized using linear tridegin (**P1**). Samples were taken at different time points during incubation at 37 °C and analyzed by HPLC, MS and MS/MS. An incubation time of 1.5 h was then selected, which yielded a low number of unspecific cleavages and showed some incompletely digested fragments that might be useful for structure elucidation. The digest was then repeated with oxidized full-length tridegin (**P2**) and analyzed by HPLC, both before and after reduction with DTT (Figure 5.13). The oxidized tridegin digest should, after reduction, show the same fragments as the linear tridegin digest, if all digestion sites have a similar accessibility in both oxidized and reduced state (Figure 5.13B and C). Although there are some differences in the HPLC profile of both samples, the overall pattern is similar, which shows that the digest is not significantly impaired in the oxidized peptide. However, differences between these samples and the oxidized digest (Figure 5.13A) are obvious. Therefore it was concluded that chymotryptic digest of the oxidized peptide was a suitable way to prepare disulfide-linked fragments.

To reduce complexity of the digest, fractions were collected from the HPLC analysis, concentrated by lyophilization and subjected to ESI-MS analysis both before and after reduction with DTT. By comparing the MS spectra, mass peaks that were present in the non-reduced and absent in the reduced samples were identified. These were the potential disulfide-containing fragments. When analyzing the corresponding reduced sample, one could find either a 2 Da heavier mass peak in case of a disulfide bond within one fragment, or two new mass peaks corresponding to two fragments that were originally linked by a disulfide bond (Figure 5.14). As can be seen, unspecific cleavage was also detected, especially after arginine residues. The reason for this is not known, however, a contamination of the chymotrypsin with trypsin is suspected. Figure 5.14B shows that the tridegin sequence has been covered completely by this approach.

To ensure a correct assignment of the fragments and resolve remaining ambiguities,

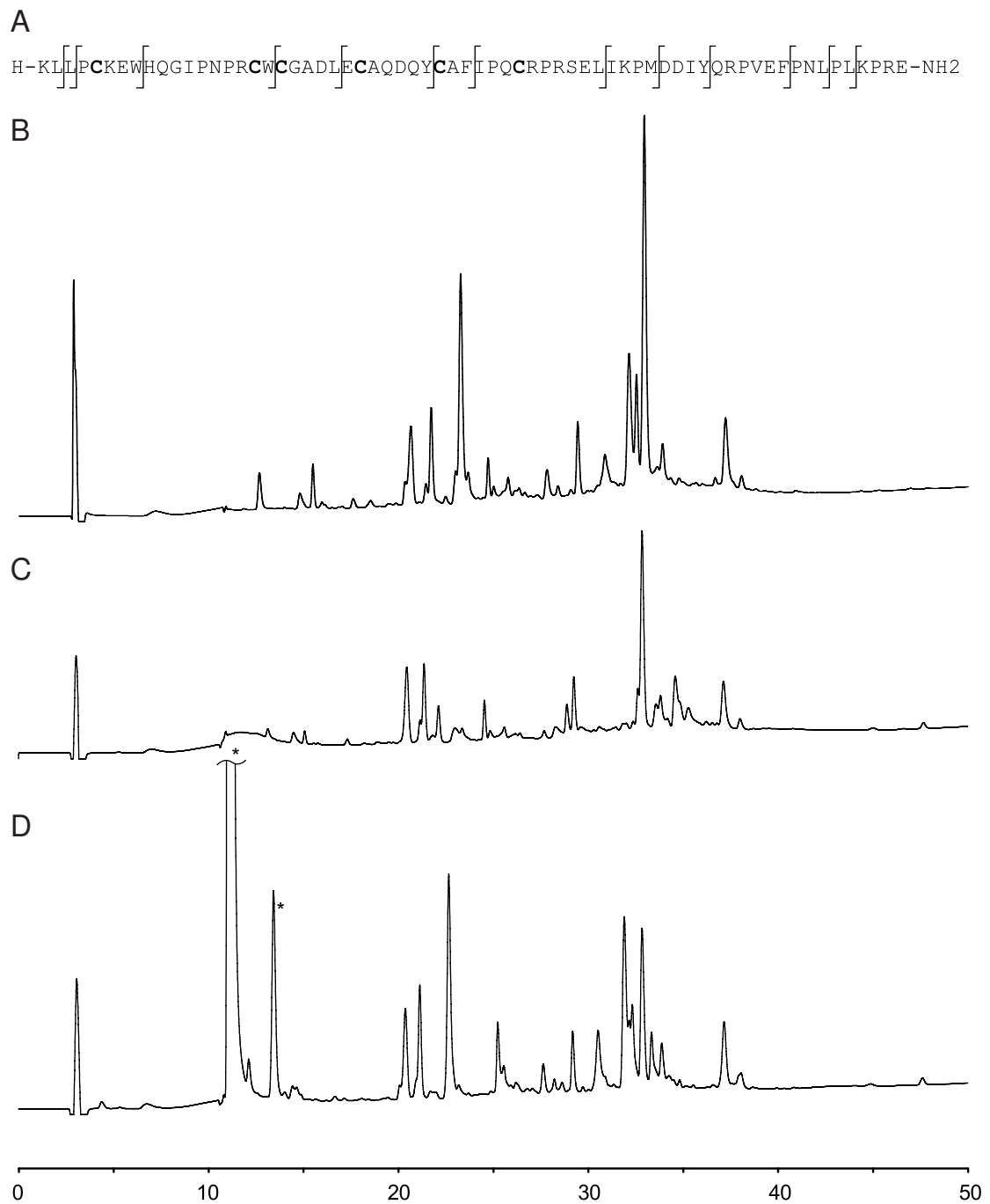


**Figure 5.13:** A) Cleavage sites for chymotrypsin in tridegin. B-D) HPLC traces (method D) of chymotryptic digest of B) linear tridegin **P1**, C) oxidized tridegin **P2** and D) oxidized tridegin **P2** and reduction of digest with DTT. \*DTT.

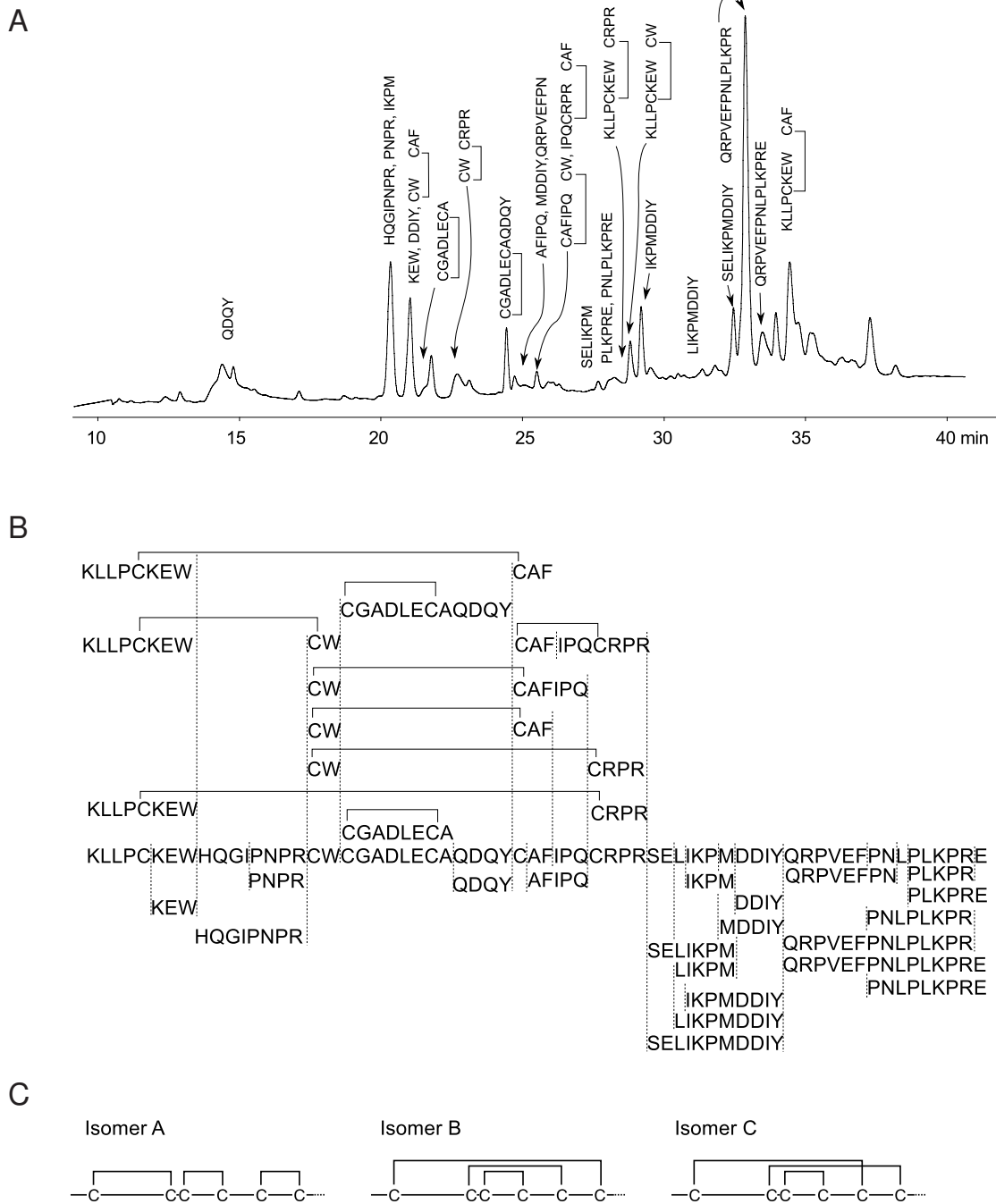


**Figure 5.14:** Analysis of the chymotryptic digest of oxidized tridegin **P2**. A) HPLC trace (method D) of **P2** digest with identified fragments. B) All detected fragments for **P2**. Cysteine containing fragments are indicated above, cysteine-free fragments below the full-length sequence. C) Concluded isomers.

fragments were analyzed in more detail by collision-induced dissociation (CID) MS/MS. One of these ambiguities is exemplified in Figure 5.15: The potential oxidized fragment C<sup>19</sup>GADLEC<sup>25</sup>A has a calculated [M+H]<sup>+</sup> ion mass of 779.270 Da, whereas oxidized C<sup>31</sup>AFI-PQC<sup>37</sup> has an [M+H]<sup>+</sup> ion mass of 779.322 Da. An ion mass of 779.270 was detected, however, the theoretical mass difference of 0.052 Da is too low to be distinguished with sufficient certainty. Both possible peptides show a mass increase of 2 Da when reduced, which does not allow differentiation just by analyzing reduced samples. Therefore, fragmentation patterns of both the oxidized and reduced species were analyzed. The fragmentation of the oxidized species did yield very few fragments, only one C-terminal alanine could be identified (Figure 5.15B). This is a well-known behavior of oxidized peptides in CID: the ion series stops at an oxidized cysteine residue.<sup>171</sup> To gain a more informative CID spectrum, the measurement was repeated with the reduced sample and, as expected, showed a clear ion series covering almost the full peptide (Figure 5.15D). From the data it was concluded that C<sup>19</sup>GADLEC<sup>25</sup>A was the correct assignment. In general, CID spectra were evaluated for all disulfide-containing fragments to ascertain the assignments.

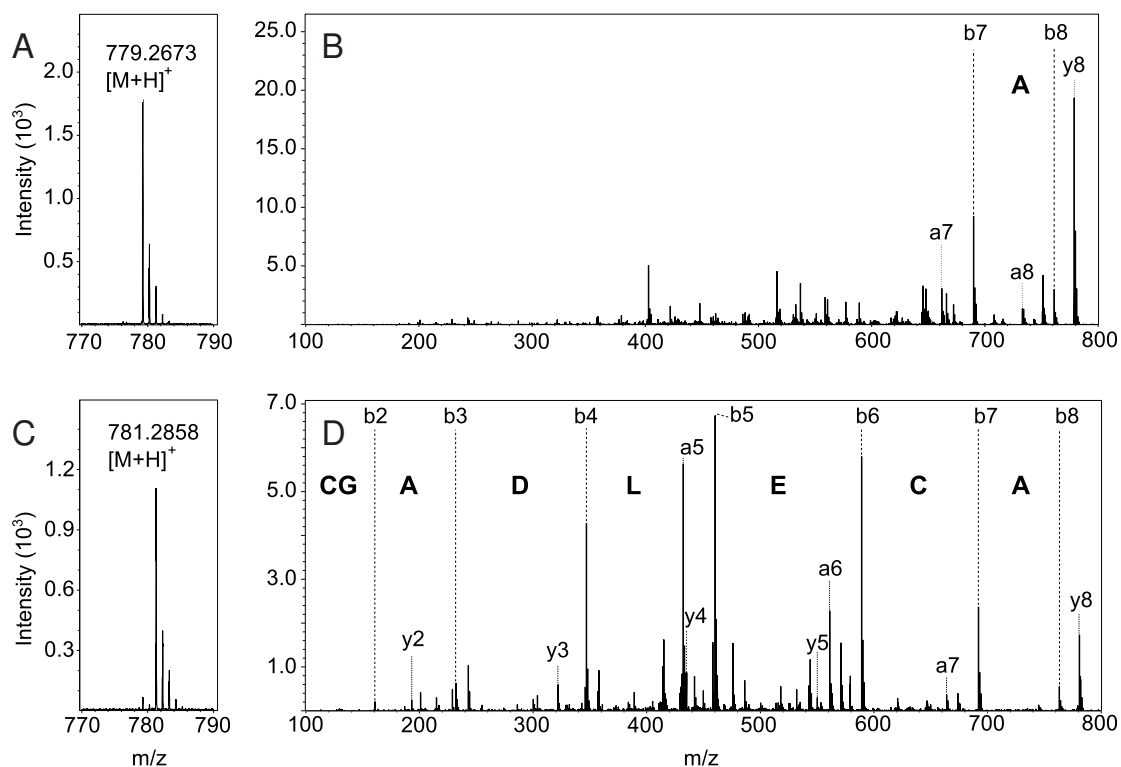


**Figure 5.15:** Detailed analysis of a disulfide-containing fragment by CID. A) mass spectrum of a disulfide-containing fragment. B) CID fragment spectrum of the same peak. C) Mass spectrum of the same fraction after reduction with DTT. D) CID fragment spectrum of the reduced fragment.



**Table 5.3:** Disulfide-connected fragments identified by mass spectrometry.

Fragment	full-length tridegin <b>P2</b>		N-terminal part <b>P6</b>		Connection	Isomer
	[M+H] <sup>+</sup> expected	[M+H] <sup>+</sup> found <sup>a</sup>	[M+H] expected	[M+H] <sup>+</sup> found <sup>a</sup>		
<u>KLLPC<sup>5</sup>KEW</u> C <sup>17</sup> W	1321.644	1321.628	1321.644	1321.637	C5-C17	A
LPC <sup>5</sup> K C <sup>17</sup> W	765.342	–	765.342	765.321	C5-C17	A
<u>KLLPC<sup>5</sup>KEW</u> C <sup>31</sup> AF	1353.670	1353.673	1353.670	1353.659	C5-C31	C
LPC <sup>5</sup> K C <sup>31</sup> AF	797.368	–	797.368	797.341	C5-C31	C
<u>KLLPC<sup>5</sup>KEW</u> C <sup>37</sup> RPR	1544.819	1544.817	–	–	C5-C37	B
<u>KLLPC<sup>5</sup>KEW</u> IPQC <sup>37</sup>	–	–	1472.775	1472.812	C5-C37	B
C <sup>17</sup> W C <sup>31</sup> AF	645.217	645.203	645.217	645.204	C17-C31	B
C <sup>17</sup> W C <sup>31</sup> AFIPQ	983.412	983.399	983.412	–	C17-C31	B
C <sup>17</sup> W C <sup>37</sup> RPR	836.366	836.362	–	–	C17-C37	C
C <sup>17</sup> W IPQC <sup>37</sup>	–	–	764.322	764.322	C17-C37	C
C <sup>31</sup> AF IPQC <sup>37</sup> RPR	1206.588	1206.589	–	–	C31-C37	A
C <sup>31</sup> AF IPQC <sup>37</sup>	–	–	796.351	796.338	C31-C37 <sup>b</sup>	A
C <sup>31</sup> AFIPQC <sup>37</sup>	–	–	778.351	778.337	C31-C37 <sup>b</sup>	A
C <sup>19</sup> GADLEC <sup>25</sup> A	779.270	779.270	779.270	–	C19-C25	A,B,C
C <sup>19</sup> GADLEC <sup>25</sup> AQDQY	1313.482	1313.480	1313.482	1313.464	C19-C25	A,B,C

<sup>a</sup> if detected in a higher charged state, [M+H]<sup>+</sup> was calculated. <sup>b</sup> In case of **P6**, C37 is the amidated C-terminus of the peptide.

The approach was repeated in a similar manner with the isolated N-terminal region (**P6**) of tridegin. Due to a lower complexity of this peptide, the pre-separation of the digest on HPLC could be omitted and the digest was directly analyzed by LC-ESI MS. The resulting disulfide-connected fragments for full-length tridegin **P2** and the N-terminal variant **P6** are shown in Table 5.3.

In total, three different isomers could be identified in both the oxidized tridegin **P2** and the N-terminal part **P6**: isomer A with a connectivity of C5-C17, C19-C25 and C31-C37, isomer B with C5-C37, C17-C31 and C19-C25 and isomer C with C5-C31, C17-C37 and C19-C25. Remarkably, all three isomers contain the C19-C25 bridge, and, at the same time, all three possible isomers containing this bridge are present. It is noteworthy that both, **P2** and **P6**, showed the same disulfide connectivities, which indicates that the presence of the C-terminal part of tridegin does not greatly influence the folding process. Furthermore, the fact that three different disulfide-connected isomers were formed indicates that the primary sequence of tridegin does not drive the folding process under the given conditions into a

single, energy-minimized folded state. This can be either due to the folding conditions applied (i.e. oxidative self-folding in buffer in the presence of GSSG and GSH, without any protein disulfide isomerase or chaperones) or it could be an intrinsic property of the peptide. Whether or not different disulfide-linked isomers of peptides may occur in nature is not yet fully understood.

However, the presence of small amounts of dimeric tridegin in the synthetic product (section 5.2.1) could also indicate that the monomeric form is not the most stable or “native” one, which would explain the presence of different isomers in this case. Elucidation of the structure of dimeric tridegin might help to answer this question and thus represents an interesting future task.

### 5.4.3 Side-product formation during oxidation of disulfide-linked tridegin analogues

After 24 h of oxidation in buffer, there was still some partially oxidized **P6** left, which did not reach full oxidation even in the presence of air oxygen. This side product had two free thiol groups, as could be identified by iodoacetamide derivatization and subsequent MS analysis. To analyze the stable side product further, MS/MS analysis was carried out on the iodoacetamide-derivatized and subsequently reduced product. CID fragmentation of this product allowed the localization of the alkylated cysteine residues (Figure 5.16). These were found to be C19 and C37. Interestingly, C19 is in all of the fully oxidized species part of the C19-C25 bridge. In case of this by-product, C25 forms a disulfide bridge with C5, C17 or

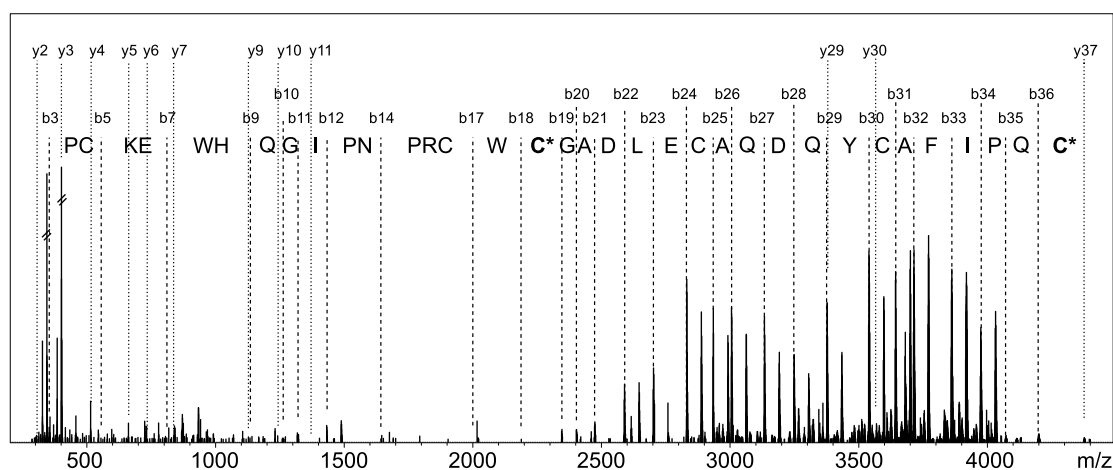


**Figure 5.16:** CID fragmentation pattern of alkylated and reduced side product occurring after **P6** oxidation. The b-ion series is indicated by dashed lines, the y-ion series by dotted lines. C\* denotes alkylated cysteine residues. Some unassigned peaks hint on at least one other partly oxidized species present. However, the assignment given here was the best fit for this spectrum.

C31, which seems to result in an irreversibly misfolded state in which C19 is not able to form a bond to the remaining C37.

Incompletely oxidized species have also been found in tridegin **P2** after oxidation, but due to the higher complexity of this peptide, detailed analysis was not accomplished. Nevertheless, one can assume that a similar misfolding may occur in **P2**.

#### 5.4.4 Disulfide connectivity of recombinant tridegin

The disulfide connectivity of recombinant tridegin was assessed as well. In this case, a pre-separation of the digest was not performed, but the digest was directly analyzed by LC-MS. Evaluation of the data was done in a semi-automated fashion, in which the digest of all 15 isomers were simulated with Bruker BioTools software and then compared to the generated data. The automatic evaluation was then manually reviewed and assignments with >50 ppm mass deviation were removed.

A full sequence coverage could only be shown for isomer B, as well as the two other possible isomers containing the C5-C37 link. However, the fragments supporting these two isomers do also fit for isomer B, i.e. they are not unambiguous, while there is one fragment (C<sup>19</sup>GADLEC<sup>25</sup>AQDQY, oxidized) that unambiguously supports isomer B (Table 5.4). Isomers A and C also give relatively high sequence coverage, but not all disulfide bonds could be confirmed by peptide fragments. It was therefore concluded that the data only supports the presence of isomer B.

**Table 5.4:** Sequence coverage for all 15 isomers in recombinant tridegin digest. In the overview, gray bars show an assigned peptide, red boxes indicate confirmation by MS/MS.

Isomer	% coverage by		Overview
	MS	MS/MS	
C5-C17,C19-C25,C31-C37 (A)	97.0	78.8	
C5-C17,C19-C31,C31-C37	68.2	50.0	
C5-C17,C31-C37,C25-C31	86.4	68.2	
C5-C19,C17-C25,C31-C37	81.8	63.6	
C5-C19,C17-C31,C25-C37	71.2	53.0	
C5-C19,C17-C37,C25-C31	68.2	50.0	
C5-C25,C17-C19,C31-C37	81.8	63.6	
C5-C25,C17-C31,C19-C37	89.4	72.7	
C5-C25,C17-C37,C19-C31	68.2	50.0	
C5-C31,C17-C19,C25-C37	71.2	65.2	
C5-C31,C17-C25,C19-C37 (C)	89.4	83.3	
C5-C31,C17-C37,C19-C25	86.4	45.5	
C5-C37,C17-C19,C25-C31	100	93.9	
C5-C37,C17-C25,C19-C31	100	93.9	
C5-C37,C17-C31,C19-C25 (B)	100	93.9	

## 5.5 Molecular Modeling of Tridegin

Molecular modeling of all three isomers of **P2** was performed by Dr. A. Biswas (University Hospital Bonn) using Yasara (Figure 5.17).<sup>173</sup> All three isomers show primarily flexible loops,  $\beta$ - and  $\gamma$ -turns as well as 3-4 helices (between 32 % and 41 % in total). The helix content is somewhat higher than predicted from former CD spectra (5 %).<sup>53</sup> Interestingly, the helices between residues 5-8, 24-27 and 41-50 are present in all three isomers, which suggests that these helices form the core structural fold of the peptide (Figure 5.18). Helices have already been predicted (without prior knowledge of cysteine connectivity) for the residues 6-9 and 47-51 using PSIPRED.<sup>53,174</sup> Apart from this similarity, however, the different disulfide connectivities in the isomers result in three different overall structures, which cannot be superposed.

Besides the secondary structure of the peptide backbone, the conformation of the disulfide bonds is also of major interest. They can be classified according to Schmidt (see section 2.6).<sup>145</sup> Table 5.5 reflects this classification. The C19-C25 disulfide bond that is present in all three isomers, shows the same +/-LHHook conformation in all the models. Furthermore, isomers A and B each contain one bridge with a -RHStaple conformation, which has been described as allosteric disulfide bond conformation that can induce functional changes in a protein when cleaved or oxidized. They also tend to have a high potential energy. This might indicate that these disulfide bonds are of importance for the structural stability of tridegin.

**Table 5.5:** Configuration of disulfide bonds in computational models of tridegin. The  $\chi$ -angles were derived from PDBsum,<sup>172</sup> classification was performed according to Schmidt *et al.*<sup>145</sup>

Disulfide bridge	Configuration	$\chi_1$	$\chi_2$	$\chi_3$	$\chi'_2$	$\chi'_1$
<b>Isomer A</b>						
Cys5 – Cys17	-RHStaple	-137.6	-67.4	162.4	-85.2	-156.7
Cys19 – Cys25	+/-LHHook	-68.4	-71.6	-164.2	68.6	22.9
Cys31 – Cys37	-/+RHHook	69.8	113.4	97.2	-77.9	-63.1
<b>Isomer B</b>						
Cys5 – Cys37	+/-LHSpiral	167.6	-96	-60.3	-177.4	-163.4
Cys17 – Cys31	-RHStaple	-160.9	-5.2	163.9	-49.1	-48.1
Cys19 – Cys25	+/-LHHook	-46.4	-48.7	-144.7	74.3	61.7
<b>Isomer C</b>						
Cys5 – Cys31	-RHHook	-74.2	-92.7	137.8	40.1	-176
Cys17 – Cys37	-/+LHHook	23.1	109.7	-82.5	-32	-55.8
Cys19 – Cys25	+/-LHHook	67.8	-139.9	-103.4	73.3	-83.6

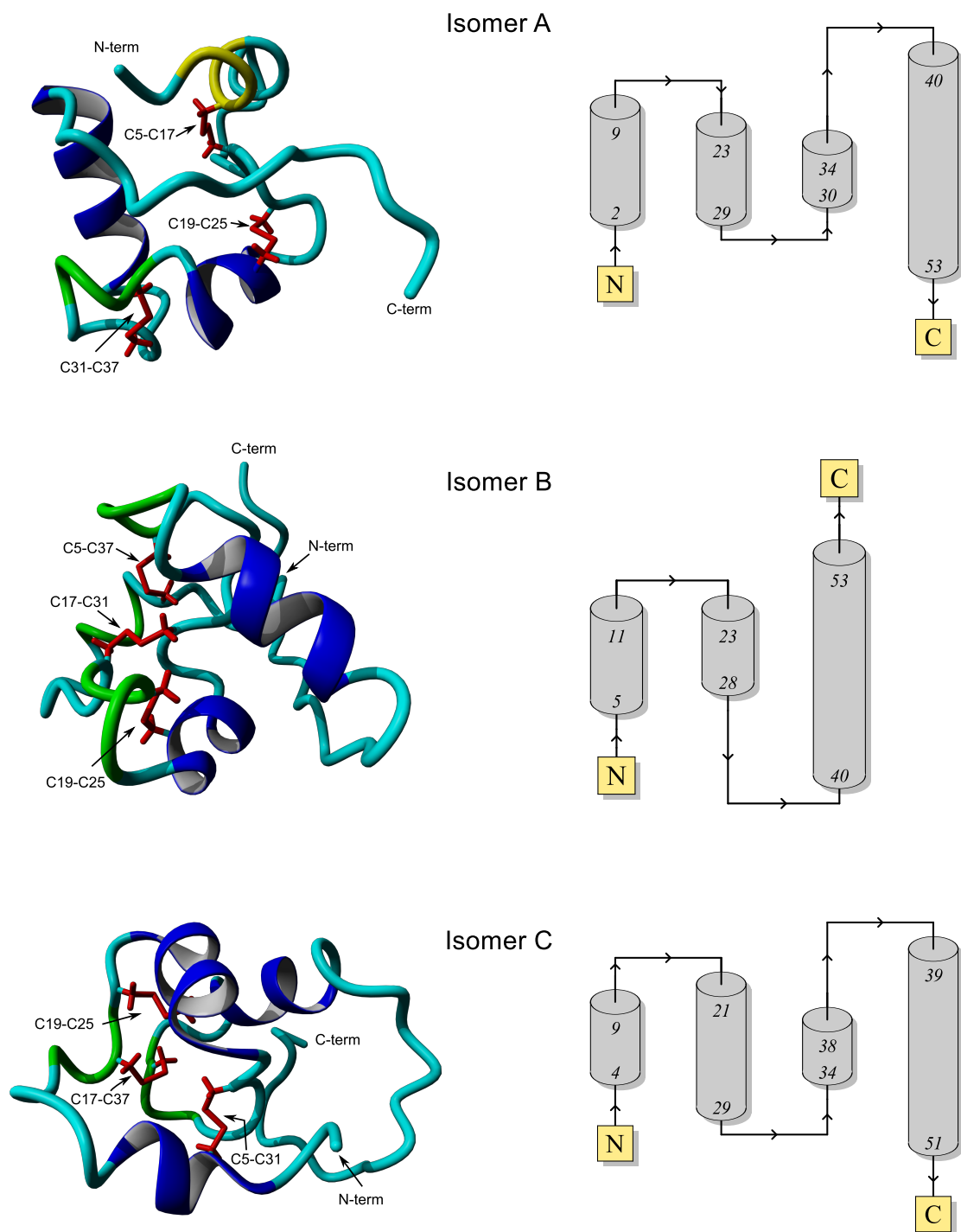


**Figure 5.17:** Computational models of the three tridegin isomers (left, by YASARA) and schematic topology (right, by PDBsum<sup>172</sup>). The structures are colored according to secondary structure:  $\alpha$ -helix (blue), turns and coils (cyan),  $3_{10}$ -helix (yellow) and  $\pi$ -helix (green). Disulfide bonds are highlighted in red.

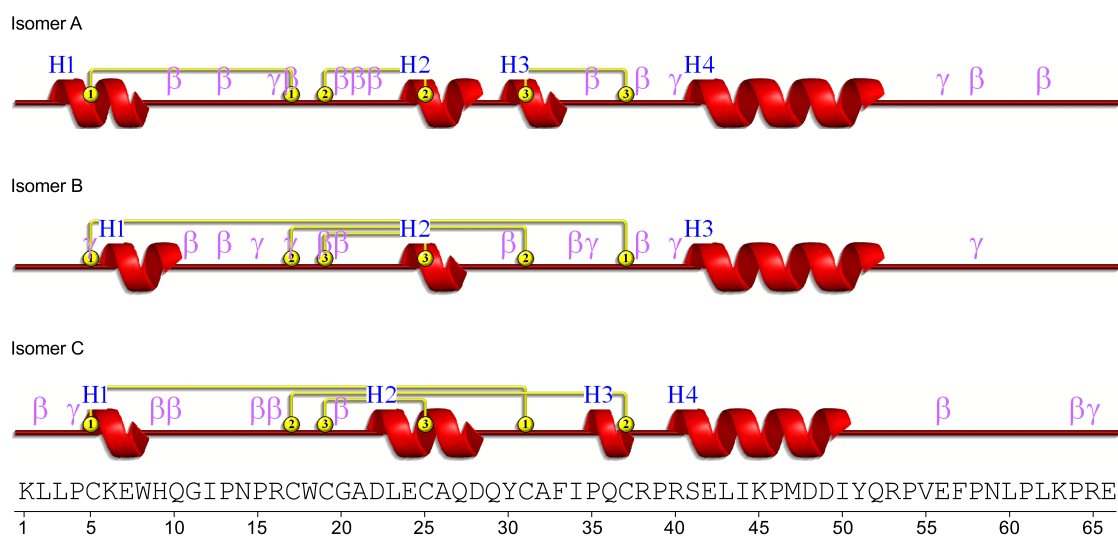


**Figure 5.18:** Comparison of secondary structures of the three different tridegin isomers (generated by PDBsum<sup>172</sup>).

### 5.5.1 Comparison with other peptides and proteins

There are two major groups of cysteine connectivities described for leech-derived anti-coagulants. One of them is the antistasin-type, which contains among others Antistasin, Hirustasin and Guamerin as well as Ghilanten that is also derived from *H. ghilani*. These peptides/miniproteins contain 5 disulfide bonds which are connected 1-3, 2-4,5-8,6-9 and 7-10.<sup>175</sup> The other one is the so-called leech antihemostatic protein (LAP) motif, which includes Decorsin, Hirudin, Haemadin and Ornatin. These peptides contain six cysteine residues with a disulfide pattern 1-2,3-5 and 4-6.<sup>176,177</sup> Although the number of cysteine residues and even their spacing in tridegin is similar to the LAP representatives (see also Figure 2.8), tridegin clearly shows a different disulfide connectivity. This also results in a different secondary structure: for Hirudin, Decorsin and Haemadin crystal- and/or NMR structures are available, and none of them shows  $\alpha$ -helices in their secondary structure (e.g. PDB entries 1HIC,<sup>165</sup> 2PW8,<sup>178</sup> 1DEC,<sup>179</sup> 1E0F<sup>177</sup>).

## 5.6 Structure-Activity-Relationship

### 5.6.1 General relationships of the tridegin-FXIIIa-interaction

The interaction of tridegin with FXIIIa is rather complex. Simply removing parts of the structure changes the way of interaction extensively. It has been shown that some amino acids in the C-terminal region, such as Ile50, Gln52 and Leu62 are important for potency of the inhibitor.<sup>151</sup> In general, the C-terminal part shows inhibition of FXIIIa, however, this

inhibition is more precisely described as substrate competition. Addition of all N-terminal amino acids does not increase inhibitor potency much, but prevents the substrate-like behavior of the inhibitor in the presence of FXIIIa. In contrast, oxidation of the 6 cysteine residues in the N-terminus is not necessary for preventing the substrate-like behavior, but does increase inhibitor potency. The isolated N-terminal part, however, independently of being oxidized or not, does not inhibit FXIIIa. This already indicates a contribution to inhibitor binding, but not direct interaction of the N-terminal region of tridegin with the active site of FXIIIa. Binding studies support this hypothesis and could show that the isolated, oxidized N-terminal part does efficiently bind to FXIIIa, possibly to a binding site in some distance to the active center of the enzyme. Up to now, no experimental data is available on which of the three different isomers present in the monomeric tridegin preparation shows the highest affinity or inhibitor potency to FXIIIa. However, the high potency of the dimeric tridegin suggests that this might be the biologically relevant form.

With this information in mind, docking studies of the three monomeric isomers to FXIII-A° were performed and evaluated.

### 5.6.2 Docking of tridegin to FXIII-A°

The new crystal structure of activated FXIII-A° was used for docking experiments with the three modeled isomers of tridegin. Docking was performed by A. Biswas (University Hospital Bonn) who kindly provided the docking data.

First, the general docking regions of the three different isomers were analyzed. While isomers A and B bind to a region close to the active site, the best dock for isomer C is in a completely different part of the FXIII-A° structure and does not interact directly with atoms of FXIII-A°. Figure 5.19 gives a superposition of the docking sites for all three isomers.

In general, isomers A and B showed a number of putative interactions with residues in or close to the active site of FXIII-A°, while isomer C did not show any interactions even in the best fitted docks. Therefore, mainly isomer A and B will be discussed. The putative interactions of these two isomers with the FXIII-A° structure are listed in Table 5.6. Some of these interactions are also indicated in Figure 5.20. From these data it becomes clear that the two different isomers A and B bind in completely different ways to the active site of FXIII-A°. Isomer A binds predominantly with the N-terminal part to FXIII-A° and shows direct interactions between the active site cysteine (Cys314) in FXIII-A° and Gln10 in tridegin. This is surprising, because Gln10 has not yet been associated with inhibitory potency of tridegin, however a targeted mutation of this site has never been evaluated. Interestingly, the N-terminal region of isomer A penetrates the substrate tunnel of FXIII-A° in a way that the peptide chain enters through the side of the tunnel that is assumed to normally allow



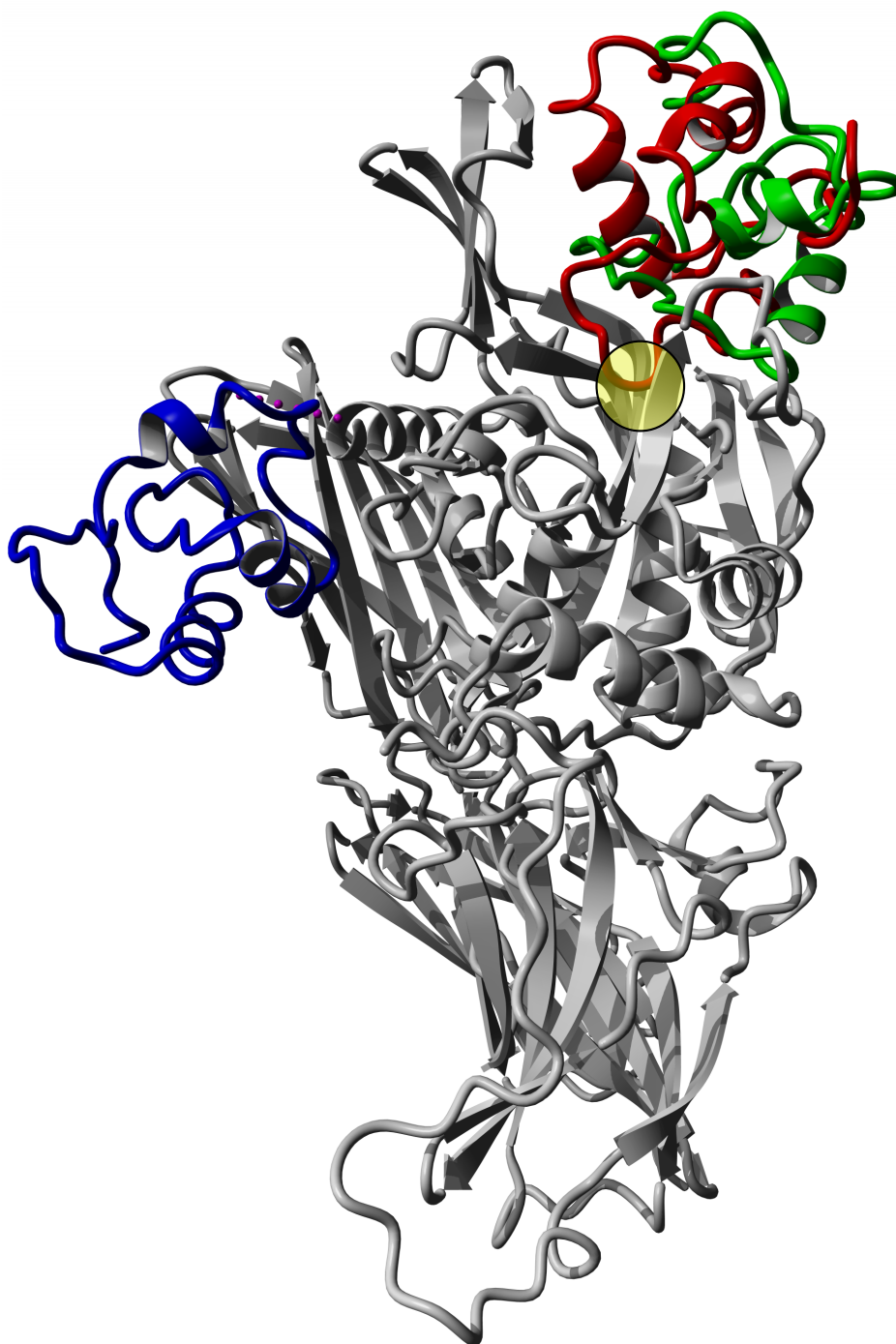


**Figure 5.19:** Docking of the three different tridegin isomers to the FXIII-A° structure. Isomer A is shown in red, B in green and C in blue. The localization of the active site is indicated with a yellow circle.

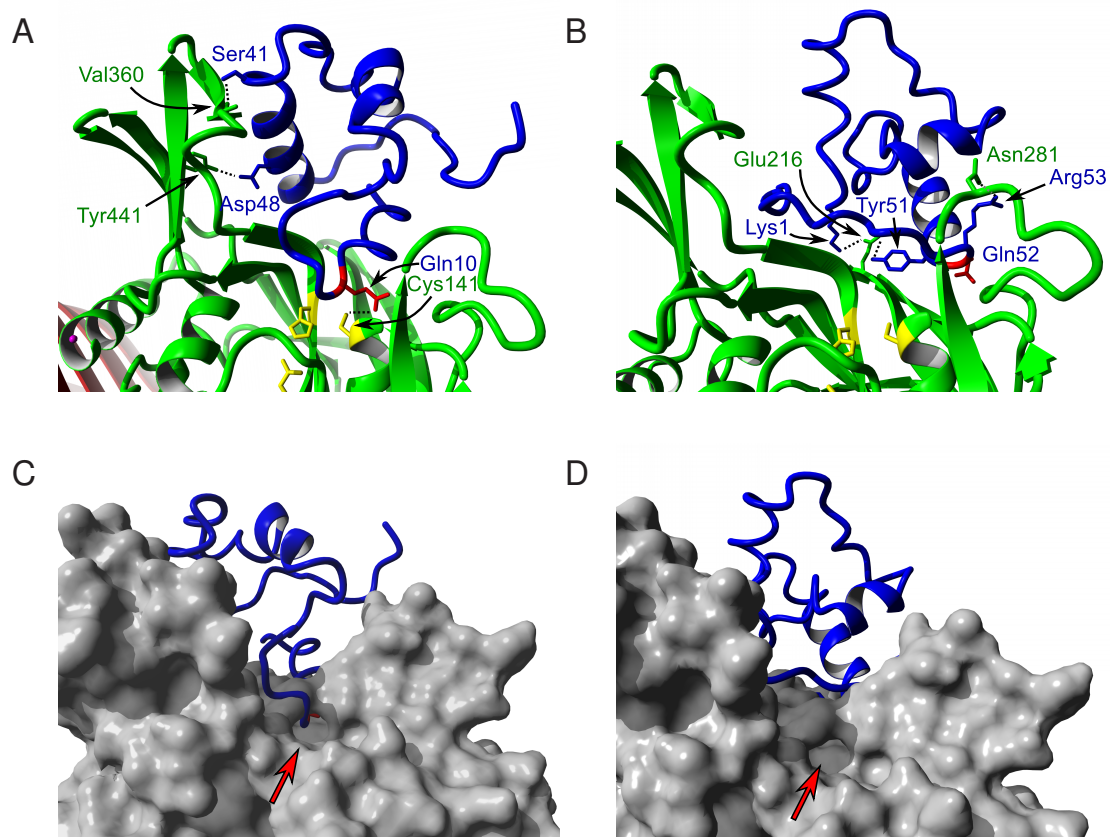


**Figure 5.20:** Details and interactions of the docking region for A) isomer A and B) isomer B. The backbone of FXIII<sup>o</sup> is shown in green, tridegin in blue. Active site residues are indicated in yellow and Gln10 and Gln52 in red. The surface representation (C and D) of FXIII<sup>o</sup> shows the tunnel for entrance of the amine substrate (arrow) and the relative localization of isomer A and B, respectively.

entrance of the amine substrate (Figure 5.20). This would effectively inhibit the enzyme. Whether or not this mode of binding contributes to inhibitory action of tridegin remains questionable, as long as no experimental proof is found. In any case, this type of binding is completely different to what has been observed for isolated C-terminal parts of tridegin, where Gln52 clearly interacts with the active site of FXIIIa and Gln10 is not even present.

Most interactions of isomer B with FXIII-A<sup>o</sup>, in contrast, are located in the C-terminal part of the peptide. In this case, Gln52 is located relatively close to the active site cysteine residue (12 Å), but too far away for direct interaction. Still, given the inaccuracy generated by the modeling and the docking step, this binding mode might explain the effects seen in C-terminal peptides of tridegin. In contrast to isomer A, isomer B does not penetrate the tunnel near the active site of the enzyme, but probably blocks access from the entrance site for the glutamine containing substrate. This type of binding would therefore also be expected to inhibit FXIII-A<sup>o</sup>.

**Table 5.6:** List of putative interactions of the tridegin isomers A and B with FXIII-A°. The atoms taking part in the putative interaction are given in square brackets and follow the PDB nomenclature.<sup>180</sup>

Isomer A			Isomer B		
Tridegin	Dist. [Å]	FXIII A°	Tridegin	Dist. [Å]	FXIII A°
<b>Hydrogen bonds</b>			<b>Hydrogen bonds</b>		
Asn14 [N]	2.90	Ser368 [OG]	Lys1 [NZ]	3.3	Glu216 [OE1]
Glu7 [O]	3.72	Trp279 [NE1]	Tyr51 [OH]	2.10	Gly215 [O]
Gln10 [O]	3.29	His373 [ND1]	Arg53 [NH2]	3.26	Asn281 [OD1]
Gln10 [OE1]	3.21	Cys314 [SG]	Val55 [N]	3.51	Gln313 [OE1]
Gln10 [OE1]	3.32	Cys314 [N]	Lys63 [NZ]	2.56	Asp456 [OD2]
Gln10 [OE1]	3.39	Trp315 [N]	Tyr51 [O]	2.96	Arg223 [NH2]
Pro13 [O]	3.76	Val369 [N]	Tyr51 [O]	3.86	Tyr372 [OH]
Ser41 [O]	2.24	Val360 [N]	Tyr51 [OH]	3.70	Glu216 [N]
Ser41 [OG]	3.43	Val360 [N]	Asn59 [O]	3.01	Val369 [N]
Ser41 [OG]	3.45	Asn361 [N]	Pro61 [O]	3.59	His459 [NE2]
Asp48 [OD2]	3.33	Tyr441 [OH]			
<b>Salt bridges</b>			<b>Salt bridges</b>		
Asp48 [OD1]	3.90	His459 [NE2]	Lys1 [NZ]	3.33	Glu216 [OE1]
			Lys63 [NZ]	2.56	Asp456 [OD2]

In general it is encouraging that two out of three isomers readily fit into the active site of FXIII° in a way that would inhibit the enzyme. The orientation of isomer A is surprising and generates a new hypothesis that would be worthwhile to be tested by e.g. synthesizing a Gln10Ala mutant. The discrepancy between experimental findings for the reaction of Gln52 with the active site of FXIIIa and the docking of isomer A might also explain in parts the different binding modes suggested for N-terminally truncated and full-length tridegin. However, this binding mode would nicely explain the high affinity of the isolated N-terminal part of tridegin to FXIIIa. The binding of isomer B relates more closely to the experimental findings for the importance of Gln52, although a direct interaction with the active site was not demonstrated. On the other hand, this model fails to explain the affinity of the N-terminal region of tridegin to FXIIIa, as most interactions are located in the C-terminal part of the inhibitor. Isomer C did not interact with FXIII-A° in the present docking study, which, however, does not need to be true in reality.

For further studies, experimental confirmation of the models and docking studies would be of high interest. The targeted synthesis of all three isomers via solid-phase peptide synthesis

and orthogonal protecting group strategies is challenging, but a successful preparation of the single isomers would allow individual structural and functional studies which would in turn refine the findings presented here.

## 6 Conclusion

Factor XIIIa (FXIIIa), a transglutaminase catalyzing the covalent cross-linking of fibrin in the final step of blood coagulation, is an interesting pharmaceutical target due to its multiple functions and involvement in a number of pathophysiological processes. Moreover, there is still a lot of research ongoing to further elucidate the role of this enzyme in- and outside of cells. Therefore, there is a need for specific, effective and well-characterized inhibitors for FXIIIa. The only natural peptidic FXIIIa inhibitor available so far, tridegin, has been isolated from the giant amazon leech *Hamenteria ghiliani* in 1997. The detailed structural and functional characterization of this 66mer peptide was the aim of this thesis.

**Synthesis** First, the inhibitor was synthesized according to a protocol already established in the laboratory. Different full-length variants of the peptide (synthetic, recombinant, monomeric, dimeric) were prepared as well as a series of N-terminally truncated peptides. Additionally, the peptide sequence was separated into a 37-mer N-terminal part and a 29-mer C-terminal part, both of which were synthesized. An overview of the synthesized linear precursors is given in Figure 6.1.

The isolated N-terminal part as well as the full-length peptide were allowed to self-fold and form disulfide bonds, which is a way to prepare disulfide-bonded peptides with unknown native disulfide connectivity. From peptides **P1**, **P2**, **P6** and **P7** fluorescence-labeled derivatives were prepared by N-terminal coupling of carboxyfluoresceine, resulting in peptides **P15**, **P16**, **P17** and **P18**, respectively.

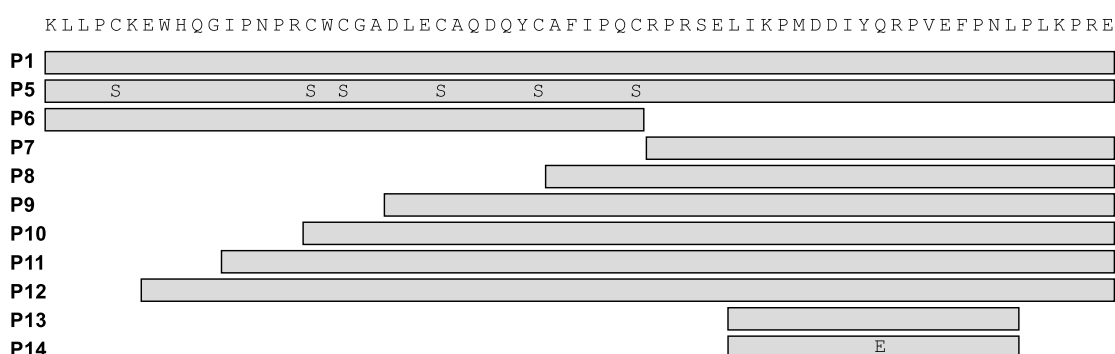


**Figure 6.1:** Overview over all synthesized linear precursors. Peptide **P1** was oxidized to a monomeric (**P2**) and a dimeric (**P3**) form. Peptide **P6** was prepared only in an oxidized version. Peptides with indicated amino acids contain mutations of the original sequence at the given positions.

In an orthogonal approach, tridegin was also expressed recombinantly in *E. coli*. Expression of the peptide was reproduced and optimized from a formerly published protocol using an artificial DNA, since the original cDNA sequence encoding tridegin is not known.

**Functional assays** The different tridegin variants were subjected to functional analyses. The inhibitory potency of the compounds was analyzed by enzyme activity assays. It was shown that the C-terminal part **P7** did inhibit FXIIIa with only about 4fold higher  $IC_{50}$  values than those measured for oxidized full-length tridegin **P2** (2.2  $\mu$ M and 0.5  $\mu$ M, respectively). In contrast, the N-terminal part **P6** did not inhibit FXIIIa at all. Furthermore, the linear variant of tridegin showed an  $IC_{50}$  of 1.5  $\mu$ M, which strengthens the assumption that the disulfide connectivity plays an important role in inhibitor function. This was further confirmed by assaying a mutant peptide containing only serine residues instead of cysteine (**P5**) which resulted in a similar potency ( $IC_{50}$  2.1  $\mu$ M). Therefore it was concluded, that the presence of the N-terminal part only increases inhibitor potency when disulfide bonds are formed. However, an interesting finding remains: while the isolated C-terminal part **P7** loses its inhibitory function over time in presence of FXIIIa (i.e. is a competing substrate of the enzyme, in which Gln52 is turned into Glu), this behavior could not be observed with any of the full-length derivatives, oxidized or not. This either means that the full-length variants are not substrates of FXIIIa or that the product of this hypothetical reaction (i.e. the Glu52 mutant) still inhibits FXIIIa.

Furthermore, the recombinantly expressed peptide **P4** was analyzed, but showed a lower potency ( $IC_{50}$  of 1.2  $\mu$ M) than the synthesized, oxidized peptide. In contrast, a synthetic, covalent dimer (**P3**) displayed an  $IC_{50}$  value of 0.1  $\mu$ M. This leads to the assumption that the dimeric form might be the native one.

In general, the inhibition of FXIIIa by tridegin seems to be very complex and cannot be described by e.g. a simple competitive mechanism. Also, the analyses performed did indicate a 1:2 stoichiometry between FXIIIa and tridegin.

To further assess the function of the non-inhibitory N-terminal part, binding assays were performed. In a thermophoresis experiment, the fluorescence-labeled peptides were incubated with different forms of FXIII and binding was monitored. These experiments revealed that linear and oxidized tridegin as well as the isolated N- and C-terminal parts did bind to FXIIIa, but none of the peptides bound to non-activated FXIII (A-subunit) or the carrier B-subunit. A potential explanation for the impact of the N-terminal part on inhibitor potency is that it enhances binding of the inhibitor to the enzyme, potentially by association with a secondary binding site different from the active center.

The structure-activity relationships gained from these experiments are summarized in Figure 6.2.

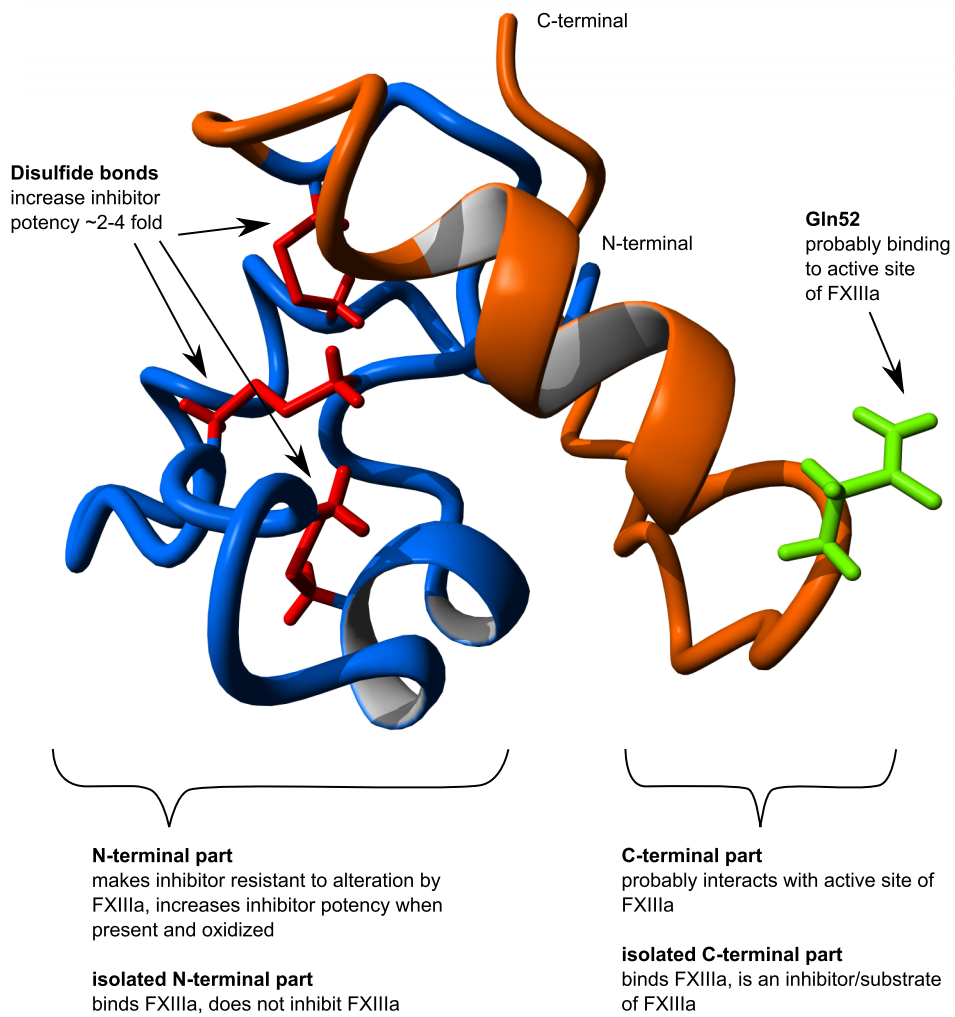


**Figure 6.2:** Structure-Activity-Relationships in tridegin (isomer B). Disulfide bonds are indicated in red, the N-terminal part of the peptide (1-37) is colored blue, the C-terminal part (38-66) orange. The important Gln52 position is highlighted in green.

**Structure elucidation** For a detailed understanding of the tridegin structure, elucidation of the disulfide connectivity is of major importance. No suitable homologue for directly inferring disulfide connectivity could be found, therefore the disulfide bonds had to be determined *de novo* from both the synthetic and recombinant material. Crystallization of tridegin in presence and absence of factor XIII was attempted in cooperation with Dr. M. Than (FLI Jena) but was not successful. Thus, the oxidized peptides – full length tridegin synthetic (**P2**) and recombinant (**P4**) as well as the isolated N-terminal analogue **P6** – were subjected to enzymatic digestion and subsequent mass spectrometric analysis. This method was successful, and three different isomers could be identified in both **P2** and **P6**. One of them could also be confirmed in recombinant tridegin.

This information was then used to perform molecular modeling of the structures (in cooperation with Dr. A. Biswas, University Hospital Bonn) and docking of the modeled tridegin isomers to the structure of active FXIII. Two of the three identified isomers were shown to dock to the active site of FXIIIa *in silico* exhibiting different binding modes.

**Outlook** In summary, this work greatly enhances the understanding of the FXIIIa inhibitor tridegin. Further experimental studies are needed to assess the inhibitor potency and binding of the three different isomers individually. Also, evaluation of full-length variants with single amino acid mutations based on the docking experiments would be useful to confirm the *in silico* studies and pinpoint interaction sites between FXIIIa and tridegin. Subsequently, further optimization of the inhibitor might be possible.

Although some questions still remain, tridegin is now one of the best-characterized inhibitors for FXIIIa and might therefore serve both as research tool for the investigation of FXIIIa function *in vitro* and *in vivo*, as well as a lead structure for FXIIIa inhibitor development.



## Abbreviations

Abbreviations of amino acids and their derivatives are used according to the recommendation of the *Nomenclature Committee of IUB* (NC-IUB) and the *IUPAC-IUB Joint Commission on Biochemical Nomenclature* (JCBN).<sup>181</sup> If not stated otherwise, amino acids and amino acid derivatives are L-configured.

$\alpha_2$ AP	$\alpha_2$ -Antiplasmin
5-FAM	5-Carboxyfluorescein
Abz	2-Aminobenzoic acid
APCE	Antiplasmin cleaving enzyme
APS	Ammonium persulfate
bp	base pairs
CD	Circular dichroism
cFXIII	Cellular factor XIII
CID	Collision induced dissociation
CMK	Chloro methyl ketone
DCM	Dichlormethane
DIEA	<i>N,N</i> -Diisopropylethylamine
DMF	<i>N,N</i> -Dimethylformamide
DTT	Dithiothreitol
DVT	Deep vein thrombosis
EDTA	Ethylenediaminetetraacetic acid
eq.	Equivalents
ESI	Electro spray ionization
EST	Expressed sequence tag
Fmoc	Fluorenylmethyloxycarbonyl protecting group
FRET	Förster resonance energy transfer
FXIII	Factor XIII
FXIIIa	Activated factor XIII
GSH	Glutathione (reduced)
GSSG	Glutathione (oxidized)
H-Gly-OEt	Glycine ethyl ester

## Abbreviations

---

HBTU	<i>O</i> -benzotriazol- <i>N,N,N',N'</i> -tetramethyl-uronium-hexafluoro-phosphate
HPLC	High performance liquid chromatography
IAA	Iodoacetamide
IC <sub>50</sub>	Half maximal inhibitory concentration
IPTG	Isopropyl β-D-1-thiogalactopyranoside
LC	Liquid chromatography
MALDI	Matrix assisted laser desorption/ionization
MAP	Michael acceptor pharmacophore
MASP1	Mannan-binding lectin-associated serine protease-1
MS	Mass spectrometry
NMR	Nuclear magnetic resonance
PAGE	Polyacrylamide gel electrophoresis
PAI-2	Plasminogen activator inhibitor 2
PCR	Polymerase chain reaction
pFXIII	Plasma factor XIII
PyBOP	Benzotriazol-1-yl-oxytripyrrolidinophosphonium hexafluorophosphate
SDS	Sodium dodecyl sulfate
SPPS	Solid phase peptide synthesis
t-PA	Tissue-type plasminogen activator
TAFI	Thrombin activatable fibrinolysis inhibitor
TAFIa	Thrombin activatable fibrinolysis inhibitor (activated)
TEMED	<i>N,N,N',N'</i> -Tetramethylethane-1,2-diamine
TFA	Trifluoroacetic acid
Tgase	Transglutaminase
TLC	Thin layer chromatography
TOF	Time of flight
Tris	Tris(hydroxymethyl)aminomethane
u-PA	Urokinase-type plasminogen activator
VTE	Venous thromboembolism

## List of Figures

2.1	Overview over the reactions catalyzed by transglutaminases . . . . .	3
2.2	Activation of plasma FXIII . . . . .	6
2.3	Activation of cellular FXIII . . . . .	7
2.4	Structures of FXIII-A and FXIII-A° . . . . .	8
2.5	Fibrinolytic and anti-fibrinolytic processes . . . . .	12
2.6	Physiological functions of FXIIIa. . . . .	14
2.7	Overview over different complications arising from thrombus formation. . . . .	17
2.8	Published tridegin sequences and putative homologues . . . . .	22
2.9	Early truncation and mutation studies on tridegin . . . . .	24
2.10	$\chi$ -angles of the disulfide bond . . . . .	26
4.1	Cloning strategy for recombinant tridegin . . . . .	39
5.1	IC <sub>50</sub> values of peptides from the C-terminal part of tridegin . . . . .	45
5.2	Gel filtration chromatogram and SDS-PAGE of dimeric tridegin . . . . .	49
5.3	Recombinant expression of tridegin . . . . .	50
5.4	HPLC of FXIIIa-catalyzed modification of <b>P13</b> . . . . .	52
5.5	Progress curve and IC <sub>50</sub> -values of truncated tridegin derivatives . . . . .	53
5.6	Progress curve and IC <sub>50</sub> -values of selected tridegin derivatives . . . . .	54
5.7	IC <sub>50</sub> determination of tridegin with a chromogenic and a fluorogenic assay . . . . .	56
5.8	Analysis of FXIIIa-tridegin stoichiometry . . . . .	58
5.9	Hill plots of the dimer <b>P3</b> and the C-terminal peptide <b>P7</b> . . . . .	59
5.10	Binding curves for <b>P16</b> , <b>P17</b> and <b>P18</b> to FXIIIa . . . . .	60
5.11	CD-spectrum of tridegin . . . . .	61
5.12	Gel filtration chromatogram of FXIII, tridegin and a FXIII/tridegin mixture . . . . .	62
5.13	Cleavage sites for chymotrypsin in tridegin and HPLC traces of digests . . . . .	64
5.14	Analysis of the chymotryptic digest of oxidized tridegin. . . . .	65
5.15	Detailed analysis of a disulfide-containing fragment by CID . . . . .	66
5.16	CID fragmentation pattern of alkylated and reduced side product after <b>P6</b> oxidation . . . . .	68

*LIST OF FIGURES*

---

5.17	Computational models of the three tridegin isomers . . . . .	72
5.18	Comparison of secondary structures of the three different tridegin isomers . .	73
5.19	Docking of the three different tridegin isomers to the FXIII-A <sup>o</sup> structure . . . .	75
5.20	Details and interactions of the docking region for isomers A and B . . . . .	76
6.1	Overview over all synthesized linear precursors . . . . .	79
6.2	Structure-activity-relationships in tridegin (molecular model of isomer B) . .	81

## List of Tables

2.1	Human transglutaminases. . . . .	4
2.2	Selected glutamine containing substrates of FXIIIa . . . . .	10
2.3	FXIIIa inhibitors . . . . .	19
2.4	Effect of mutations in the sequence of tridegin or a truncated analogue on inhibitor potency . . . . .	25
4.1	Chemicals and reagents . . . . .	29
4.2	Composition of buffers and media . . . . .	32
4.3	HPLC methods applied for semi-preparative and analytical separations. . . . .	34
4.4	Chemical characterization of synthesized peptides . . . . .	36
5.1	Yields of synthesized peptides . . . . .	48
5.2	Calculation of $K_i$ values for tridegin using different assays and inhibition types. . . . .	57
5.3	Disulfide-connected fragments identified by mass spectrometry. . . . .	67
5.4	Sequence coverage for all possible 15 isomers in recombinant tridegin digest . . . . .	70
5.5	Configuration of disulfide bonds in computational models of tridegin . . . . .	71
5.6	List of putative interactions of the tridegin isomers A and B with FXIII-A° . . . . .	77



## Bibliography

- [1] Whitaker, I. S.; Rao, J.; Izadi, D.; Butler, P. E. Historical Article: *Hirudo medicinalis*: ancient origins of, and trends in the use of medicinal leeches throughout history. *Br. J. Oral Maxillofac. Surg.* **2004**, *42*, 133–7.
- [2] Hyson, J. M. Leech therapy: a history. *J. Hist. Dent.* **2005**, *53*, 25–7.
- [3] Franz, F. Über den die Blutgerinnung aufhebenden Bestandteil des medizinischen Blutegels. *Naunyn Schmiedebergs Arch. Exp. Pathol. Pharmacol.* **1903**, 342–357.
- [4] Sawyer, R. T. Thrombolytics and anti-coagulants from leeches. *Biotechnology. (N. Y.)* **1991**, *9*, 513–5, 518.
- [5] Salzet, M. Anticoagulants and inhibitors of platelet aggregation derived from leeches. *FEBS Lett.* **2001**, *492*, 187–92.
- [6] Griffin, M.; Casadio, R.; Bergamini, C. M. Transglutaminases: nature's biological glues. *Biochem. J.* **2002**, *368*, 377–96.
- [7] Lorand, L.; Graham, R. M. Transglutaminases: crosslinking enzymes with pleiotropic functions. *Nat. Rev. Mol. Cell Biol.* **2003**, *4*, 140–56.
- [8] Klöck, C.; Khosla, C. Regulation of the activities of the mammalian transglutaminase family of enzymes. *Protein Sci.* **2012**, *21*, 1781–91.
- [9] Sugimura, Y.; Hosono, M.; Kitamura, M.; Tsuda, T.; Yamanishi, K.; Maki, M.; Hitomi, K. Identification of preferred substrate sequences for transglutaminase 1—development of a novel peptide that can efficiently detect cross-linking enzyme activity in the skin. *FEBS J.* **2008**, *275*, 5667–77.
- [10] Sugimura, Y.; Hosono, M.; Wada, F.; Yoshimura, T.; Maki, M.; Hitomi, K. Screening for the preferred substrate sequence of transglutaminase using a phage-displayed peptide library: identification of peptide substrates for TGASE 2 and Factor XIIIa. *J. Biol. Chem.* **2006**, *281*, 17699–706.

- [11] Yamane, A.; Fukui, M.; Sugimura, Y.; Itoh, M.; Alea, M. P.; Thomas, V.; El Alaoui, S.; Akiyama, M.; Hitomi, K. Identification of a preferred substrate peptide for transglutaminase 3 and detection of in situ activity in skin and hair follicles. *FEBS J.* **2010**, *277*, 3564–74.
- [12] Fukui, M.; Kuramoto, K.; Yamasaki, R.; Shimizu, Y.; Itoh, M.; Kawamoto, T.; Hitomi, K. Identification of a highly reactive substrate peptide for transglutaminase 6 and its use in detecting transglutaminase activity in the skin epidermis. *FEBS J.* **2013**, *280*, 1420–9.
- [13] Gundemir, S.; Colak, G.; Tucholski, J.; Johnson, G. V. W. Transglutaminase 2: a molecular Swiss army knife. *Biochim. Biophys. Acta* **2012**, *1823*, 406–19.
- [14] Martin, A.; De Vivo, G.; Iannaccone, M.; Stefanile, A.; Serretiello, E.; Gentile, V. Pathophysiological roles of transglutaminase - catalyzed reactions in the pathogenesis of human diseases. *Inflamm. Allergy Drug Targets* **2012**, *11*, 278–84.
- [15] Iismaa, S. E.; Mearns, B. M.; Lorand, L.; Graham, R. M. Transglutaminases and disease: lessons from genetically engineered mouse models and inherited disorders. *Physiol. Rev.* **2009**, *89*, 991–1023.
- [16] Eckert, R. L.; Sturniolo, M. T.; Broome, A.-M.; Ruse, M.; Rorke, E. a. Transglutaminase function in epidermis. *J. Invest. Dermatol.* **2005**, *124*, 481–92.
- [17] Candi, E.; Schmidt, R.; Melino, G. The cornified envelope: a model of cell death in the skin. *Nat. Rev. Mol. Cell Biol.* **2005**, *6*, 328–40.
- [18] Huber, M.; Rettler, I.; Bernasconi, K.; Frenk, E.; Lavrijsen, S. P.; Ponc, M.; Bon, A.; Lautenschlager, S.; Schorderet, D. F.; Hohl, D. Mutations of keratinocyte transglutaminase in lamellar ichthyosis. *Science* **1995**, *267*, 525–8.
- [19] Matsuki, M. et al. Defective stratum corneum and early neonatal death in mice lacking the gene for transglutaminase 1 (keratinocyte transglutaminase). *Proc. Natl. Acad. Sci. U. S. A.* **1998**, *95*, 1044–9.
- [20] Dubbink, H. J.; de Waal, L.; van Haperen, R.; Verkaik, N. S.; Trapman, J.; Romijn, J. C. The human prostate-specific transglutaminase gene (TGM4): genomic organization, tissue-specific expression, and promoter characterization. *Genomics* **1998**, *51*, 434–44.
- [21] Jiang, W. G.; Ye, L.; Sanders, A. J.; Ruge, F.; Kynaston, H. G.; Ablin, R. J.; Mason, M. D. Prostate transglutaminase (TGase-4, TGaseP) enhances the adhesion of prostate



- cancer cells to extracellular matrix, the potential role of TGase-core domain. *J. Transl. Med.* **2013**, *11*, 269.
- [22] Thomas, H.; Beck, K.; Adamczyk, M.; Aeschlimann, P.; Langley, M.; Oita, R. C.; Thiebach, L.; Hils, M.; Aeschlimann, D. Transglutaminase 6: a protein associated with central nervous system development and motor function. *Amino Acids* **2013**, *44*, 161–77.
- [23] Laki, K.; Lóránd, L. On the Solubility of Fibrin Clots. *Science* **1948**, *108*, 280.
- [24] Lorand, L.; Konishi, K. Activation of the Fibrin Stabilizing Factor of Plasma by Thrombin. *Arch. Biochem. Biophys.* **1964**, *105*, 58–67.
- [25] Muszbek, L.; Ariëns, R. a.; Ichinose, A. Factor XIII: recommended terms and abbreviations. *J. Thromb. Haemost.* **2007**, *5*, 181–3.
- [26] Muszbek, L.; Bagoly, Z.; Bereczky, Z.; Katona, E. The involvement of blood coagulation factor XIII in fibrinolysis and thrombosis. *Cardiovasc. Hematol. Agents Med. Chem.* **2008**, *6*, 190–205.
- [27] Bagoly, Z.; Koncz, Z.; Hársfalvi, J.; Muszbek, L. Factor XIII, clot structure, thrombosis. *Thromb. Res.* **2012**, *129*, 382–7.
- [28] Katona, E.; Haramura, G.; Kárpáti, L.; Fachel, J.; Muszbek, L. A simple, quick one-step ELISA assay for the determination of complex plasma factor XIII (A2B2). *Thromb. Haemost.* **2000**, *83*, 268–73.
- [29] Katona, E.; Péntes, K.; Csapó, A.; Fazakas, F.; Udvardy, M. L.; Bagoly, Z.; Orosz, Z. Z.; Muszbek, L. Interaction of factor XIII subunits. *Blood* **2014**,
- [30] Lorand, L. Factor XIII: structure, activation, and interactions with fibrinogen and fibrin. *Ann. N. Y. Acad. Sci.* **2001**, *936*, 291–311.
- [31] Lewis, S. D.; Janus, T. J.; Lorand, L.; Shafer, J. a. Regulation of formation of factor XIIIa by its fibrin substrates. *Biochemistry* **1985**, *24*, 6772–7.
- [32] Radek, J. T.; Jeong, J. M.; Wilson, J.; Lorand, L. Association of the A subunits of recombinant placental factor XIII with the native carrier B subunits from human plasma. *Biochemistry* **1993**, *32*, 3527–34.
- [33] Kristiansen, G. K.; Andersen, M. D. Reversible activation of cellular factor XIII by calcium. *J. Biol. Chem.* **2011**, *286*, 9833–9.

- [34] Bagoly, Z.; Katona, E.; Muszbek, L. Factor XIII and inflammatory cells. *Thromb. Res.* **2012**, *129 Suppl*, S77–81.
- [35] Ando, Y.; Imamura, S.; Yamagata, Y.; Kitahara, A.; Saji, H.; Murachi, T.; Kannagi, R. Platelet factor XIII is activated by calpain. *Biochem. Biophys. Res. Commun.* **1987**, *144*, 484–90.
- [36] Muszbek, L.; Bereczky, Z.; Bagoly, Z.; Komáromi, I.; Katona, E. Factor XIII: A Coagulation Factor With Multiple Plasmatic and Cellular Functions. *Physiol. Rev.* **2011**, *91*, 931–972.
- [37] Yee, V. C.; Pedersen, L. C.; Le Trong, I.; Bishop, P. D.; Stenkamp, R. E.; Teller, D. C. Three-dimensional structure of a transglutaminase: human blood coagulation factor XIII. *Proc. Natl. Acad. Sci. U. S. A.* **1994**, *91*, 7296–300.
- [38] Yee, V. C.; Pedersen, L. C.; Bishop, P. D.; Stenkamp, R. E.; Teller, D. C. Structural evidence that the activation peptide is not released upon thrombin cleavage of factor XIII. *Thromb. Res.* **1995**, *78*, 389–97.
- [39] Fox, B. a.; Yee, V. C.; Pedersen, L. C.; Le Trong, I.; Bishop, P. D.; Stenkamp, R. E.; Teller, D. C. Identification of the calcium binding site and a novel ytterbium site in blood coagulation factor XIII by x-ray crystallography. *J. Biol. Chem.* **1999**, *274*, 4917–23.
- [40] Weiss, M. S.; Metzner, H. J.; Hilgenfeld, R. Two non-proline cis peptide bonds may be important for factor XIII function. *FEBS Lett.* **1998**, *423*, 291–6.
- [41] Pinkas, D. M.; Strop, P.; Brunger, A. T.; Khosla, C. Transglutaminase 2 undergoes a large conformational change upon activation. *PLoS Biol.* **2007**, *5*, e327.
- [42] Komáromi, I.; Bagoly, Z.; Muszbek, L. Factor XIII: novel structural and functional aspects. *J. Thromb. Haemost.* **2011**, *9*, 9–20.
- [43] Woofter, R. T.; Maurer, M. C. Role of calcium in the conformational dynamics of factor XIII activation examined by hydrogen-deuterium exchange coupled with MALDI-TOF MS. *Arch. Biochem. Biophys.* **2011**, *512*, 87–95.
- [44] Andersen, M. D.; Faber, J. H. Structural characterization of both the non-proteolytic and proteolytic activation pathways of coagulation Factor XIII studied by hydrogen–deuterium exchange mass spectrometry. *Int. J. Mass Spectrom.* **2011**, *302*, 139–148.

- [45] Stieler, M.; Weber, J.; Hils, M.; Kolb, P.; Heine, A.; Büchold, C.; Pasternack, R.; Klebe, G. Structure of active coagulation factor XIII triggered by calcium binding: basis for the design of next-generation anticoagulants. *Angew. Chem. Int. Ed. Engl.* **2013**, *52*, 11930–4.
- [46] Ahvazi, B.; Boeshans, K. M.; Rastinejad, F. The emerging structural understanding of transglutaminase 3. *J. Struct. Biol.* **2004**, *147*, 200–7.
- [47] Souri, M.; Kaetsu, H.; Ichinose, A. Sushi domains in the B subunit of factor XIII responsible for oligomer assembly. *Biochemistry* **2008**, *47*, 8656–64.
- [48] Carrell, N. a.; Erickson, H. P.; McDonagh, J. Electron microscopy and hydrodynamic properties of factor XIII subunits. *J. Biol. Chem.* **1989**, *264*, 551–6.
- [49] Lorand, L.; Rule, N. G.; Ong, H. H.; Furlanetto, R.; Jacobsen, A.; Downey, J.; Oner, N.; Bruner-Lorand, J. Amine specificity in transpeptidation. Inhibition of fibrin cross-linking. *Biochemistry* **1968**, *7*, 1214–23.
- [50] Richardson, V. R.; Cordell, P.; Standeven, K. F.; Carter, A. M. Substrates of Factor XIII-A: roles in thrombosis and wound healing. *Clin. Sci. (Lond)*. **2013**, *124*, 123–37.
- [51] Nikolajsen, C. L.; Dyrland, T. F.; Toftgaard Poulsen, E.; Enghild, J. J.; Scavenius, C. Coagulation Factor XIIIa Substrates in Human Plasma. Identification and Incorporation Into the Clot. *J. Biol. Chem.* **2014**, 0–15.
- [52] Csoz, E.; Meskó, B.; Fésüs, L. Transdab wiki: the interactive transglutaminase substrate database on web 2.0 surface. *Amino Acids* **2009**, *36*, 615–7.
- [53] Böhm, M. Untersuchung funktioneller und struktureller Aspekte des Faktor XIIIa-Inhibitors Tridegin. Diplomarbeit, Friedrich-Schiller-Universität Jena, 2010.
- [54] McDonagh, J.; Fukue, H. Determinants of substrate specificity for factor XIII. *Semin. Thromb. Hemost.* **1996**, *22*, 369–76.
- [55] Péntzes, K.; Kövér, K. E.; Fazakas, F.; Haramura, G.; Muszbek, L. Molecular mechanism of the interaction between activated factor XIII and its glutamine donor peptide substrate. *J. Thromb. Haemost.* **2009**, *7*, 627–33.
- [56] Valnickova, Z.; Enghild, J. J. Human Procarboxypeptidase U, or Thrombin-activable Fibrinolysis Inhibitor, Is a Substrate for Transglutaminases: Evidence for transglutaminase-catalyzed cross-linking to fibrin. *J. Biol. Chem.* **1998**, *273*, 27220–27224.

- [57] Jensen, P. H.; Schüler, E.; Woodrow, G.; Richardson, M.; Goss, N.; Højrup, P.; Petersen, T. E.; Rasmussen, L. K. A unique interhelical insertion in plasminogen activator inhibitor-2 contains three glutamines, Gln83, Gln84, Gln86, essential for transglutaminase-mediated cross-linking. *J. Biol. Chem.* **1994**, *269*, 15394–8.
- [58] Takagi, J.; Aoyama, T.; Ueki, S.; Ohba, H.; Saito, Y.; Lorand, L. Identification of factor-XIIIa-reactive glutaminyl residues in the propolypeptide of bovine von Willebrand factor. *Eur. J. Biochem.* **1995**, *232*, 773–7.
- [59] Francis, R. T.; McDonagh, J.; Mann, K. G. Factor V is a substrate for the transamidase factor XIIIa. *J. Biol. Chem.* **1986**, *261*, 9787–92.
- [60] Cleary, D. B.; Maurer, M. C. Characterizing the specificity of activated Factor XIII for glutamine-containing substrate peptides. *Biochim. Biophys. Acta* **2006**, *1764*, 1207–17.
- [61] Gorman, J. J.; Folk, J. E. Structural features of glutamine substrates for transglutaminases. Specificities of human plasma factor XIIIa and the guinea pig liver enzyme toward synthetic peptides. *J. Biol. Chem.* **1981**, *256*, 2712–5.
- [62] Mockros, L. F.; Roberts, W. W.; Lorand, L. Viscoelastic properties of ligation-inhibited fibrin clots. *Biophys. Chem.* **1974**, *2*, 164–9.
- [63] Weisel, J. W. The mechanical properties of fibrin for basic scientists and clinicians. *Biophys. Chem.* **2004**, *112*, 267–76.
- [64] Fraser, S. R.; Booth, N. A.; Mutch, N. J. The antifibrinolytic function of factor XIII is exclusively expressed through  $\alpha$ 2-antiplasmin cross-linking. *Blood* **2011**, *117*, 6371–4.
- [65] Carpenter, S. L.; Mathew, P. Alpha2-antiplasmin and its deficiency: fibrinolysis out of balance. *Haemophilia* **2008**, *14*, 1250–4.
- [66] Medcalf, R. L.; Stasinopoulos, S. J. The undecided serpin. The ins and outs of plasminogen activator inhibitor type 2. *FEBS J.* **2005**, *272*, 4858–67.
- [67] Ritchie, H.; Robbie, L. a.; Kinghorn, S.; Exley, R.; Booth, N. a. Monocyte plasminogen activator inhibitor 2 (PAI-2) inhibits u-PA-mediated fibrin clot lysis and is cross-linked to fibrin. *Thromb. Haemost.* **1999**, *81*, 96–103.
- [68] Rijken, D. C.; Lijnen, H. R. New insights into the molecular mechanisms of the fibrinolytic system. *J. Thromb. Haemost.* **2009**, *7*, 4–13.

- [69] Katona, E.; Ajzner, E.; Tóth, K.; Kárpáti, L.; Muszbek, L. Enzyme-linked immunosorbent assay for the determination of blood coagulation factor XIII A-subunit in plasma and in cell lysates. *J. Immunol. Methods* **2001**, *258*, 127–35.
- [70] Hevessy, Z.; Haramura, G.; Boda, Z.; Udvardy, M.; Muszbek, L. Promotion of the crosslinking of fibrin and alpha 2-antiplasmin by platelets. *Thromb. Haemost.* **1996**, *75*, 161–7.
- [71] Rao, K. M.; Newcomb, T. F. Clot retraction in a factor XIII free system. *Scand. J. Haematol.* **1980**, *24*, 142–8.
- [72] Kasahara, K.; Souri, M.; Kaneda, M.; Miki, T.; Yamamoto, N.; Ichinose, A. Impaired clot retraction in factor XIII A subunit-deficient mice. *Blood* **2010**, *115*, 1277–9.
- [73] Serrano, K.; Devine, D. V. Intracellular factor XIII crosslinks platelet cytoskeletal elements upon platelet activation. *Thromb. Haemost.* **2002**, *88*, 315–20.
- [74] Schroeder, V.; Kohler, H. P. New developments in the area of factor XIII. *J. Thromb. Haemost.* **2013**, *11*, 234–44.
- [75] Schroeder, V.; Kohler, H. P. Factor XIII Deficiency: An Update. *Semin. Thromb. Hemost.* **2013**, *39*, 632–41.
- [76] Inbal, A.; Lubetsky, A.; Krapp, T.; Castel, D.; Shaish, A.; Dickneite, G.; Modis, L.; Muszbek, L.; Inbal, A. Impaired wound healing in factor XIII deficient mice. *Thromb. Haemost.* **2005**, *94*, 432–7.
- [77] Dardik, R.; Krapp, T.; Rosenthal, E.; Loscalzo, J.; Inbal, A. Effect of FXIII on monocyte and fibroblast function. *Cell. Physiol. Biochem.* **2007**, *19*, 113–20.
- [78] Dardik, R.; Loscalzo, J.; Inbal, a. Factor XIII (FXIII) and angiogenesis. *J. Thromb. Haemost.* **2006**, *4*, 19–25.
- [79] Dardik, R.; Solomon, A.; Loscalzo, J.; Eskaraev, R.; Bialik, A.; Goldberg, I.; Schiby, G.; Inbal, A. Novel proangiogenic effect of factor XIII associated with suppression of thrombospondin 1 expression. *Arterioscler. Thromb. Vasc. Biol.* **2003**, *23*, 1472–7.
- [80] Dardik, R.; Leor, J.; Skutelsky, E.; Castel, D.; Holbova, R.; Schiby, G.; Shaish, A.; Dickneite, G.; Loscalzo, J.; Inbal, A. Evaluation of the pro-angiogenic effect of factor XIII in heterotopic mouse heart allografts and FXIII-deficient mice. *Thromb. Haemost.* **2006**, *95*, 546–50.

- [81] Sharief, L. a. T.; Kadir, R. a. Congenital factor XIII deficiency in women: a systematic review of literature. *Haemophilia* **2013**, *19*, e349–57.
- [82] Kappelmayer, J.; Bacskó, G.; Kelemen, E.; Adány, R. Onset and distribution of factor XIII-containing cells in the mesenchyme of chorionic villi during early phase of human placentation. *Placenta* **1994**, *15*, 613–23.
- [83] Asahina, T.; Kobayashi, T.; Okada, Y.; Goto, J.; Terao, T. Maternal blood coagulation factor XIII is associated with the development of cytotrophoblastic shell. *Placenta* **2000**, *21*, 388–93.
- [84] Ichinose, A. Factor XIII is a key molecule at the intersection of coagulation and fibrinolysis as well as inflammation and infection control. *Int. J. Hematol.* **2012**, *95*, 362–70.
- [85] Loof, T. G.; Mörgelin, M.; Johansson, L.; Oehmcke, S.; Olin, A. I.; Dickneite, G.; Norrby-Teglund, A.; Theopold, U.; Herwald, H. Coagulation, an ancestral serine protease cascade, exerts a novel function in early immune defense. *Blood* **2011**, *118*, 2589–98.
- [86] Hess, K.; Ajjan, R.; Phoenix, F.; Dobó, J.; Gál, P.; Schroeder, V. Effects of MASP-1 of the complement system on activation of coagulation factors and plasma clot formation. *PLoS One* **2012**, *7*, e35690.
- [87] Nahrendorf, M. et al. Factor XIII deficiency causes cardiac rupture, impairs wound healing, and aggravates cardiac remodeling in mice with myocardial infarction. *Circulation* **2006**, *113*, 1196–202.
- [88] Souri, M.; Koseki-Kuno, S.; Takeda, N.; Yamakawa, M.; Takeishi, Y.; Degen, J. L.; Ichinose, A. Male-specific cardiac pathologies in mice lacking either the A or B subunit of factor XIII. *Thromb. Haemost.* **2008**, *99*, 401–8.
- [89] Nahrendorf, M.; Weissleder, R.; Ertl, G. Does FXIII deficiency impair wound healing after myocardial infarction? *PLoS One* **2006**, *1*, e48.
- [90] Aeschlimann, D.; Mosher, D.; Paulsson, M. Tissue transglutaminase and factor XIII in cartilage and bone remodeling. *Semin. Thromb. Hemost.* **1996**, *22*, 437–43.
- [91] Johnson, K. a.; Rose, D. M.; Terkeltaub, R. a. Factor XIII mobilizes transglutaminase 2 to induce chondrocyte hypertrophic differentiation. *J. Cell Sci.* **2008**, *121*, 2256–64.
- [92] Naukkarinen, J.; Surakka, I.; Pietiläinen, K. H.; Rissanen, A.; Salomaa, V.; Ripatti, S.; Yki-Järvinen, H.; van Duijn, C. M.; Wichmann, H.-E.; Kaprio, J.; Taskinen, M.-R.;

- Peltonen, L. Use of genome-wide expression data to mine the "Gray Zone" of GWA studies leads to novel candidate obesity genes. *PLoS Genet.* **2010**, *6*, e1000976.
- [93] Myneni, V. D.; Hitomi, K.; Kaartinen, M. T. Factor XIII-A transglutaminase promotes plasma fibronectin assembly into preadipocyte extracellular matrix which modulates insulin signalling and preadipocyte proliferation and differentiation. *Blood* **2014**,
- [94] Perez, D. L.; Diamond, E. L.; Castro, C. M.; Diaz, A.; Buonanno, F.; Nogueira, R. G.; Sheth, K. Factor XIII deficiency related recurrent spontaneous intracerebral hemorrhage: a case and literature review. *Clin. Neurol. Neurosurg.* **2011**, *113*, 142–5.
- [95] Board, P. G.; Losowsky, M. S.; Miloszewski, K. J. Factor XIII: inherited and acquired deficiency. *Blood Rev.* **1993**, *7*, 229–42.
- [96] Biswas, A.; Ivaskevicius, V.; Seitz, R.; Thomas, A.; Oldenburg, J. An update of the mutation profile of Factor 13 A and B genes. *Blood Rev.* **2011**, *25*, 193–204.
- [97] Luo, Y.-Y.; Zhang, G.-S. Acquired factor XIII inhibitor: clinical features, treatment, fibrin structure and epitope determination. *Haemophilia* **2011**, *17*, 393–8.
- [98] Biswas, a.; Ivaskevicius, V.; Thomas, A.; Oldenburg, J. Coagulation factor XIII deficiency. Diagnosis, prevalence and management of inherited and acquired forms. *Hamostaseologie* **2014**, *34*, 1–7.
- [99] Muszbek, L.; Berczky, Z.; Bagoly, Z.; Shemirani, A. H.; Katona, E. Factor XIII and atherothrombotic diseases. *Semin. Thromb. Hemost.* **2010**, *36*, 18–33.
- [100] Van Hylckama Vlieg, A.; Komanasin, N.; Ariëns, R. a. S.; Poort, S. R.; Grant, P. J.; Bertina, R. M.; Rosendaal, F. R. Factor XIII Val34Leu polymorphism, factor XIII antigen levels and activity and the risk of deep venous thrombosis. *Br. J. Haematol.* **2002**, *119*, 169–75.
- [101] Cushman, M.; O'Meara, E. S.; Folsom, A. R.; Heckbert, S. R. Coagulation factors IX through XIII and the risk of future venous thrombosis: the Longitudinal Investigation of Thromboembolism Etiology. *Blood* **2009**, *114*, 2878–83.
- [102] Kucher, N.; Schroeder, V.; Kohler, H. P. Role of blood coagulation factor XIII in patients with acute pulmonary embolism. Correlation of factor XIII antigen levels with pulmonary occlusion rate, fibrinogen, D-dimer, and clot firmness. *Thromb. Haemost.* **2003**, 434–438.

- [103] Berezky, Z.; Balogh, E.; Katona, E.; Czuriga, I.; Edes, I.; Muszbek, L. Elevated factor XIII level and the risk of myocardial infarction in women. *Haematologica* **2007**, *92*, 287–8.
- [104] Muszbek, L. Deficiency causing mutations and common polymorphisms in the factor XIII-A gene. *Thromb. Haemost.* **2000**, *84*, 524–7.
- [105] Ariëns, R. a.; Philippou, H.; Nagaswami, C.; Weisel, J. W.; Lane, D. a.; Grant, P. J. The factor XIII V34L polymorphism accelerates thrombin activation of factor XIII and affects cross-linked fibrin structure. *Blood* **2000**, *96*, 988–95.
- [106] Li, B.; Zhang, L.; Yin, Y.; Pi, Y.; Yang, Q.; Gao, C.; Fang, C.; Wang, J.; Li, J. Lack of evidence for association between factor XIII-A Val34Leu polymorphism and ischemic stroke: A meta-analysis of 8,800 subjects. *Thromb. Res.* **2011**,
- [107] AbdAlla, S.; Lothar, H.; Langer, A.; el Faramawy, Y.; Quitterer, U. Factor XIIIa transglutaminase crosslinks AT1 receptor dimers of monocytes at the onset of atherosclerosis. *Cell* **2004**, *119*, 343–54.
- [108] Simon, A.; Bagoly, Z.; Hevessy, Z.; Csáthy, L.; Katona, E.; Vereb, G.; Ujfalusi, A.; Szerafin, L.; Muszbek, L.; Kappelmayer, J. Expression of coagulation factor XIII subunit A in acute promyelocytic leukemia. *Cytometry B. Clin. Cytom.* **2012**, *82*, 209–16.
- [109] Lee, S. H.; Suh, I. B.; Lee, E. J.; Hur, G. Y.; Lee, S. Y.; Lee, S. Y.; Shin, C.; Shim, J. J.; In, K. H.; Kang, K. H.; Yoo, S. H.; Kim, J. H. Relationships of coagulation factor XIII activity with cell-type and stage of non-small cell lung cancer. *Yonsei Med. J.* **2013**, *54*, 1394–9.
- [110] Palumbo, J. S.; Barney, K. a.; Blevins, E. a.; Shaw, M. a.; Mishra, a.; Flick, M. J.; Kombrinck, K. W.; Talmage, K. E.; Souri, M.; Ichinose, a.; Degen, J. L. Factor XIII transglutaminase supports hematogenous tumor cell metastasis through a mechanism dependent on natural killer cell function. *J. Thromb. Haemost.* **2008**, *6*, 812–9.
- [111] Bárdos, H.; Molnár, P.; Csécei, G.; Adány, R. Fibrin deposition in primary and metastatic human brain tumours. *Blood Coagul. Fibrinolysis* **1996**, *7*, 536–48.
- [112] Feund, K. F.; Gaul, S. L.; Doshi, K. P.; Claremon, D. A.; Remy, D. C.; Baldwin, J. J.; Friedman, P. A.; Stern, A. M. A novel factor XIIIa inhibitor enhances clot lysis rates. *Fibrinolysis* **1988**, *2*, 67.



- [113] Freund, K. F.; Doshi, K. P.; Gaul, S. L.; Claremon, D. a.; Remy, D. C.; Baldwin, J. J.; Pitzenberger, S. M.; Stern, a. M. Transglutaminase inhibition by 2-[(2-oxopropyl)thio]imidazolium derivatives: mechanism of factor XIIIa inactivation. *Biochemistry* **1994**, *33*, 10109–19.
- [114] Tymiak, A. A.; Tuttle, J. G.; Kimball, S. D.; Wang, T.; Lee, V. G. A simple and rapid screen for inhibitors of factor XIIIa. *J. Antibiot. (Tokyo)*. **1993**, *46*, 204–6.
- [115] Kogen, H.; Kiho, T.; Tago, K.; Miyamoto, S.; Fujioka, T.; Otsuka, N.; Suzuki-Konagai, K.; Ogita, T. Alutacenoic Acids A and B, Rare Naturally Occurring Cyclopropanone Derivatives Isolated from Fungi: Potent Non-Peptide Factor XIIIa Inhibitors. *J. Am. Chem. Soc.* **2000**, *122*, 1842–1843.
- [116] Iwata, Y.; Tago, K.; Kiho, T.; Kogen, H.; Fujioka, T.; Otsuka, N.; Suzuki-Konagai, K.; Ogita, T.; Miyamoto, S. Conformational analysis and docking study of potent factor XIIIa inhibitors having a cyclopropanone ring. *J. Mol. Graph. Model.* **2000**, *18*, 591–9, 602–4.
- [117] Shebuski, R. J.; Sitko, G. R.; Claremon, D. a.; Baldwin, J. J.; Remy, D. C.; Stern, a. M. Inhibition of factor XIIIa in a canine model of coronary thrombosis: effect on reperfusion and acute reocclusion after recombinant tissue-type plasminogen activator. *Blood* **1990**, *75*, 1455–9.
- [118] Reed, G. L.; Houn, a. K. The Contribution of Activated Factor XIII to Fibrinolytic Resistance in Experimental Pulmonary Embolism. *Circulation* **1999**, *99*, 299–304.
- [119] Matlung, H. L.; VanBavel, E.; van den Akker, J.; de Vries, C. J. M.; Bakker, E. N. T. P. Role of transglutaminases in cuff-induced atherosclerotic lesion formation in femoral arteries of ApoE3 Leiden mice. *Atherosclerosis* **2010**, *213*, 77–84.
- [120] Lorand, L.; Gray, A. J.; Brown, K.; Credo, R. B.; Curtis, C. G.; Domanik, R. A.; Stenberg, P. Dissociation of the subunit structure of fibrin stabilizing factor during activation of the zymogen. *Biochem. Biophys. Res. Commun.* **1974**, *56*, 914–22.
- [121] Reinhardt, G. alpha-Halogenmethyl carbonyl compounds as very potent inhibitors of factor XIIIa in vitro. *Ann. N. Y. Acad. Sci.* **1981**, *370*, 836–42.
- [122] Atkinson, J. G.; Baldwin, J. J.; Claremon, D. A.; Friedman, P. A.; Remy, D. C.; Stern, A. M. Factor XIIIa inhibitor compounds useful for thrombolytic therapy. **1988**, Patent, EP0294016.

- [123] Barsigian, C.; Stern, A. M.; Martinez, J. Tissue (type II) transglutaminase covalently incorporates itself, fibrinogen, or fibronectin into high molecular weight complexes on the extracellular surface of isolated hepatocytes. Use of 2-[(2-oxopropyl)thio]imidazolium derivatives as cellular transg. *J. Biol. Chem.* **1991**, *266*, 22501–9.
- [124] Baldwin, J. J.; Remy, D. C.; Claremon, D. A. Certain imidazole compounds as transglutaminase inhibitors. **1990**, US Patent, US4968713.
- [125] Heil, A.; Weber, J.; Büchold, C.; Pasternack, R.; Hils, M. Differences in the inhibition of coagulation factor XIII-A from animal species revealed by Michael Acceptor- and thioimidazol based blockers. *Thromb. Res.* **2013**, *131*, e214–22.
- [126] Zedira GmbH, Newsletter via E-mail. 31.07.2014.
- [127] Hils, M.; Heil, A.; Weber, J.; Pasternack, R. Recombinant factor XIII from animal species for preclinical drug development. 2012; [http://zedira.com/resources/content/pdf/poster\\_p528.pdf](http://zedira.com/resources/content/pdf/poster_p528.pdf).
- [128] Harges, K.; Zouhir Hammamy, M.; Steinmetzer, T. Synthesis and characterization of novel fluorogenic substrates of coagulation factor XIII-A. *Anal. Biochem.* **2013**, *442*, 223–30.
- [129] Finney, S.; Seale, L.; Sawyer, R. T.; Wallis, R. B. Tridegin, a new peptidic inhibitor of factor XIIIa, from the blood-sucking leech *Haementeria ghilianii*. *Biochem. J.* **1997**, *324*, 797–805.
- [130] Sawyer, R. T.; Wallis, R. B.; Seale, L.; Finney, S. Inhibitors of fibrin cross-linking and/or transglutaminases. **2000**, US Patent, 6025330.
- [131] Giersiefen, H.; Stöckel, J.; Pamp, T.; Ohlmann, M. Modifizierte Tridegine, ihre Herstellung und Verwendung als Transglutaminase-Inhibitoren. **2002**, Patent, EP1458866B1.
- [132] Linxweiler, W.; Burger, C.; Pöschke, O.; Hofmann, U.; Wolf, A. Glucose-Dehydrogenase-Fusionsproteine und ihre Verwendung in Expressionssystemen. **2000**, Patent, WO 00/49039.
- [133] Faria, F.; Junqueira-de Azevedo, I. D. L. M.; Ho, P. L.; Sampaio, M. U.; Chudzinski-Tavassi, A. M. Gene expression in the salivary complexes from *Haementeria depressa* leech through the generation of expressed sequence tags. *Gene* **2005**, *349*, 173–85.
- [134] Kühl, T. Untersuchungen zur Darstellung des Faktor XIIIa-Inhibitors Tridegin durch Festphasenpeptidsynthese und chemische Ligation. Diplomarbeit, Friedrich-Schiller-Universität Jena, 2009.

- [135] Rost, B. Twilight zone of protein sequence alignments. *Protein Eng.* **1999**, *12*, 85–94.
- [136] Simakov, O. et al. Insights into bilaterian evolution from three spiralian genomes. *Nature* **2013**, *493*, 526–31.
- [137] Slaughter, T. F.; Achyuthan, K. E.; Lai, T. S.; Greenberg, C. S. A microtiter plate transglutaminase assay utilizing 5-(biotinamido)pentylamine as substrate. *Anal. Biochem.* **1992**, *205*, 166–71.
- [138] Fickenscher, K.; Aab, A.; Stüber, W. A photometric assay for blood coagulation factor XIII. *Thromb. Haemost.* **1991**, *65*, 535–40.
- [139] Kárpáti, L.; Penke, B.; Katona, E.; Balogh, I.; Vámosi, G.; Muszbek, L. A modified, optimized kinetic photometric assay for the determination of blood coagulation factor XIII activity in plasma. *Clin. Chem.* **2000**, *46*, 1946–55.
- [140] Oertel, K.; Hunfeld, A.; Specker, E.; Reiff, C.; Seitz, R.; Pasternack, R.; Dodt, J. A highly sensitive fluorometric assay for determination of human coagulation factor XIII in plasma. *Anal. Biochem.* **2007**, *367*, 152–8.
- [141] Hardes, K.; Becker, G. L.; Hammamy, M. Z.; Steinmetzer, T. Design, synthesis, and characterization of chromogenic substrates of coagulation factor XIIIa. *Anal. Biochem.* **2012**, *428*, 73–80.
- [142] Arkona, C.; van de Locht, A. Tridegin: Recombinant expression, purification, and characterization of the highly specific coagulation factor XIIIa inhibitor from *Haementeria ghilianii*. MipTec – Lead. Eur. Event Drug Discov. Basel, Switzerland, 2009; p P 160.
- [143] Coch, R. Darstellung und biologische Wirksamkeit von Analoga des Faktor XIIIa-Inhibitors Tridegin. Diplomarbeit, Friedrich-Schiller-Universität Jena, 2010.
- [144] Thornton, J. M. Disulphide bridges in globular proteins. *J. Mol. Biol.* **1981**, *151*, 261–87.
- [145] Schmidt, B.; Ho, L.; Hogg, P. J. Allosteric disulfide bonds. *Biochemistry* **2006**, *45*, 7429–33.
- [146] Wong, J. W. H.; Hogg, P. J. Analysis of disulfide bonds in protein structures. *J. Thromb. Haemost.* **2010**, 9385.
- [147] Richardson, J. S. The anatomy and taxonomy of protein structure. *Adv. Protein Chem.* **1981**, *34*, 167–339.

- [148] Schmidt, B.; Hogg, P. J. Search for allosteric disulfide bonds in NMR structures. *BMC Struct. Biol.* **2007**, *7*, 49.
- [149] Stieler, M.; Weber, J.; Hils, M.; Kolb, P.; Heine, A.; Büchold, C.; Pasternack, R.; Klebe, G. Kristallstruktur des aktiven Gerinnungsfaktors XIIIa, induziert durch Calciumbindung: Grundlage für die Entwicklung neuartiger Antikoagulantien. *Angew. Chemie* **2013**, *125*, 12148–12153.
- [150] Candiano, G.; Bruschi, M.; Musante, L.; Santucci, L.; Ghiggeri, G. M.; Carnemolla, B.; Orecchia, P.; Zardi, L.; Righetti, P. G. Blue silver: a very sensitive colloidal Coomassie G-250 staining for proteome analysis. *Electrophoresis* **2004**, *25*, 1327–33.
- [151] Böhm, M.; Kühn, T.; Hards, K.; Coch, R.; Arkona, C.; Schlott, B.; Steinmetzer, T.; Imhof, D. Synthesis and functional characterization of tridegin and its analogues: inhibitors and substrates of factor XIIIa. *ChemMedChem* **2012**, *7*, 326–33.
- [152] Liu, Y.; Kati, W.; Chen, C. M.; Tripathi, R.; Molla, a.; Kohlbrenner, W. Use of a fluorescence plate reader for measuring kinetic parameters with inner filter effect correction. *Anal. Biochem.* **1999**, *267*, 331–5.
- [153] Wienken, C. J.; Baaske, P.; Rothbauer, U.; Braun, D.; Duhr, S. Protein-binding assays in biological liquids using microscale thermophoresis. *Nat. Commun.* **2010**, *1*, 100.
- [154] Z-dock docking server. <http://zdock.umassmed.edu>.
- [155] Böhm, M.; Bäuml, C. A.; Hards, K.; Steinmetzer, T.; Roeser, D.; Schaub, Y.; Than, M. E.; Biswas, A.; Imhof, D. Novel Insights into Structure and Function of Factor XIIIa-Inhibitor Tridegin. *J. Med. Chem.* **2014**, *57*, 10355–65.
- [156] Bäuml, C. Structural and Functional Analysis of Factor XIIIa Inhibitor Tridegin. Master Thesis, University of Cologne, 2014.
- [157] Kojer, K.; Riemer, J. Balancing oxidative protein folding: The influences of reducing pathways on disulfide bond formation. *Biochim. Biophys. Acta* **2014**, *1844*, 1383–1390.
- [158] Brandt, R. B.; Laux, J. E.; Yates, S. W. Calculation of inhibitor  $K_i$  and inhibitor type from the concentration of inhibitor for 50% inhibition for Michaelis-Menten enzymes. *Biochem. Med. Metab. Biol.* **1987**, *37*, 344–9.
- [159] Dixon, M. The determination of enzyme inhibitor constants. *Biochem. J.* **1953**, *55*, 170–1.

- [160] Segel, I. H. *Enzyme Kinetics: Behavior and Analysis of Rapid Equilibrium and Steady-State Enzyme Systems*; John Wiley & Sons, Inc.: New York, 1975; pp 465–473.
- [161] Kovalevsky, A. Y.; Ghosh, A. K.; Weber, I. T. Solution kinetics measurements suggest HIV-1 protease has two binding sites for darunavir and amprenavir. *J. Med. Chem.* **2008**, *51*, 6599–603.
- [162] Böhm, G.; Muhr, R.; Jaenicke, R. Quantitative analysis of protein far UV circular dichroism spectra by neural networks. *Protein Eng.* **1992**, *5*, 191–5.
- [163] Greenfield, N.; Fasman, G. D. Computed circular dichroism spectra for the evaluation of protein conformation. *Biochemistry* **1969**, *8*, 4108–16.
- [164] Hofmann, A. ACDP – a Java application for data processing and analysis of protein circular dichroism spectra. *J. Appl. Crystallogr.* **2008**, *42*, 137–139.
- [165] Szyperski, T.; Güntert, P.; Stone, S. R.; Wüthrich, K. Nuclear magnetic resonance solution structure of hirudin(1-51) and comparison with corresponding three-dimensional structures determined using the complete 65-residue hirudin polypeptide chain. *J. Mol. Biol.* **1992**, *228*, 1193–205.
- [166] Tietze, A. A.; Tietze, D.; Ohlenschläger, O.; Leipold, E.; Ullrich, F.; Kühl, T.; Mischo, A.; Buntkowsky, G.; Görlach, M.; Heinemann, S. H.; Imhof, D. Structurally diverse  $\mu$ -conotoxin PIIIA isomers block sodium channel NaV 1.4. *Angew. Chem. Int. Ed. Engl.* **2012**, *51*, 4058–61.
- [167] Sicker, T. Strukturelle Untersuchungen von Blutgerinnungsfaktor XIII. Dissertation, Friedrich-Schiller-Universität Jena, 2007.
- [168] Gray, W. R. Disulfide structures of highly bridged peptides: a new strategy for analysis. *Protein Sci.* **1993**, *2*, 1732–48.
- [169] Tang, H.-Y.; Speicher, D. W. Determination of disulfide-bond linkages in proteins. *Curr. Protoc. Protein Sci.* **2004**, *Chapter 11*, Unit 11.11.
- [170] Bhattacharyya, M.; Gupta, K.; Gowd, K. H.; Balaram, P. Rapid mass spectrometric determination of disulfide connectivity in peptides and proteins. *Mol. Biosyst.* **2013**, *9*, 1340–50.
- [171] Nicolardi, S.; Giera, M.; Kooijman, P.; Kraj, A.; Chervet, J.-P.; Deelder, A. M.; van der Burgt, Y. E. M. On-line electrochemical reduction of disulfide bonds: improved FTICR-CID and -ETD coverage of oxytocin and hepcidin. *J. Am. Soc. Mass Spectrom.* **2013**, *24*, 1980–7.

- [172] Laskowski, R. a. PDBsum new things. *Nucleic Acids Res.* **2009**, *37*, D355–9.
- [173] Krieger, E.; Darden, T.; Nabuurs, S. B.; Finkelstein, A.; Vriend, G. Making optimal use of empirical energy functions: force-field parameterization in crystal space. *Proteins* **2004**, *57*, 678–83.
- [174] Jones, D. T. Protein secondary structure prediction based on position-specific scoring matrices. *J. Mol. Biol.* **1999**, *292*, 195–202.
- [175] Rester, U.; Bode, W.; Sampaio, C. A.; Auerswald, E. A.; Lopes, A. P Cloning, purification, crystallization and preliminary X-ray diffraction analysis of the antistasin-type inhibitor ghilanten (domain I) from *Haementeria ghiliani* in complex with porcine beta-trypsin. *Acta Crystallogr. D. Biol. Crystallogr.* **2001**, *57*, 1038–41.
- [176] Krezel, A. M.; Wagner, G.; Seymour-Ulmer, J.; Lazarus, R. A. Structure of the RGD protein decorsin: conserved motif and distinct function in leech proteins that affect blood clotting. *Science* **1994**, *264*, 1944–7.
- [177] Richardson, J. L.; Kröger, B.; Hoeffken, W.; Sadler, J. E.; Pereira, P.; Huber, R.; Bode, W.; Fuentes-Prior, P. Crystal structure of the human alpha-thrombin-haemadin complex: an exosite II-binding inhibitor. *EMBO J.* **2000**, *19*, 5650–60.
- [178] Liu, C. C.; Brustad, E.; Liu, W.; Schultz, P. G. Crystal structure of a biosynthetic sulfo-hirudin complexed to thrombin. *J. Am. Chem. Soc.* **2007**, *129*, 10648–9.
- [179] Krezel, A. M.; Wagner, G.; Seymour-Ulmer, J.; Lazarus, R. A. Structure of the RGD protein decorsin: conserved motif and distinct function in leech proteins that affect blood clotting. *Science* **1994**, *264*, 1944–7.
- [180] Protein Data Bank Contents Guide: Atomic Coordinate Entry Format Description. Version 3.30. 2008; <http://www.wwpdb.org/documentation/format33/v3.3.html>.
- [181] Jones, J. H. Abbreviations and symbols in peptide science: a revised guide and commentary. *J. Pept. Sci.* **2006**, *12*, 1–12.

## Acknowledgement

Most of all I would like to thank Prof. Dr. Diana Imhof, who supported me throughout the work on my thesis and gave me advice, guidance and motivation.

Furthermore I thank Prof. Dr. Michael Gütschow for being the second referee of this thesis.

Special thanks are also addressed to Prof. Dr. Torsten Steinmetzer and Kornelia Hardes (University of Marburg) for giving me the possibility to perform FXIIIa activity assays in Marburg and for the help and advice in numerous questions.

Moreover, I am very grateful to Dr. Manuel Than (FLI Jena) and his co-workers for a huge number of crystallization experiments as well as to Dr. Arijit Biswas (University Hospital Bonn) for performing computational modeling and docking.

For the possibility to perform thermophoresis experiments I would like to thank Prof. Dr. Michael Famulok and Dr. Anton Schmitz (LIMES Bonn). I also would like to express my gratitude towards Dr. Marianne Engeser for uncomplicated access to MALDI-MS and Prof. Dr. Christa E. Müller for the possibility to work in the S1 lab.

Many thanks also to the other members of the Imhof group, namely Toni, Dorle, Pascal, Ming and Henning as well as to Charlotte and Amelie for their support, the motivating atmosphere and stimulating paper discussions.

Last but not least I would like to thank Robert and my family for their continuous support.





# Publications

## Articles

Böhm, M.; Kühl, T.; Harges, K.; Coch, R.; Arkona, C.; Schlott, B.; Steinmetzer, T.; Imhof, D. Synthesis and functional characterization of tridegin and its analogues: inhibitors and substrates of factor XIIIa. *ChemMedChem* **2012**, 7 (2), 326–33.

Böhm, M.; Tietze, A.A.; Heimer, P.; Chen, M.; Imhof, D. Ionic liquids as reaction media for oxidative folding and native chemical ligation of cysteine-containing peptides. *J. Mol. Liq.* **2014**, 192, 67-70.

Böhm, M.; Bäuml, C.; Harges, K.; Steinmetzer, T.; Roesner, D.; Schaub, Y.; Than, M.; Biswas, A.; Imhof, D. Novel insights into structure and function of factor XIIIa-inhibitor tridegin. *J. Med. Chem.* **2014**, 57 (24), 10355-10365.

Heimer, P.; Tietze, A.A.; Böhm, M.; Giernoth, R.; Kuchenbuch, A.; Stark, A.; Leipold, E.; Heinemann, S.H.; Imhof, D. Application of room temperature aprotic and protic ionic liquids for oxidative folding of cysteine-rich peptides. *ChemBioChem* **2014**, 15 (18), 2754-2765.

## Posters

Kühl, T.; Böhm, M.; Tietze, A.; Imhof, D. Native Chemical Ligation and Oxidation in Ionic Liquids. *Workshop SPP1191* **2011**, Heimerzheim.

Böhm, M.; Kühl, T.; Imhof, D. Targeting the final step of blood coagulation: Tridegin as a valuable tool to inhibit FXIIIa. *11. Deutsches Peptidsymposium* **2013**, Garching (München).

Böhm, M.; Bäuml, C.; Imhof, D. Tridegin, an interesting peptide targeting factor XIIIa. *GRC: Transglutaminases in Human Disease Processes* **2014**, Lucca (Italien).